



저작자표시-비영리-변경금지 2.0 대한민국

이용자는 아래의 조건을 따르는 경우에 한하여 자유롭게

- 이 저작물을 복제, 배포, 전송, 전시, 공연 및 방송할 수 있습니다.

다음과 같은 조건을 따라야 합니다:



저작자표시. 귀하는 원저작자를 표시하여야 합니다.



비영리. 귀하는 이 저작물을 영리 목적으로 이용할 수 없습니다.



변경금지. 귀하는 이 저작물을 개작, 변형 또는 가공할 수 없습니다.

- 귀하는, 이 저작물의 재이용이나 배포의 경우, 이 저작물에 적용된 이용허락조건을 명확하게 나타내어야 합니다.
- 저작권자로부터 별도의 허가를 받으면 이러한 조건들은 적용되지 않습니다.

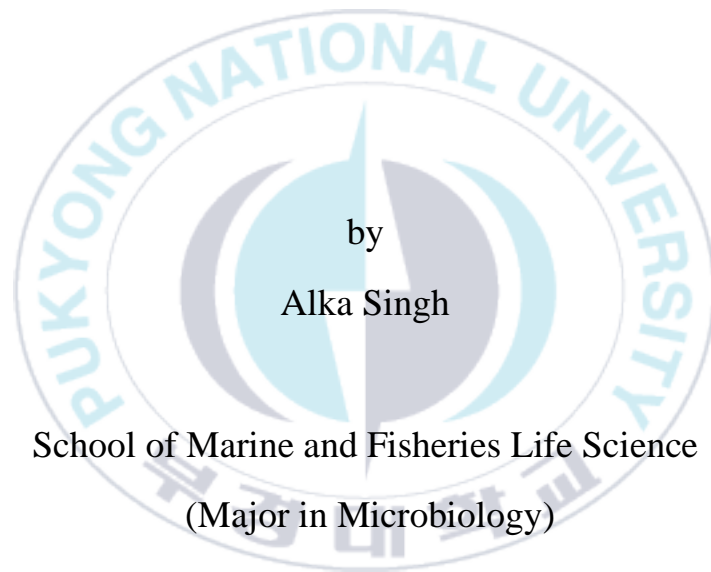
저작권법에 따른 이용자의 권리는 위의 내용에 의하여 영향을 받지 않습니다.

이것은 [이용허락규약\(Legal Code\)](#)을 이해하기 쉽게 요약한 것입니다.

[Disclaimer](#)

Thesis for the Degree of Doctor of Philosophy

**Induction of apoptosis in AGS and HepG2 cancer
cells using Indole-3-Carbinol and
Angelica keiskei extracts**



by

Alka Singh

School of Marine and Fisheries Life Science

(Major in Microbiology)

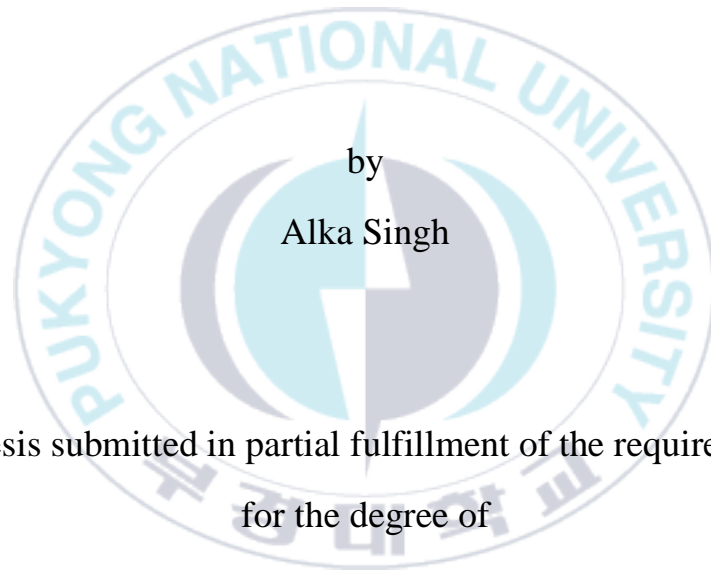
The Graduate School
Pukyong National University

February 2024

**Induction of apoptosis in AGS and HepG2 cancer cells
using Indole-3-Carbinol and *Angelica keiskei* extracts
(Indole-3-Carbinol 및 *Angelica keiskei* 추출물을 이용한**

AGS 및 HepG2 암 세포의 세포사멸 유도)

Advisor: Prof. Gun-Do Kim



by

Alka Singh

A thesis submitted in partial fulfillment of the requirements
for the degree of
Doctor of Philosophy

School of Marine and Fisheries Life Science

(Major in Microbiology)

The Graduate School
Pukyong National University

February 2024

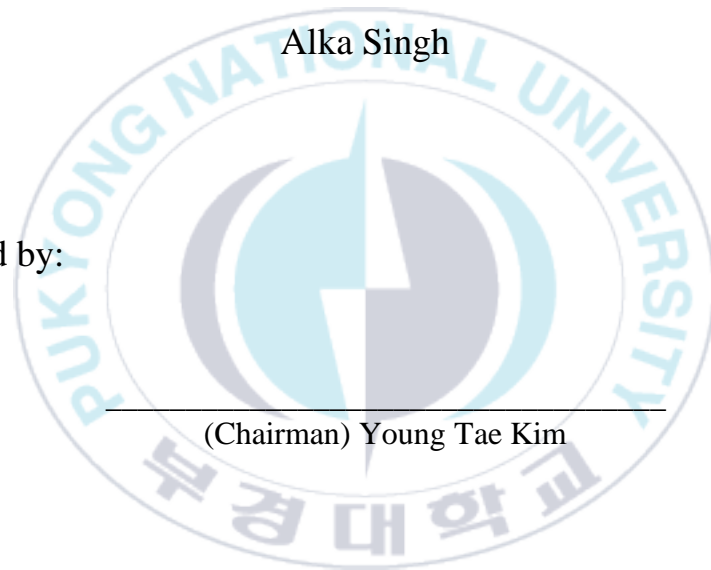
**Induction of apoptosis in AGS and HepG2 cancer cells
using Indole-3-Carbinol and *Angelica keiskei* extracts**

A dissertation

by

Alka Singh

Approved by:



(Chairman) Young Tae Kim

(Member) Young Jae Jeon

(Member) Soo-Wan Nam

(Member) Nam Gyu Park

(Member) Gun-Do Kim

February 16, 2024

Contents

List of Figures	vii
List of Tables	x
List of Abbreviations	xi
Abstract	xiii
Chapter 1. General Introduction	1
1.1. Cancer.....	3
1.2. Gastric Cancer	4
1.3. <i>Helicobacter pylori</i> (<i>H. pylori</i>)	6
1.3.1. The virulence and pathogenicity of <i>H. pylori</i>	8
1.3.2. Metabolic Modification by <i>H. pylori</i>	9
1.4. Treatment of gastric cancer	11
1.4.1. Surgery.....	11
1.4.2. Chemotherapy.....	12
1.4.3. Radiation therapy.....	13
1.4.4. Targeted therapy	14
1.4.5. Immunotherapy.....	14
1.5. Hepatocellular Carcinoma (HCC).....	15
1.6. Cellular malignancy-related markers	16
1.7. HCC Sequential Development	16
1.7.1. Tumor necrosis factor-alpha and interleukin-6 (TNF- α and IL-6)	16
1.7.2. Nuclear Factor- $\kappa\beta$ (NF- $\kappa\beta$).....	17
1.7.3. Transforming growth factor alpha (TGF α).....	17

1.8.	Hepatocellular Carcinoma's (HCCs) Molecular Targeted Therapies	18
1.8.1.	Anti-Angiogenic Agents	18
1.8.2.	Immunotherapy in the Treatment of HCC	19
1.9.	Treatment Challenges for HCC Patients	19
1.10.	Indole-3-carbinol	20
1.11.	<i>Angelica keiskei</i>	24
1.12.	Aims of the present study	27

Chapter 2. Indole-3-Carbinol Regulates Apoptosis in AGS Cancer Cells via the BCL-Family Genes 28

2.1.	Abstract	28
2.2.	Introduction	29
2.3.	Materials and methods	33
2.3.1.	Reagents	33
2.3.2.	Cell culture	33
2.3.3.	Cell viability assay	33
2.3.4.	DAPI staining (4',6-diamidino-2-phenylindole staining)	34
2.3.5.	DNA fragmentation	35
2.3.6.	RNA extraction and cDNA synthesis	35
2.3.7.	Real-Time quantitative PCR	36
2.3.8.	Molecular Docking Analysis of I3C with P53	38
2.3.9.	Statistical analysis	38
2.4.	Results	38

2.4.1.	Effects of I3C on normal cells and AGS cells.....	38
2.4.2.	Nuclei express consistent morphological changes during apoptosis by I3C.	41
2.4.3.	DNA degradation and cellular death	43
2.4.4.	Apoptosis induction via mitochondrial pathway by expressing BH-3 subfamily genes.	45
2.4.5.	Molecular docking between I3C and p53 protein.....	48
2.5.	Discussion	50
2.6.	Conclusion.....	61
Chapter 3. <i>Angelica keiskei</i>: A potential antioxidant and anticancer agent for photothermal drug delivery applications		63
3.1.	Abstract	63
3.2.	Introduction	64
3.3.	Materials and methods.....	68
3.3.1.	Sample collection.....	68
3.3.2.	Crude extraction.....	68
3.3.3.	Total phenolic content (TPC) and antioxidant activity assay	71
3.3.4.	GC-MS.....	71
3.3.5.	Synthesis of Hydroxyapatite (HAp)	72
3.3.6.	UV-Vis study	72
3.3.7.	Drug loading and releasing study	73
3.3.8.	Cell cytotoxicity test	75

3.3.9.	Fluorescence imaging of MDA-MB 231 cells.....	75
3.3.10.	Photothermal therapy.....	76
3.3.11.	Hemolysis study.....	76
3.3.12.	Molecular docking analysis to check antibacterial activities	77
3.4.	Results	77
3.4.1.	Total phenolic content (TPC) and Radical Scavenging Activity.....	77
3.4.2.	Compound identification and chromatogram by GC-MS analysis based on Wileylib.	80
3.4.3.	The biological function of the 2,3-dihydro-3,5-dihydroxy-6-methyl-4 <i>H</i> -pyran-4-one (DDMP):	84
3.4.4.	XRD analysis of HAp.....	84
3.4.5.	UV-Vis study.....	85
3.4.6.	Drug loading and releasing study	88
3.4.7.	Effect of AKLE on MDA-MB 231 cells	92
3.4.8.	Double labeling for AO and PI fluorescence analysis of cell viability	92
3.4.9.	Photothermal therapies (PTT).....	94
3.4.10.	Hemolysis study.....	98
3.4.11.	Molecular Interaction between DDMP and beta-lactamase using docking analysis.....	103

3.4.12.	Molecular Interaction between DDMP and penicillin-binding proteins using docking analysis.....	105
3.5.	Discussion	107
3.6.	Conclusion.....	108
Chapter 4. <i>Angelica keiskei</i> extracts induce apoptosis in HepG2 cells by neutralizing the function of IGFBP1 protein		112
4.1.	Abstract	112
4.2.	Introduction	113
4.3.	Materials and methods.....	116
4.3.1.	Reagents.....	116
4.3.2.	Cell culture.....	116
4.3.3.	MTT assay	116
4.3.4.	Human Apoptotic Array Screening	117
4.3.5.	Sample preparation	117
4.3.6.	Antibody array assay	118
4.3.7.	Data analysis.....	119
4.3.8.	Protein extraction and Western blotting	120
4.3.9.	Molecular docking analysis	121
4.4.	Results	121
4.4.1.	Cytotoxic effect and morphological alteration of <i>Angelica keiskei</i> on HepG2 cells	121
4.4.2.	Protein expression alteration using the apoptotic array analysis.	123

4.4.3.	Identification of differentially expressed apoptotic proteins using cluster heatmap.....	126
4.4.4.	Protein-protein interaction network investigation	129
4.4.5.	Functional enrichment analysis	132
4.4.6.	Western blotting analysis of apoptotic proteins.....	134
4.4.7.	Computational analysis of DDMP with IGFPB1, Bcl-2 and P53 protein.	136
4.5.	Discussion	138
4.6.	Conclusion.....	142
References		144
요약		174
Acknowledgement		176

List of Figures

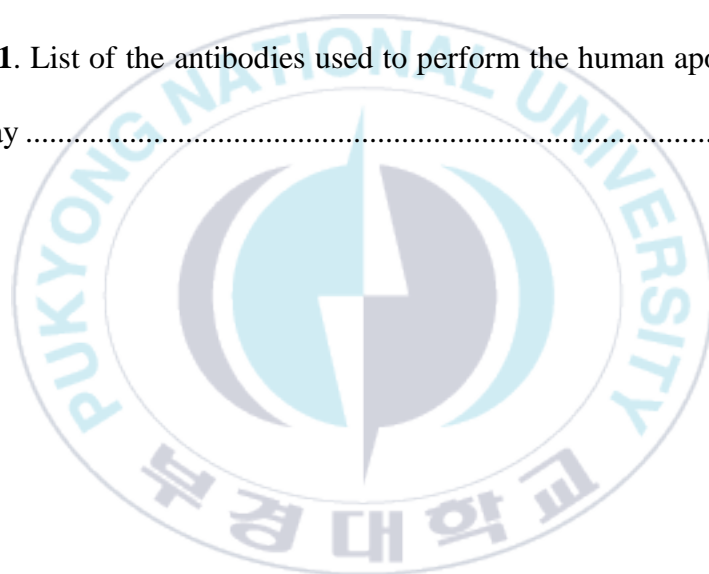
Figure 1.1. Chemical structure of Indole-3-Carbinol	23
Figure 1.2. <i>Angelica keiskei</i> plant.....	26
Figure 2.1. Cell viability of normal cells treated with I3C (The data has shown mean \pm SE).....	39
Figure 2.2. AGS cell viability after I3C treatment. (The data has shown mean \pm SE.).....	40
Figure 2.3. The morphological alteration of AGS cells after I3C treatment on dose-dependent manner.	42
Figure 2.4. DNA fragmentation of I3C treated AGS cells on dose-dependent manner.	44
Figure 2.5. RT-qPCR results of relative gene expression in AGS cells after I3C treatment.	47
Figure 2.6. (a)Molecular docking analysis of I3C with p53; and (b) The ligand interactions with p53 shown in 2D diagram.	49
Figure 2.7. Schematic diagram of the intrinsic pathway of apoptosis involved in I3C-treated AGS cells.	60
Figure 3.1. Schematic diagram of a batch subcritical water extractor.	70

Figure 3.2. Total phenolic content (a) and radical scavenging activity (b) of <i>Angelica keiskei</i> extracts obtained from subcritical water treatment at different temperatures.....	79
Figure 3.3. (a) GC-MS chromatogram of crude <i>Angelica keiskei</i> extract, (b) The compound identification from <i>Angelica keiskei</i> extract based on Wileylib, (c) Chemical structure of DDMP.	83
Figure 3.4. (a) XRD analysis of synthesized HAp nanomaterials (b) UV-Vis study of <i>Angelica keiskei</i> extract.....	87
Figure 3.5. (a) UV-Vis study of <i>Angelica keiskei</i> extract (drug) loaded on synthesized HAp nanomaterials (b) drug-releasing study at different pH with/without laser irradiation for sustainable release (72 hours).	91
Figure 3.6. MTT assay and AO/PI study of the MDA-MB 231 treated cell line.....	93
Figure 3.7. Photothermal (PTT) study of <i>Angelica keiskei</i> extract (drug) loaded on synthesized HAp.....	97
Figure 3.8. Hemolysis study of hydroxyapatite loaded with <i>Angelica keiskei</i> extract.....	102
Figure 3.9. Protein-ligand interaction between beta-lactamase and 2,3-Dihydro-3,5-dihydroxy-6-methyl-4H-pyran-2-one (DDMP)	104

Figure 3.10. Protein-ligand interaction between penicillin-binding protein and 2,3-Dihydro-3,5-dihydroxy-6-methyl-4H-pyran-2-one (DDMP)	106
Figure 4.1. Morphological alteration and cell viability representation of HepG2 cell after treatment with <i>Angelica keiskei</i> on dose-dependent manner.	122
Figure 4.2. The fluorescence image of expressed proteins at different concentrations on dose-dependent manner based on the sequence of the antibodies in the table 4.1.	125
Figure 4.3. The substantial response level of the AK therapy on HepG2 cells.	128
Figure 4.4. Protein-protein interactions of BAD, HTRA2, IGFBP1, IGFBP5, and CDKN1A.	131
Figure 4.5. The differentially expressed signaling pathways	133
Figure 4.6. Western blot analysis of the BAD, BID, IGFBP1 protein (0, 50, 100, 400µg/ml)	135
Figure 4.7. (A) IGFBP1 (B) Bcl-2 and (C) p53 protein docking with DDMP has binding affinity -4.7, -5.3 and -5.4 respectively.	137

List of Tables

Table 2.1. A list of the designed primers used for RT-qPCR.....	37
Table 3.1. List of the parameters for extracting bioactive components from Angelica Kieskei using subcritical water extraction method.	69
Table 3.2. List of identified compounds by GC-MS analysis	81
Table 4.1. List of the antibodies used to perform the human apoptotic array assay	124



List of Abbreviations

AITC	Allyl isothiocyanate
AKLE	<i>Angelica keiskei</i> leaf extract
AO/PI	Acridine orange/propidium iodide
APAF1	Apoptotic protease activating factor-1
ATCC	American type culture collection
BAD	BCL2 antagonist of cell death
BAK	BCL-2 Antagonist/killer
BAX	Bcl-2 Associated X protein
CDK-6	Cyclin-dependent kinase 6
CDKN1A	Cyclin-dependent kinase inhibitor 1A
Cyt-c	Cytochrome c
DAPI	4',6-diamidino-2-phenylindole
DDMP	2, 3, -Dihydro-3, 5-dihydroxy-6-methyl-4H-pyran-4-one
DILI	Drug-induced liver injury
DIM	Diindolylmethane
DMEM	Dulbecco's modified eagle's medium
DMSO	Dimethyl sulfoxide
DPPH	2,2'-diphenyl-1-picrylhydrazyl radical
EGFR	Epithelial growth factor receptor
ESP	Epithioapecifier protein
GC-MS	Gas chromatography-mass spectrometry
HaCaT	Human keratinocyte
HAp	Hydroxyapatite
HCB	Hepatitis B virus
HCC	Hepatocellular carcinoma

HCV	Hepatitis C virus
HEK-293	Human embryonic kidney 293
HepG2	Hepatoblastoma cell line
HPCs	Hepatic progenitor cells
HTRA2	HtrA serine peptidases 2
I3C	Indole-3-Carbinol
IC50	50% Inhibitory concentration
IFNs	Interferons
IGFBP1	Insulin-like growth factor binding proteins1
IGFBP5	Insulin-like growth factor binding proteins5
IL-6	Interleukin 6
MDA-MB231	Breast cancer cells
MEM	Minimum essential medium
MTT	3-(4,5-dimethylthiazol-2-yl)-2,5-diphenyl tetrazolium bromide
NCSP	National cancer screening program
NIR	Near-infrared
PARP	Poly (ADP-ribose) polymerase (PARP)
PC-3	Human prostate cancer cell line
PDB	Protein data bank
PTT	Photothermal therapy
qPCR	Quantitative polymerase chain reaction
RPMI	Roswell park memorial institute medium
TNF- α	Tumor necrosis factor-alpha
TPC	Total phenolic compounds
UGIS	Upper gastrointestinal series
UV-Vis	UV visible spectroscopy
XRD	X-ray powder diffraction

Induction of apoptosis in AGS and HepG2 cancer cells using Indole-3-Carbinol and *Angelica keiskei* extracts

Alka Singh

Department of Microbiology, The Graduate School,

Pukyong National University

Abstract

One of the most common diseases in the world is cancer. Action is still required in the face of the formidable global health challenge posed by cancer. Cancer is a disease that occurs when specific body cells proliferate abnormally out of control and migrate to other body areas. Following the standard view of the disease, cancer is an assortment of progressive genetic abnormalities caused by mutations in tumor-suppressor genes, oncogenes, and chromosomal abnormalities. Cancer chemoprevention uses natural or biological compounds to reduce the risk of developing cancer in healthy people. Chemopreventive drugs prevent cancer growth by preventing DNA damage, which results in spite, or by reversing or preventing the division of premalignant cells with DNA damage. Most of the pharmaceuticals employed nowadays are derived from plants, making them one of the more significant sources of medicine. Differential drug response and safe dosages are the main challenges to such prediction. It is safe to treat with IC50 doses to avoid the side effects of the drugs that kill normal cells and cancer cells. Clinical studies have shown that phytochemicals and herbs are the most efficient way to treat cancer,

whether added to chemotherapy or taken separately to boost the immune system without any side effects.

Gastric cancer is the second-leading cause of cancer-related deaths globally. One known fact is that *Helicobacter pylori* infects the stomach's inner lining and causes cancer. In this research, Indole-3-Carbinol is used as an anticancer drug against the AGS cancer cells. Cell viability was performed to check the compound's anticancer activity. DNA fragmentation was utilized to assess DNA degradation, and DAPI labeling was employed to identify nuclear condensation. The qPCR technique was used to measure apoptotic gene expression. I3C demonstrated a strong affinity for the apoptotic protein 3DCY per molecular docking study.

This work explores the remarkable anticancer, antioxidant, and antibacterial properties and the safest drug delivery applications. *Angelica keiskei* Crude was extracted using the subcritical water extraction method. Antioxidant activity was evaluated using a DPPH radical scavenging assay. MTT assay was done to check the compound's anticancer activity on MDA-MB-231 cells. HAp was used for drug delivery. UV-Vis study was performed to check the photothermal efficacy, drug loading, and releasing capacity. A hemolysis research was conducted to determine the biocompatibility and safety of the compounds. Molecular docking was performed to check the binding affinity with the bacterial proteins.

Hepatocellular carcinoma (HCC) is the most common type of primary liver cancer. In the present study, the *Angelica keiskei* extract's active compound identified by GC-MS is 3, - Dihydro-3, 5-dihydroxy-6-methyl-4H-pyran-4-one (DDMP) induced apoptosis in HepG2 cells. Cell viability was decreased in a dose-dependent manner after the MTT test. The study's main emphasis, the Antibody Apoptotic Array that has checked the 43 genes' expression together, identified significant changes in apoptotic proteins. Western blot analysis and molecular docking further confirmed the expression of apoptotic proteins and binding affinity.

This work is distinct and has never been done using the mentioned cells and techniques. This can help further study the precise molecular mechanism of action.



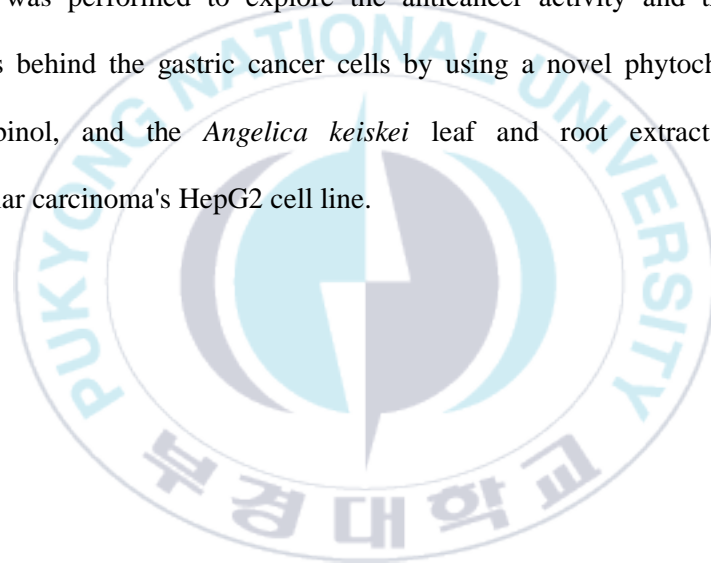
Chapter 1. General Introduction

On a global scale, cancer incidence and mortality are increasing rapidly. The reasons are complicated, but they include changes in the prevalence and distribution of primary cancer risk factors and population aging and growth. Cancer remains one of the leading causes of mortality worldwide, necessitating the continuous search for novel and effective therapeutic strategies. Transformation of the normal cells can be achieved in various ways like chemical or physical mutagen that change the properties of the cells, resulting in malignant cells. It is routine to check the preliminary safety aspects of the particles intended for in vivo applications. According to the latest data, gastric cancer (stomach cancer) is the fourth leading cause of death and the fifth most commonly diagnosed worldwide malignancy. In 2020, gastric cancer accounted for 1.1 million new cases, representing 1,089,103 (5.6%) of all cancer cases, and recent deaths representing 7,687,933 (7.7%) globally in 2020. Stomach cancer is a critical worldwide health issue because of its high incidence, poor prognosis, and cellular and molecular heterogeneity, among other factors (Thrift and El-Serag 2020). Most patients die from secondary tumors generated by cells separated from the primary ones rather than the primary ones. Most frequently, the primary tumor suffers from the lack of oxygen, which goes to stress and loungers the mechanism of metastasis and worsens the chance of recovery.

In terms of gene expression and function, immortalized hepatocyte cell lines bear only a slight resemblance to primary hepatocytes, limiting their efficacy in predicting drug-induced liver injury (DILI). According to a medical review by Gabriela Pichardo, MD,

on November 10, 2019, most liver cancers are secondary or metastatic, which means they begin somewhere else in the body. Liver cancer can be caused by chronic infection with hepatitis C virus (HCV) or hepatitis B virus (HBV). In the United States, primary liver cancer, which starts in the liver, accounts for about 2% of all cancers. However, in some emerging regions, cancer accounts for up to 50% of all cancers. The most prevalent type of primary liver cancer is hepatocellular carcinoma (HCC).

This study was performed to explore the anticancer activity and the molecular mechanisms behind the gastric cancer cells by using a novel phytochemical drug, indole-3carbinol, and the *Angelica keiskei* leaf and root extract against the hepatocellular carcinoma's HepG2 cell line.



1.1. Cancer

Cancer is one of the most prevalent health concerns in the world and significantly negatively influences the quality of life for millions of people of all ages and genders. Cancer, also known as malignant tumors and neoplasms, is the outcome of interactions between a person's genetic makeup and environmental circumstances, which, over time, cause aberrant cell changes into tumors. The frequency of new cancer cases is growing along with the average age of the world's population, which raises the annual death toll from cancer. According to "The Global Cancer Observatory, owned by the World Health Organization/International Agency for Research on Cancer," worldwide cancer data published the most common cancer in 2020 (excluding non-melanoma), estimated at 18.1 million cancer cases worldwide. Of these, 9.3 million cases were in men and 8.8 million in women. More than 19.3 million (19,300,000) new cancer cases were diagnosed and reported recently, leading to approximately 10 million deaths in 2020 based on the reported data (Chhikara, Bhupender S., and Keykavous Parang 2022).

Cancer is a type of tumor that becomes progressively invasive. The ability of cells to grow and divide rapidly irrespective of any growth signal. The growth and division are tightly regulated in different stages by various growth hormones. When the development and division of the cells are triggered in the hyper stage, a cell will never stop dividing throughout time to produce an immortal line of cells called a tumor. When the tumor becomes progressively invasive, it could transfer from one place to another, resulting in cancer metastasis. It can develop when cancer cells from the primary tumor break off and grow in nearby areas such as the lungs, liver, or bones. The majority of

malignancies that have tumors are staged into five major categories. Roman numerals are frequently used when referring to them. Other staging methods exist for different types, including brain cancer, lymphoma, and blood malignancies.

Cancer staging and grading play crucial roles in predicting the clinical behavior of malignancies, determining suitable treatments, and enabling accurate information exchange among clinicians. The universally recognized standards for cancer staging, known as the tumor-node-metastasis (TNM) system, encompass three key factors: (1) the size and local growth of the tumor (T); (2) the degree of lymph node metastases (N); and (3) the presence of distant metastases (M) (Telloni, Stacy M. 2017).

Apoptosis has become a valuable target for developing new anticancer medications since it is thought to be one of the key processes in cancer treatment. Apoptosis can be triggered by a stimulant factor, such as a chemical, or by removing repressor agents. The cell disintegrates into membrane-bound particles that are then eliminated by phagocytosis, a process called "programmed cell death."

1.2. Gastric Cancer

A vital part of the digestive system is the stomach, an organ with a sac-like appearance. The etiology of gastric cancer is complicated and varied and reflects genetic, molecular, and morphological variability. According to the latest statistics, gastric cancer (also known as stomach cancer) is the fifth most often diagnosed malignancy globally and the fourth most common cause of death. In 2020, there were 1.1 million new cases of stomach cancer, which accounted for 1,089,103 (5.6%) of all cancer cases and

7,687,933 (7.7%) of all cancer deaths worldwide. Due to its high prevalence, poor prognosis, cellular and molecular heterogeneity, and other variables, stomach cancer is a serious global health concern (Aaron and El-Serag, 2020). To provide screening for those over 40 years old, the National Cancer Screening Program (NCSP) for stomach cancer was developed in South Korea in 1999. The NCSP advises doing an upper gastrointestinal series (UGIS) or upper endoscopy every two years to screen for stomach cancer in men and women who are 40 years of age or older. Despite several drawbacks, a recent study found that the NCSP successfully lowered gastric cancer mortality (Kim *et al.*, 2020). Gastric carcinoma is classified into cardia and non-cardia as types of stomach cancer. *Helicobacter pylori* is a well-known cause of non-cardia gastric cancer, which develops remarkably from chronic inflammation to dysplasia and carcinoma.

Gastric cancer, on the other hand, primarily affects white, obese people and results in oesophageal adenocarcinoma (Bray *et al.*, 2018). Primary tumors are less common than secondary tumors, produced by primary tumor cells that have been removed and cause death. Lack of oxygen is a common cause of the primary tumor, which brings it under stress, promotes metastasis, and diminishes its probability of recovery (Kelley *et al.*, 2003). Despite recent developments in therapy and diagnostic technologies, doctors and researchers still haven't discovered a reliable way to treat stomach cancer. It is widely acknowledged that some caspases (caspases 8, 9, and 10 in humans) function as an upstream "initiator" of apoptosis by activating a downstream "effector" caspase (caspases 3, 7) (Walsh *et al.*, 2008). The most common forms of stomach cancer are

intestinal and diffuse gastric cancer. Hereditary gastric cancer is caused by inherited high-risk mutations, which have been found only for the diffuse histotype. In contrast, sporadic gastric cancer is associated with environmental and genetic low-risk variables. This phenotypic diversity among diffuse gastric cancer poses a significant challenge to our knowledge of the molecular pathways driving carcinogenesis (Garcia-Pelaez *et al.*, 2021).

1.3. Helicobacter pylori (H. pylori)

The stomach is a typical habitat for the gram-negative, microaerophilic, spiral (helical) bacteria *H. pylori*, formerly known as *Campylobacter pylori*. *H. pylori* are helix-shaped, about three μm long, with a diameter of about $0.5\mu\text{m}$ (Stark *et al.*, 1999). In 1982, doctors Barry Marshall and Robin Warren from Perth, Western Australia, found *H. pylori* in the stomachs of people suffering from gastritis and ulcers. Conventional wisdom at the time held that no bacteria could survive in the acidic conditions of the human gut. The Nobel Prize in Physiology or Medicine for 2005 was given to Marshall and Warren for their groundbreaking discovery (Gilman, 2018). When *H. pylori* pass from the micro aerobic stomach into the anaerobic intestinal system, they morphologically become viable but non-culturable coccoid forms (Hirukawa *et al.*, 2018). It has been claimed that the risk of stomach cancer can be reduced in asymptomatic people living in high-risk locations by eliminating *H. pylori* infection. It is uncertain how much of a benefit eradicating *H. pylori* will have in populations with varying stomach cancer risks and various therapeutic settings (Lee *et al.*, 2016). Most occurrences of gastric adenocarcinoma, especially those outside of the stomach's cardia

(i.e., the esophagus-stomach junction), have been associated with *H. pylori* (Laird-Fick *et al.*, 2016). The treatment for this cancer is quite aggressive, and even localized disease is treated sequentially with chemotherapy and radiation before surgical resection. This is done to maximize the chance of curing the malignancy (Badgwell *et al.*, 2017). Treatment with antibiotic-proton pump inhibitor regimens is not employed for this malignancy since it does not respond to them and does not depend on *H. pylori* infection (Laird-Fick *et al.*, 2016). Pylori's potential to induce cancer through two interconnected pathways is now the subject of investigation. An increased rate of host cell mutation may result from the increased generation of free radicals in the vicinity of *H. pylori*. A "perigenetic pathway" is the term for the alternative process, and it entails modifications to cell proteins, including adhesion proteins, to improve the altered host cell phenotype. It has been hypothesized that *H. pylori* causes inflammation and raises tumor necrosis factor-alpha (TNF- α) levels and interleukin 6 (IL-6) (Tsuji *et al.*, 2003). The likelihood of acquiring stomach cancer may vary depending on the specific strain of *H. pylori* to which a person is exposed. More extensive tissue damage is shown in *H. pylori* strains that generate more of two proteins, vacuolating toxin A (VacA) and the cytotoxin-associated gene A (CagA), than in those that produce less of these proteins or lack these genes altogether (Alfarouk *et al.*, 2019). These proteins powerfully alert the immune system to the fact that an invasion is occurring and are directly harmful to cells lining the stomach. As a defense mechanism against microbial attack, neutrophils and macrophages populate the affected tissue (Kim and Moss 2008).

1.3.1. The virulence and pathogenicity of *H. pylori*

Pathogenesis, or the capacity of this organism to produce disease, is the primary focus for studies into the *H. pylori* genome. The Cag pathogenicity island (PAI) (Pathogenicity island is part of a genome that has evidence of horizontal origins), which is thought to be responsible for the pathogenesis and is present in both of the sequenced strains, is around 40 kilobases in length and comprises more than 40 genes. Asymptomatic *H. pylori* carriers typically harbor strains of the bacteria that lack this pathogenicity island (Baldwin *et al.*, 2007). Gastrin, a hormone produced by G cells in the pyloric antrum in response to an inflammatory reaction, is transported by the blood to parietal cells in the fundus (Blaser *et al.*, 2004). Over time, gastrin increases the number of parietal cells, increasing acid secretion into the stomach lumen and growing more parietal cells with time (Schubert and Peura 2008). The increased acid load harms the duodenum, which can lead to the development of duodenal ulcers. The inflammatory reaction caused by *H. pylori* colonization can lead to atrophy of the stomach lining and, eventually, stomach ulcers. The possibility of developing stomach cancer is also raised (Schreiber *et al.*, 2004). People in the West infected with strains containing the cag PAI are more likely to develop peptic ulcers or stomach cancer than those infected with strains lacking the island (Kusters *et al.*, 2006). *H. pylori* "injects" peptidoglycan, an inflammatory substance, from their cell walls into the stomach epithelial cells upon attachment via the type IV secretion system produced by the cag PAI. Cytoplasmic pattern recognition receptor (immune sensor) Nod1 recognizes the injected peptidoglycan and inflammation by increasing the production of cytokines (Viala *et al.*, 2004). The cag PAI-encoded protein CagA is also injected into stomach

epithelial cells through the type-IV secretion mechanism, which interferes with cytoskeleton organization, cell adhesion, intracellular signaling, and cell polarity (Backert and Selbach 2008). CagA is a membrane-associated protein kinase that, once inside the cell, is phosphorylated on tyrosine residues by a host cell TK. Afterward, CagA stimulates the protein tyrosine phosphatase/protooncogene Shp2 in an allosteric manner (Hatakeyama, 2004). Epidermal growth factor receptor (EGFR), a membrane protein containing a TK domain, is activated by pathogenic *H. pylori*. The epithelial growth factor receptor (EGFR) activation by *Helicobacter pylori* is linked to changes in signal transduction and gene expression in the host epithelial cells, which may play a role in pathogenesis. It has also been proposed that the C-terminal region of the CagA protein (amino acids 873-1002) can affect host cell gene transcription in a manner distinct from protein tyrosine phosphorylation (Baldwin *et al.*, 2007). Individual outcomes can be predicted based on the specific *H. pylori* strain that infects a patient.

1.3.2. Metabolic Modification by *H. pylori*

H. pylori virulence factors cause the recruitment of immunologically active cells, which then secrete cytokines, tumor necrosis factor (TNF), and interferons (IFNs), all of which can function independently of *H. pylori*'s natural environment (Buzás, 2014). *H. pylori* utilizes its flagella to burrow through the mucus lining of the stomach to reach the epithelial cells beneath, which are located in an area of the stomach that is less acidic. This allows the bacteria to escape the more acidic environment of the lumen, which is the inside of the stomach (Amieva *et al.*, 2008). *H. pylori* may detect a less acidic location in the mucus and migrate there (a process known as chemotaxis).

Because mucus is continually being produced at the epithelium and broken down at the lumen interface, this prevents the bacteria from being whisked away into the lumen by the mucus (Schreiber *et al.*, 2004). The spatial orientation of *H. pylori* in the gastric mucus. *H. pylori* survives in mucus, on the epithelium's inner surface, and, rarely, within the epithelial cells themselves (Petersen and Krogfelt 2003). The adhesion it secretes attaches to lipids and carbohydrates on the surface of the epithelial cells, allowing it to cling to them. BabA is an adhesin that recognizes and binds to the Lewis B antigen expressed by stomach epithelial cells. *H. pylori* adhesin binding fucosylated histo-blood group antigens revealed by retagging (Ilver *et al.*, 1998). The BabA-mediated adhesion of *H. pylori* can be blocked entirely by lowering the pH of the stomach. It is hypothesized that BabA's acid responsiveness facilitates adhesion and allows for an efficient escape from an adverse environment at pH damaging to the organism (Bugaytsova *et al.*, 2017). SabA is another adhesin that binds to sLeX antigen, which is highly expressed on stomach mucosa. Multiple ways allow *H.pylori* to cause damage to the stomach and duodenal linings. *H. pylori* biochemicals, including the ammonia generated to control pH, certain phospholipases, and vacuolating cytotoxin A (VacA) (which damages epithelial cells, destroys tight junctions, and induces apoptosis), are all hazardous to epithelial cells (Smoot, 1997). CagA, a gene related to cytokines, has been linked to inflammation and may even be carcinogenic (Hatakeyama and Higashi 2005). The association between *H. pylori* infection and metabolic changes is inconsistent and subject to controversy in epidemiological studies. Growth delay has primarily been observed in low-income regions with a high prevalence of infection, where additional nutritional and social factors may also play a role. Timely eradication

of the infection is crucial for promoting the young population's healthy development and preventing peptic ulcers and gastric cancer.

1.4. Treatment of gastric cancer

Several variables have been linked to the development of stomach cancer, and it is most likely that the etiology of the disease is complex. Even though they play a substantial role, genetic anomalies (such as DNA aneuploidy, oncogene amplification or mutation, and allelic loss of tumor suppressor genes) are not known well enough to permit the creation of a sequence of progression that leads to the formation of gastric cancer (Layke and Lopez 2004). For stomach cancer, a variety of therapies are available. The treatment strategy, which could involve many treatments, will be decided upon in collaboration with the cancer care team. The cancer's stage, general health, and preferences are just a few variables that will be considered. A treatment plan will outline the malignancy, the intended therapy outcomes, the feasible treatment options, any potential adverse effects, and the anticipated treatment time.

1.4.1. Surgery

Stomach cancer surgery mainly entails gastrectomy or the removal of all or part of the stomach. Stomach cancer is often treated with surgery. Surgical procedures are tailored to the specifics of each cancer case.

In addition to surgery, the following therapies may be administered:

Preoperative therapy, or neoadjuvant therapy, is treatment administered before surgery.

The tumor can be shrunk, and the quantity of healthy tissue removed after surgery by

administering chemotherapy beforehand. Researchers are exploring chemoradiation to reduce the cancer's size before surgery.

Adjuvant therapy is treatment administered after surgery to reduce the likelihood of cancer returning. Once the visible cancer has been removed, some patients may have chemotherapy, radiation treatment, or both to eradicate any remaining cancer cells (Orditura *et al.*, 2014). Although surgical excision is the primary curative therapy for stomach cancer, these tumors are frequently detected at an advanced stage, which is when it is no longer advised that surgery be performed. The effectiveness of other therapies, such as radiation and chemotherapy, is only slightly above average (Marin *et al.*, 2016).

1.4.2. Chemotherapy

Unfortunately, there is currently no cure for advanced stomach cancer. Palliative chemotherapy has increased survival without negatively impacting patients' quality of life. In the fight against metastatic illness, a wide variety of single drugs and drug combinations have been validated as effective. Adjuvant and neoadjuvant chemotherapy and radiotherapy are considered when treating patients with locally advanced illnesses. Adjuvant chemotherapy is not routinely used since most trials showing a survival benefit have failed to replicate these results. Korea and Japan have made significant contributions to the development of adjuvant immunochemotherapy. Immunotherapy has been demonstrated by a meta-analysis of phase III studies using OK-432 to increase survival in patients with curatively resected stomach cancer. Even though neoadjuvant chemotherapy and chemoradiation are still in the experimental

stages, they have shown encouraging outcomes in numerous phase II- III trials (Sastre *et al.*, 2006).

To combat stomach cancer, A phase II-III study conducted in Germany, comparing eight cycles of peri-operative 5-FU–leucovorin–oxaliplatin–docetaxel (FLOT) to six cycles of ECF/epirubicin–cisplatin–capecitabine (ECX), revealed a noteworthy enhancement in the primary endpoint of overall survival (OS). The median OS was 50 months with FLOT compared to 35 months with ECF/ECX (HR 0.77; 95% CI 0.63-0.94; P = 0.012), and no significant concerns regarding toxicity were reported. Based on these findings, the peri-operative application of FLOT (four cycles pre- and four cycles post-operative) is now considered the standard of care for patients capable of tolerating a triple cytotoxic drug regimen. For patients unable to undergo triplet chemotherapy, a combination of a fluoropyrimidine with cisplatin or oxaliplatin is recommended (Lordick *et al.*, 2022).

1.4.3. Radiation therapy

High-powered X-rays or other forms of radiation are used in radiation treatment to destroy cancer cells or stop their growth. Radiation treatment delivered from outside the body is one option for treating stomach cancer. External beam radiation treatment involves directing radiation from a machine outside the body to the affected region. Postoperative radiation therapy has been shown to improve locoregional control, as was demonstrated in early investigations. Patient compliance with postoperative radiation is often subpar because of the difficulties inherent in its administration. Therefore, preoperative radiation is being assessed for its potential usefulness. Most patients

receiving radiation treatment in a palliative care context report improving their symptoms. Radiation and chemotherapy (chemo) are sometimes used together before surgery to try to reduce the size of a tumor so that it may be more easily removed from a patient. Chemoradiation is the term for this hybrid treatment method (Minsky, 1996).

1.4.4. Targeted therapy

Gastric cancer patients now have specific therapeutic choices because of novel molecular pathways. Trastuzumab, an HER-2 antibody, improves survival in advanced gastric cancer patients with gene amplification and HER-2 overexpression. It is also being studied in adjuvant and neoadjuvant settings. Ramucirumab, a VEGFR-2 antibody, performed well in clinical studies. EGFR (cetuximab), VEGF-A (bevacizumab), and mTOR (everolimus) inhibitors did not improve survival. Biomarker-selected cohorts are testing c-MET/HGF-targeting drugs with encouraging outcomes (Smyth and Cunningham 2012).

1.4.5. Immunotherapy

After surgery, chemotherapy, radiation, and targeted therapy, immunotherapy has emerged as an effective therapeutic strategy for cancer. Immunotherapies are anticipated to be brought to the forefront through combination treatments with other modalities, such as targeted therapies. Advanced unresectable or recurrent gastric cancer (AGC) is typically treated with combination regimens consisting of a fluoropyrimidine and a platinum agent (plus trastuzumab as an anti-HER2 monoclonal antibody for HER2-positive cases) in the first-line setting, and paclitaxel with or without ramucirumab in the second-line setting (Takei *et al.*, 2022).

1.5. Hepatocellular Carcinoma (HCC)

The most common cancer that results in death worldwide is liver cancer. Due to liver cancer's dismal prognosis, patients frequently receive advanced-stage diagnoses. More than 90% of instances of liver cancer are HCC, for which chemotherapy and immunotherapy are the most effective forms of treatment (Anwanwan *et al.*, 2020). The primary justification for screening and follow-up is cirrhosis, the most significant risk factor for this malignancy. Instead of strictly needing to take a tissue sample, diagnosing HCC may frequently and uniquely be done using distinctive cross-sectional imaging based on multiphase contrast. HCC is one of the leading causes of cancer-related mortality worldwide, despite improvements in medicinal, locoregional, and surgical therapy (Hartke *et al.*, 2017). HCC manifests as a symptomatic condition that decompensates the underlying cirrhosis in some hepatitis C virus infected (HCV-infected) or alcoholic individuals. However, the percentage of cases attributable to HCV infection has only slightly increased with the rise in HCC incidence (Llovet and Beaugrand 2003). Avoiding exposure to the risk factors may lower the prevalence of HCC. Most hepatitis B virus-related (HBV) HCCs dramatically decreased when HBV immunization programs were implemented (Chang *et al.*, 2016). Additionally, the treatment of antiviral medications that prevented persistent HBV and HCV infections slowed the disease's course. It likely prevented the formation of HCC (Papatheodoridis *et al.*, 2015).

1.6. Cellular malignancy-related markers

DNA ploidy: Regarding the predictive importance of DNA ploidy in HCC patients, controversy still rages. Numerous studies suggest that DNA ploidy may serve as a marker for the prognosis of HCC (Mise *et al.*, 1998). Patients with aneuploid cells have a considerably worse overall survival rate than those with diploid cells, and those with numerous G0/G1 peaks are at the most significant risk. Early recurrence rates are more excellent in patients with higher cell proportions in the proliferative phases (Nolte *et al.*, 1998).

1.7. HCC Sequential Development

The formation of HCC is a complicated, multi-step process that results from a combination of genetic and environmental factors, similar to the development of other neoplasia. Identical to other neoplasia, the formation of HCC is a complicated, multi-step process. According to estimates, HBV and the hepatitis C virus (HCV) are responsible for 32% and 19% of infection-related cancer cases, primarily liver cancer, in less developed nations. Environmental and genetic factors contribute to this (Torre *et al.*, 2015).

1.7.1. Tumor necrosis factor-alpha and interleukin-6 (TNF- α and IL-6)

Chronic hepatic damage causes the release of IL-6 and TNF- α , which stimulates the STAT3 transcription factor's downstream targets and promotes neoplastic development in the liver microenvironment (Villanueva and Luedde 2016). TNF- α also encourages

the development of liver tumors and HCC recurrence. According to a recent study by Jing *et al.*, TNF-overexpression increases the risk of HCC by activating hepatic progenitor cells (HPCs). At the same time, TNF-knockdown decreases HPC activation and proliferation, lowering tumor incidence. This demonstrated the critical impact TNF- α plays on liver damage and prognosis (Alqahtani *et al.*, 2019).

1.7.2. Nuclear Factor- $\kappa\beta$ (NF- $\kappa\beta$)

A critical transcriptional regulator of the inflammatory response and cell death is the nuclear factor (NF- $\kappa\beta$) (Luedde and Schwabe 2011). Numerous studies have supported the involvement of NF- in developing liver fibrosis, HCC, and hepatocellular damage. Regardless of the origin, activated NF- $\kappa\beta$ is a frequent and early occurrence in HCC and is associated with developing a transformed phenotype during hepatocarcinogenesis. As a result, it is suggested that NF- $\kappa\beta$ is a crucial factor connecting hepatic damage, fibrosis, and HCC (Ramakrishna *et al.*,).

1.7.3. Transforming growth factor alpha (TGF α)

TGF-a polypeptide that encourages cell division and transformation is hypothesized to have a solid connection to the development of hepatocarcinogenesis. TGF- α is not highly expressed in healthy liver cells. Following hepatic damage, several cytokines released in the chronic inflammatory response consistently increase TGF- α in the liver (Thorgeirsson and Grisham 2002). And, subsequently permit hepatocyte regeneration, proliferation, dysplasia, and, ultimately, HCC formation (Zhang *et al.*, 2004). TGF- β is

also overexpressed in HCC and is essential for the disease's development by promoting tumor cell invasion and migration (Soukupova *et al.*, 2017).

1.8. Hepatocellular Carcinoma's (HCCs) Molecular Targeted Therapies

In the past two decades, there has been significant progress in molecular cell biology, leading to a deeper understanding of the complex molecular pathways that underlie the initiation and progression of tumors. The opportunity to create innovative molecular-targeted drugs that inhibit molecular aberrations as prospective cancer therapy treatments were consequently designed.

1.8.1. Anti-Angiogenic Agents

All the approved systemic therapies for HCC are molecular targeted therapies exhibiting anti-angiogenic effects by targeting the vascular endothelial growth factor signaling pathway. Sorafenib and lenvatinib stand as the primary treatments in the first line, while regorafenib, ramucirumab, and cabozantinib are considered as secondary treatment options. Despite the promising anti-tumor effects demonstrated by anti-PD-1 antibodies, including nivolumab and pembrolizumab, as monotherapy for advanced HCC in phase II clinical trials, both treatments faced setbacks in phase III studies. Consequently, anti-angiogenic treatment continues to serve as the fundamental component of systemic therapy for HCC (Zhu *et al.*, 2020).

1.8.2. Immunotherapy in the Treatment of HCC

The escape from immune monitoring characterizes tumor development. The development of immunotherapy for HCC is justified thanks to the finding of immune checkpoint molecules. This medication is used to treat a variety of carcinomas with varying degrees of effectiveness.

For individuals with advanced HCC, the United States Food and Drug Administration (US-FDA) has granted approval for several systemic therapies. In the first-line setting, the approved therapies include the combination of atezolizumab–bevacizumab, sorafenib, and lenvatinib. Additionally, cabozantinib, regorafenib, ramucirumab (specifically for patients with alpha-fetoprotein [AFP] > 400 ng/mL), pembrolizumab, nivolumab, and the combination of nivolumab-ipilimumab are reserved for patients who have experienced progression on sorafenib.

On the other hand, the European Medical Agency (EMA) has approved atezolizumab–bevacizumab, sorafenib, and lenvatinib for first-line use. In the scenario where patients have progressed on first-line therapy, cabozantinib, regorafenib, and ramucirumab (for patients with alpha-fetoprotein [AFP] > 400 ng/mL) are approved for subsequent treatment according to EMA guidelines (Tella *et al.*, 2022).

1.9. Treatment Challenges for HCC Patients

The frequency of HCC, an aggressive cancer, is growing worldwide. Treating individuals with HCC is complex, mainly because it is crucial to consider both the liver

condition and tumor stage simultaneously. Patients with advanced HCC exhibit various clinical symptoms and radiographic characteristics (Colagrande *et al.*, 2016). The treatment choices are based on the patient's factors, liver function, and clinical stage. Immunotherapy and cytotoxic chemotherapy had very modest effects on HCC. Few clinical studies investigating the effectiveness of hormone therapy in HCC patients were carried out in the last 20 years. One of the more extensive studies employed the anti-estrogen tamoxifen as a systemic therapy but found no survival benefit. Anti-androgen medication produced unfavorable outcomes as well. Hormone treatment is not currently considered a part of managing HCC since insufficient data supports the idea that it is a hormone-responsive tumor (Maio *et al.*, 2008). Recently, molecular-targeted therapies for treating advanced HCC have exhibited promising outcomes (Chen and Wang 2015). Sorafenib's acceptance as a first-line systemic therapy for HCC was a significant advance in treating the disease. In the ensuing decade, several trials examining a variety of medications as a second-line therapy for HCC were carried out, most of which produced unfavorable findings. However, there has been a noticeable development in HCC therapy choices with positive outcomes recently.

1.10. Indole-3-carbinol

Indole-3-carbinol, or C₉H₉NO, is a naturally occurring plant-derived phytochemical formed by the glucosinolate breakdown known as glucobrassicin. This glucosinolate is found in cruciferous vegetables, which are members of the Brassicaceae family.

Myrosinase catalyzes the hydrolysis of glucosinolates in intact plant cells (Zhao *et al.*, 2015). Glucosinolates are sulfur-rich compounds activated by a specific class of -thioglucosidases that participate in various metabolic processes, each associated with a unique set of biological activities (Kliebenstein *et al.*, 2005). By chewing or chopping plant material, glucosinolate is released; as a result, myrosinase comes into touch with glucosinolate and catalyzes its hydrolysis (Verhoeven *et al.*, 1997). Glucosinolate and myrosinase are physically segregated in several compartments inside plant cells. In addition, various breakdown products, such as isothiocyanate, thiocyanate, and nitrile, might result from the hydrolysis of glucosinolates (Halkier and Gershenzon 2006). An endogenous thioglucosidase catalyzes enzymatic hydrolysis, myrosinase, found inside the vacuoles of cells in the plant's matrix. Hydrolysis initially produces an unstable aglycone intermediate, thiohydroxamate-O-sulfate, which is then continuously converted into different classes of breakdown products. Additional features, including intrinsic and extrinsic factors, determine glucosinolate hydrolysis. Intrinsic factors include ferrous ions and the presence of myrosinase and ascorbic acid, a cofactor of the enzyme. Outside factors include temperature and pH, which are known to affect the hydrolysis of glucosinolates (Rungapamestry *et al.*, 2006). Along with glucobrassicin, another significant glucosinolate known as sinigrin is degraded by myrosinase into an organosulfur compound called allyl isothiocyanate (AITC), which is mediated by an epithioapecifier protein (ESP). This hydrolysis product's potential as an anticancer or biopesticide agent is only one of the many biological uses suggested for it (Halkier and Gershenzon 2006). I3C modifies gene expression, which limits cell growth, causing cell cycle arrest in several malignancies.

Several hormone-dependent cancers, including prostate cancer, are prevented by them simultaneously, and they are crucial in this regard. Bax was upregulated, while NF- κ B was downregulated in PC-3 cells, indicating apoptosis (Chinni *et al.*, 2001). These changes were also seen with the poly (ADP-ribose) polymerase (PARP) cleavage. I3C and its derivatives have substantial safety and efficacy in biomedical sectors. However, plants are regarded as a critical source of effective medicines for treating many diseases; many chemotherapeutic agents are available to treat stomach cancer.

However, they have some substantial adverse effects or only moderately effective dosages about the patient's profile. Phytochemicals present in food, including the glucosinolate glucobrassicin and its many metabolites, have been linked to several biological processes, including the ability to fight cancer, bacteria, viruses, and oxidative stress. I3C plays a critical role in tumor cell resistance to angiogenesis, proliferation, and apoptosis in a dose- and time-dependent manner. I3C has shown antimutagenic activity against genotoxic damage brought on by benzo(a)pyrene and cyclophosphamide in mouse bone marrow cells (Shukla *et al.*, 2003). In this research, we shall outline the state of the art on I3C's potential advantages and uses in human health.

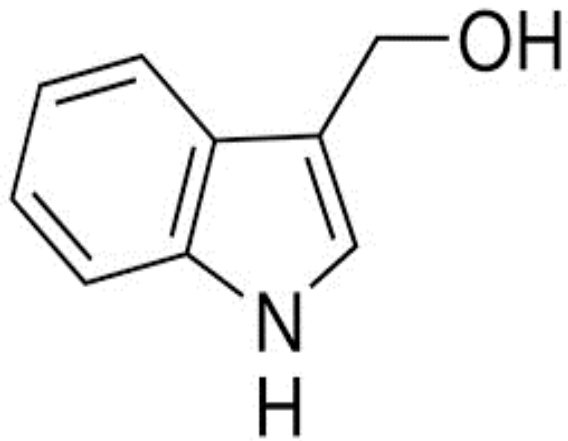
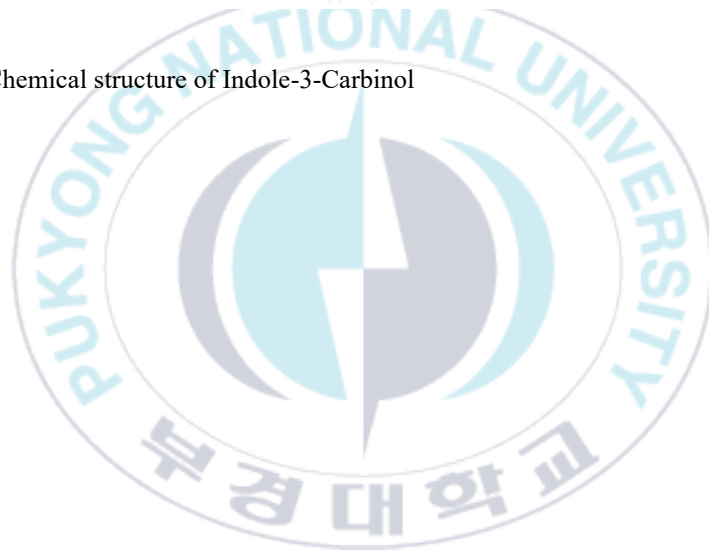


Figure 1.1. Chemical structure of Indole-3-Carbinol



1.11. *Angelica keiskei*

The Umbelliferae species of *Angelica keiskei* (Miq.) Koidz is a perennial herb, 50–120 cm tall, recognized in Japan and named Asitabha; it's a kind of nutrient-rich flowering shrub that looks like a carrot and produces flowers. It is pretty thorough and offers a variety of minerals and amino acids, which have a variety of advantageous properties in biological domains to guard against many severe illnesses and disorders. The herb *A. keiskei* is mostly a Pacific Coast Japanese plant with various culinary applications (Du *et al.*, 2019). The plant is referred to as "Shin-Sun Cho" in Korea (Kweon *et al.*, 2019). The plant components of *Angelica keiskei* (Miq.) Koidz. They were frequently utilized in culinary preparation, both as a juice and for deep frying (Imai and Imai 2008). The perennial plant *Angelica keiskei* (*A. keiskei*) belongs to the Umbelliferae family and is cold-hardy. It is indigenous to the large Japanese Pacific islands of Hachijo and Izu. It has grown to this point in the Chinese provinces of Shandong, Yunnan, Guangxi, Jiangsu, and Hainan, among others. 2019, the National Health Commission formally acknowledged it as a new food component (Fu *et al.*, 2023). Many active compounds like chalcone and coumarins, including two major chalcone compounds known for promoting antitumor activity, xanthoangelol and 4-hydroxyderricin, are present in *A. keiskei*, and its crude extracts and components have been shown to have multiple biological activities to improve human health for various diseases, including cancer (Okuyama *et al.*, 1991). Chalcone, coumarin, and phytochemicals are the bioactive substances found in *Angelica keiskei*, which provide pharmacological properties, including lipid-lowering action, anticancer activity, liver

protection, and nerve protection (Tu *et al.*, 2022). The inhabitants of Hachijo-jima, a village famous for longevity in Japan, believe that Ashitaba has improved their health. The chalcones of Ashitaba, such as 4-hydroxyderricin (4-HD), isobavachalcone, xanthokeismin A, and xanthoangelol B, E, D, and F, have been shown to exhibit a variety of pharmacological properties, including potential for anti-oxidative and anti-inflammatory effects. Due to their pharmacological potential and high quantities in this edible herb, two chalcones, particularly 4-HD and xanthoangelol, have drawn interest in developing herbal supplements or medications (Kweon *et al.*, 2019). The prevention of liver disorders, type 2 diabetes, obesity, and atherosclerosis is attributed to five components of AK, including 4-HD, according to recent metabolomic and lipidemic investigations of human plasma (Oh *et al.*, 2019). High economic value may be found in the vegetable and herb *Angelica keiskei*. *A. keiskei* has faced threats in recent years from an unparalleled anthropogenic disruption of its natural habitat and increased market demand (Zhang *et al.*, 2019). *A. keiskei* has been discovered to have antitumor effects on several cancer cell lines by engaging in multiple signaling pathways. The extract-induced apoptosis occurs in some human cancer cell lines, including breast cancer cells (MDA-MB-231) (Jeong and Kang 2011).



Figure 1.2. *Angelica keiskei* plant

1.12 Aims of the present study

This research aims to evaluate the anticancer potential of phytochemicals I3C and natural compounds from *Angelica keiskei*, focusing on their effectiveness against gastric and hepatocellular carcinoma cells. Utilizing advanced analytical methods, the study seeks to develop safer, more efficient cancer treatments.

The chapter 2 investigates the anticancer properties of Indole-3-carbinol (I3C) in human adeno gastro carcinoma (AGS) cells, focusing on its effects on cell viability, apoptosis, and molecular pathways. It highlights the potential of I3C as a novel prodrug in cancer treatment, emphasizing its anti-tumor activity and low toxicity.

The chapter 3 investigates the anticancer potential of Angelica AKLE in PTT, focusing on its efficacy in targeted drug delivery and controlled release under NIR irradiation. It highlights AKLE's effectiveness in cancer treatment along with its potential in combating methicillin-resistant bacterial infections.

The chapter 4 focuses on examining the anti-cancer effects of *Angelica keiskei* on hepatocellular carcinoma (HCC) using HepG2 cells. The study aims to understand the multiple apoptotic pathway involved in the cell death that may significantly contribute to the anti-cancer activity against HepG2 cells by using specific apoptotic proteins and utilizes techniques like antibody apoptotic array.

Chapter 2. Indole-3-Carbinol Regulates Apoptosis in AGS Cancer Cells via the BCL-Family Genes

2.1. Abstract

Indole-3-carbinol, a product of cruciferous vegetables, has been thoroughly investigated for its wide range of biological effects, both in vitro and in vivo. However, neither the anticancer activity nor the molecular mechanisms of I3C have been investigated in human adeno gastro carcinoma (AGS) cells. In the present investigation of AGS cells, cell viability assays were used to confirm cell death, nuclear condensation was detected by 4',6-diamidino-2-phenylindole (DAPI) labeling, and DNA fragmentation assays were used to detect degraded DNA at the IC₅₀ level. Apoptosis was assessed using the qPCR was done by performing the relative quantification method. The fold changes between the upregulated apoptotic proteins, Caspase-3, Cyt-c, p53, Apaf1, Caspase-9, Bak, and Bax, and the downregulated anti-apoptotic gene BCL-2 were compared with reference gene β -actin was analyzed using RT-qPCR. Cell proliferation and differentiation were significantly reduced when I3C was treated with the AGS cells in a dose-dependent manner. I3C inhibits AGS cells from proliferating and initiates apoptosis by releasing cytochrome-c from mitochondria in the intrinsic pathway. The WST-1 assay result demonstrated that I3C treatment of AGS cells had significantly decreased the cells' viability. According to molecular docking analysis, I3C had a significant affinity for the apoptotic protein p53 (3DCY). The findings

demonstrate that the caspase protein family is a critical component of the apoptotic mechanism. In context with the rapid development of tumors and oncogenesis, I3C and its metabolites target a range of cell-cycle regulatory elements through different signaling pathways. The wide range of anti-tumor activity and minimal toxicity of I3C and its metabolites in cancer emphasize its translational potential. Additionally, the novel prodrug I3C, whose fundamental actions are similar, may inspire new methods for reducing oncogenesis. The novel prodrug I3C has identical underlying processes and could encourage new approaches to minimize oncogenesis.

2.2. Introduction

According to the most recent data, gastric cancer (also known as stomach cancer) is the fifth most frequently diagnosed malignancy worldwide and the fourth most common cause of death. Gastric cancer accounted for 1.1 million new cases in 2020, 1,089,103 (5.6%) of all cancer cases, and 7,687,933 (7.7%) cancer deaths worldwide. Due to its high prevalence, poor prognosis, and cellular and molecular heterogeneity, among other considerations, stomach cancer is a serious global health concern (Hamashima 2020). To provide screening for those over 40, the National Cancer Screening Program (NCSP) for stomach cancer was developed in South Korea in 1999. The NCSP advises doing an upper gastrointestinal series (UGIS) or upper endoscopy every two years to screen for stomach cancer in men and women who are 40 years of age or older. A recent study discovered that despite several disadvantages, the NCSP successfully lowered stomach cancer mortality (Kim *et al.*, 2020). Gastric cancers classified as cardia and non-cardia are two types of stomach cancer. *Helicobacter pylori* is a well-known cause

of non-cardia gastric cancer, which develops in a remarkable series from chronic inflammation to dysplasia and carcinoma.

In contrast, cardia gastric cancer mainly affects white, obese people and results in oesophageal adenocarcinoma (Bray *et al.*, 2018). Unlike primary tumors, secondary tumors produced by primary tumor cells typically cause most patient deaths. Most often, the primary cancer is influenced by a lack of oxygen, which stresses and lounges the process of metastasis and reduces the likelihood of recovery. Adenocarcinoma, which begins in the gland cells that coat the inner surface of internal organs, is the most frequent type of malignant stomach tumor (Kelley and Duggan, 2003).

Indole-3-carbinol (I3C; C₉H₉NO) is a naturally occurring phytochemical produced by plants that is formed by the breakdown of the glucosinolate glucobrassicin found in cruciferous vegetables belonging to the Brassicaceae family (Zhao *et al.*, 2015). A specific type of β -thioglucosidases activates the sulfur-rich compound known as Glucosinolates, which is utilized for attracting a variety of metabolic functions in numerous aspects of biological activities (Kliebenstein *et al.*, 2005). Cruciferous vegetables provide a wealth of nutrients, including lutein and beta-carotene, as well as other necessary vitamins, minerals, and fibers. Apart from that, another significant substance in glucosinolate known as sinigrin is allyl isothiocyanate (AITC), which is hydrolyzed by myrosinase to other organosulfur, through an epithiospecifier protein (ESP). This substance improves the validation of anticancer effects and is currently being evaluated as a chemopreventive agent against spontaneous and chemically induced cancer development (Halkier and Gershenzon 2006). I3C alters gene

expression, which in turn prevents cell growth to cause cell cycle arrest in certain malignancies.

Additionally, they are essential in avoiding some hormone-dependent cancers, including prostate cancer. Bax up-regulation and NF- κ B down-regulation were seen in PC-3 cells with poly (ADP-ribose) polymerase (PARP) breakage, implying apoptosis (Chinni *et al.*, 2001). Many chemotherapy drugs are available for managing stomach cancer, even though plants are regarded as a critical source of effective pharmaceuticals for healing many diseases and because I3C and its derivatives have substantial safety and efficacy in biomedical disciplines. However, depending on the patient's profile, they might have significant adverse effects or minor effectiveness ranges. Phytochemicals found in food, including the glucosinolate glucobrassicin and its many metabolites, have been linked to several biological processes, including the ability to fight cancer, bacteria, viruses, and oxidative stress. I3C plays an essential role in tumor cell resistance to angiogenesis, proliferation, and apoptosis in a dose- and time-dependent manner. According to the study, I3C's anti-angiogenesis activity inhibits the process of vasculature by splitting the blood vessels (Kunimasa *et al.*, 2010). The intrinsic pathway, which results in cell death, is regulated by the caspase group of a protein family. There are two distinct forms of caspase-3: active (procaspase) and inactive (cleaved). The caspase is no longer active once created and turns to procaspase. It is known as a caspase once it is activated. Caspase-3 can be triggered by caspase-8 and caspase-9, which causes cell death. Caspase-3 controls cell death. When cytochrome-c is released, the mitochondrial mechanism of apoptosis oligomerizes, and

here is where apoptotic protease activating factor-1 (Apaf-1) plays a crucial part. Apaf-1 oligomerization, however, is not well understood (Shakeri *et al.*, 2017). According to some research, Apaf-1 is a caspase-9 inhibitor that can reduce caspase-9's activity, preventing caspase-3 from activating. To avoid this outcome, cytochrome-c will start the procaspase into caspase-3 when it is attached to caspase-9 and releases itself from Apaf-1. By using particular molecular pathways, it will result in cell death. I3C causes cells to cease migrating through the first stage of the cell cycle. Concentrating on some aspects of the cell cycle reduces the expression of the cyclin-dependent kinase 6 (CDK-6) in a time- and dose-dependent manner (Cover *et al.*, 1998). Cell cycle modulatory proteins called cyclins control CDK activity. The G1-S and G2-M transitions, triggered by cyclin complexes' activity, are regulated by cyclin-dependent kinases linked to the core cell cycle machinery (Cram *et al.*, 2001). By downregulating and inhibiting CDK6 expression by disrupting the promotor-specific factor (Sp1- is involved in cellular functions including cell growth, differentiation, and apoptosis) at a composite DNA site in the CDK6 promoter, I3C induces G1 cell cycle arrest by its tetrameric derivatives in all estrogen-dependent cancer cells such as prostate cancer and breast cancer cells. To ascertain the anticancer effects of I3C in human adeno gastro carcinoma and the underlying molecular mechanisms that underlie apoptosis, the following techniques were used: cell viability, DAPI, DNA fragmentation, docking, and qPCR. We specifically looked at the molecular processes underlying the induction of apoptosis.

2.3. Materials and methods

2.3.1. Reagents

Indole-3-Carbinol (I3C) was bought from Sigma-Aldrich, Co., and The HaCaT cell line was purchased from AddexBio (San Diego, CA, USA), while the HEK-293 and AGS cell lines were obtained from ATCC (Manassas, VA, USA).

2.3.2. Cell culture

Dimethyl sulfoxide (DMSO; Sigma, St. Louis, MO, USA) was used to dilute I3C. Under standard atmospheric conditions, the cells were cultivated in a separate medium at 37 °C, 5% CO₂, and 95% humidity. For AGS cells, Roswell Park Memorial Institute medium 1640 (RPMI 1640, GIBCO, Grand Island, New York, USA) supplemented with 10% heat-inactivated fetal bovine serum (FBS; Gibco, Grand Island, NY, USA), 100 U/ml penicillin and 10 µgml⁻¹ streptomycins (Hyclone, Logan, UT, USA) was used. MEM (Minimum Essential Medium) was utilized for HEK, and DMEM (Dulbecco's Modified Eagle's Medium) for HaCat. To investigate I3C's anticancer activity and proceed to the following experiments, HEK, HaCaT, and AGS cell lines were cultured at 85% confluency until passage three (Lee et al., 2019).

2.3.3. Cell viability assay

After passage 3, AGS cells were seeded in 96-well plates by triplicates and grown in RPMI media at 85% confluency. Then, the dish was incubated for 24 h in the incubator at 37° temperatures. After 24h, old media were removed, and cells were treated in a dose-dependent manner with different concentrations of 100 µM, 200 µM, 300 µM,

400 μ M, 500 μ M of I3C and further incubated for 24h. After that, following the manufacturer's protocol, it was then replaced with a new RPMI medium and treated with 10 μ l of EZ-Cytox (WST-1; Daeil Lab Service, Seoul, Republic of Korea) solution. WST solution was added to each well, including the control well, which had no I3C dosages, and WST-1-treated 96 well-microplates were incubated at 37 °C for 2 hours. The plates were shaken for 5 seconds at medium speed on a microplate reader. A microplate reading was taken on ELISA at 460 nm optical density, and the data acquired were utilized to quantify viable cells and display the viability of the treated cells graphically.

2.3.4. DAPI staining (4',6-diamidino-2-phenylindole staining)

The easy-to-use fluorescent dye DAPI was employed to corroborate the subsequent analyses and to visualize the changes in nuclear components in I3C-treated and non-treated cells. Cells were cultivated till passage three and seeded in the disc; after 24 hours, cells were treated with the required concentration of I3C and incubated for another 24 hours. Following treatment, the old medium was removed and washed twice with 1XPBS (135 mM sodium chloride, 2.7 mM potassium chloride, 4.3 mM sodium phosphate, and 1.4 mM potassium dihydrogen phosphate) and one μ g/mL DAPI solution (Roche Applied Science, IN, USA) was used to stain and incubated for 20 min in the dark. The DAPI solution was removed from the plates after 20 minutes and rinsed three times with 1XPBS. Remove the coverslip from the disc, place it on the mounting slide, and examine the image with a confocal microscope (ZEISS, LSM 980 airyscan) with a Prolonged Gold Antifade solution (Ferro *et al.*, 2017).

2.3.5. DNA fragmentation

The cells were grown till passage three before being seeded in the culture disk for 24 hours. The cells were subsequently treated with different concentrations of I3C (100 μ M, 200 μ M, 300 μ M, 400 μ M, 500 μ M) and incubated for another 24 hours with the I3C dosages. The next day, cells were washed with 1.5ml 1XPBS, and again, 1ml cold PBS was added to remove and detach the cells. The cells were then rinsed with 1.5 mL of 1X PBS before being detached with 1 mL of cold PBS the next day. Cells were collected in a 1.5mL Eppendorf tube and centrifuged at a cold temperature for 5 minutes at 300XG. Cells were resuspended in 1X PBS with proteinase K and RNase A and incubated at room temperature for 2 minutes. Then, according to the manufacturer's procedure, genomic DNA was extracted using "The AccuPrep Genomic DNA Extraction Kit" (Bioneer Corporation, Republic of Korea). Thermo Fisher Scientific, iBrightCL1000, was used for imaging. Gel electrophoresis was performed using 1.5% agarose gel using a 1X loading buffer with a DNA marker, and bands were observed using Chemiblot USA to access the DNA fragmentation adhering to gel electrophoresis.

2.3.6. RNA extraction and cDNA synthesis

AGS cells (1×10^5) were seeded in culture plates for 24 hours and then treated with I3C at various doses. The RNA from I3C-treated AGS cells was extracted using a QUIGEN RNeasy kit (Hilden, Germany). Cell culture plates were rinsed with 1 mL cold phosphate buffer saline (PBS), dislodged with a cell scraper, collected in a 1.5mL Eppendorf tube, and centrifuged at 8000 rpm for 10 minutes at 4°C. The cell was homogenized, and the RNA was extracted further; concentration and purity were

measured on nanodrop technology to achieve a mean RNA concentration using nanodrop 2000/2000C software, and extracted RNA was used to perform RT-PCR according to the manufacturer's protocol by dividing the RNA concentration by 1000, and cDNA was synthesized. (using the 2X, with oligo dT; GeNet Bio, Global Gene Network, Daejeon, Korea) and amplified by PCR by setting the different conditions for 60 min at 50 °C and 10 min at 70 °C for each cycle and amplified by PCR under other conditions, including 60 minutes at 50 °C and a subsequent 10 minutes at 70 °C for each cycle.

2.3.7. Real-Time quantitative PCR

After using RT-PCR, the generated cDNA was utilized for RT-qPCR. The thermal cycling parameters were followed for the activation procedure. This included a 5 s denaturation step at 95 °C and a 20 s combined annealing/extension stage at 60 °C for 30 s at 95 °C in 45 cycles. The formula $2^{-\Delta\Delta C_t}$ for relative gene expression was used to examine the specificity of the gene expression (Babavlian *et al.*, 2016). Using specific primers, real-time quantitative PCR on an SYBR green platform has been carried out to explore the expression of apoptotic genes (Kiddane *et al.*, 2022).

Table 2-1. A list of the designed primers used for RT-qPCR

Genes	Product size	Sequences
Bcl-2	103 bp	Forward 5'-CTGATGCTCCCATGCTCAGT-3'
		Reverse 5'-ACAGAACCAGACCCAGACCT-3'
Caspase-3	102 bp	Forward 5'-CTGTGAACCCTGCATTTGGC-3'
		Reverse 5'-ACTTCGGAAGCTGAACCTGG-3'
Cytochrome-c	104 bp	Forward 5'-TGGCTTAATGTGTTCCGCCCT-3'
		Reverse 5'-AAGCCCAAGCAAAGAGGGAA-3'
p53	101 bp	Forward 5'-AGTGCTTGGGTTGTGGTGAA-3'
		Reverse 5'-ACACCATGCCAGTGTCTGAG-3'
Bax	102 bp	Forward 5'-ACGAGGGTGATAGGTGGTACA-3'
		Reverse 5'-TGTTCTTCCCTTACCCACACG-3'
Apaf-1	101 bp	Forward 5'-TGGGTGACTGACCTTTGCTTT-3'
		Reverse 5'-GTCTGTGAGGATTCCCCAGTG-3'
Caspase-9	105 bp	Forward 5'-GAAGAGACCTGGCCAGAACC-3'
		Reverse 5'-ATTGCACAGCACGTTACACAC-3'
Bak	101 bp	Forward 5'-GGTTTTCCGCAGCTACGTTTT-3'
		Reverse 5'-GTTGCAGAGGTAAGGTGACCA-3'
β-Actin	104 bp	Forward 5'-TCTTCCAGCCTTGCTTCCTG-3'
		Reverse 5'-GGTGACAGGTCTTTGCGGA-3'

2.3.8. Molecular Docking Analysis of I3C with P53

To better understand the inhibitory action of I3C on p53, The I3C ligand was docked into the active region of the P53 protein. The Autodock Vina model with the lowest binding energy level was chosen after docking. The binding pockets were identified using a Prank web tool (<https://prankweb.cz/>). All critical site residues fit inside the grid box, which was specified by the binding site residues. This result thoroughly examined the molecular interactions in the complexes using the Discovery Studio visualizer tool (Koshy *et al.*, 2022).

2.3.9. Statistical analysis

This research employed each independent assay's mean and standard deviation for the experimental data. Two to three times each for each experiment. The author utilized Microsoft Excel's paired two-tail student t-tests to examine the statistical significance. * $P < 0.05$, ** $P < 0.01$, and *** $P < 0.001$ were used for the importance of various statistical values.

2.4. Results

2.4.1. Effects of I3C on normal cells and AGS cells

The WST assay was used to perform a dose- and time-dependent cell viability experiment to evaluate the activity of I3C on normal cells (HEK, HaCaT) (**Figure 2.1**) and AGS cancer cells (**Figure 2.2**). I3C was not acutely affecting normal cells for 24 hours and in a dose-dependent manner, it influenced the proliferation and

differentiation of AGS cancer cells. Increasing the concentration dose-dependently, I3C dramatically inhibited the proliferation of AGS cells.

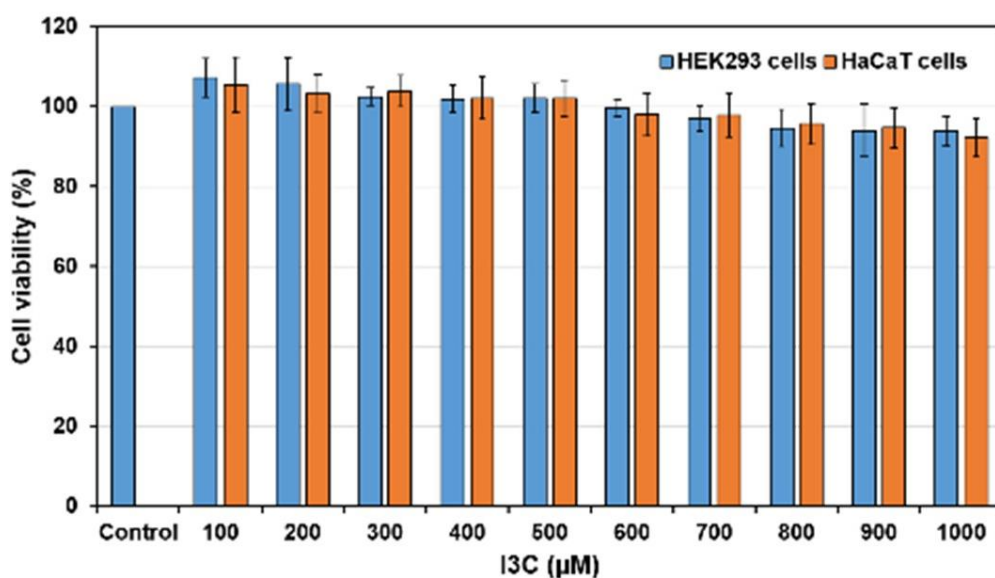


Figure 2.1. Cell viability of normal cells treated with I3C (The data has shown mean \pm SE).

Result shows undergoing dose-dependent treatment with I3C, both HEK293 and HaCaT cells demonstrate an absence of observable toxicity.

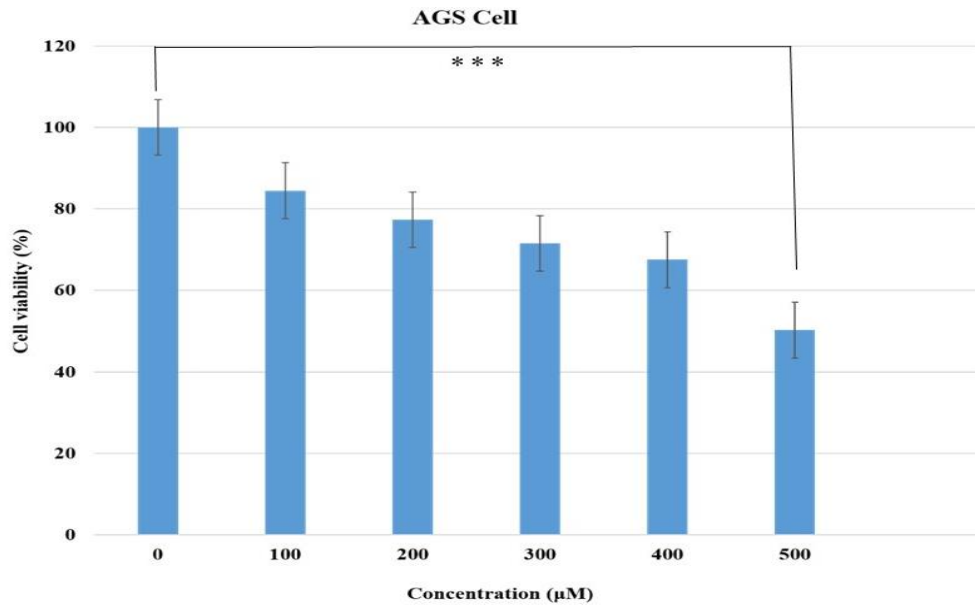


Figure 2.2. AGS cell viability after I3C treatment. (The data has shown mean \pm SE.)

The experimental groups were exposed to I3C at different concentrations (100 μ M, 200 μ M, 300 μ M, 400 μ M, and 500 μ M) for 24 hours, while the control group (C = 100% viability) did not receive any I3C treatment. As the concentration of I3C increased in a dose-dependent manner, there was a significant inhibition of AGS cell proliferation.

2.4.2. Nuclei express consistent morphological changes during apoptosis by I3C.

In this study, we employed I3C to treat AGS cells for 24 hours at five doses ranging from 100 μM to 500 μM . We observed morphological changes, including nuclei going through distinct phases of apoptosis brought on by chromatin condensation. Cells exhibit a shattered-like structure and discontinuity in the early stages of chromatin condensation, generating a ring-shaped condensed morphology. It starts to contract with a beaded anticipation when the I3C dosages steadily increase, and the nuclear structure collapses to form an apoptotic body. One of the hallmarks of the execution of apoptosis is the observance of significant alterations in the nuclear chromatin's compact structure. It is poorly understood how chromatin becomes condensed and identified as a distinct chromosome during the mitotic stage. This study demonstrates that an I3C-treated AGS cell possesses an apoptotic-specific mechanism that controls chromatin condensation activity. Surprisingly, only a limited number of factors have been identified as determining the mechanism behind chromatin condensation during apoptosis. As a result, I3C occurs in AGS cells during chromatin condensation via the mitochondrial apoptosis path, and the outcomes are shown in **Figure 2.3**.

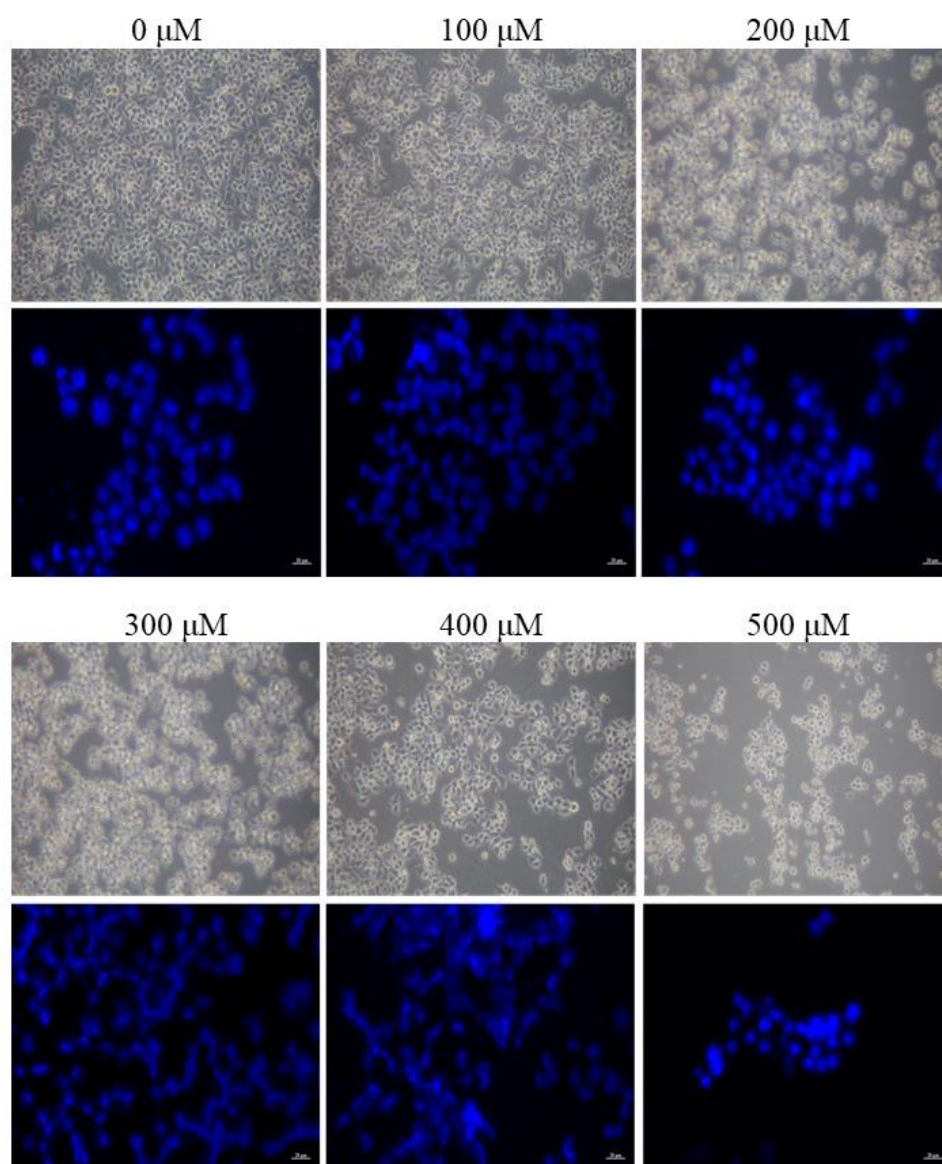


Figure 2.3. The morphological alteration of AGS cells after I3C treatment on dose-dependent manner.

The experimental group received I3C at doses of 100 μM, 200 μM, 300 μM, 400 μM, and 500 μM during 24 hours, whereas the control group received no treatment. Comparing the control group to higher-dose treatment groups, DAPI staining indicated intact nuclei in the control group.

2.4.3. DNA degradation and cellular death

DNA fragmentation has long been seen as a crucial step in apoptosis since it is a sign of intended cell death. The results of the DNA fragmentation experiment demonstrate how the genomic DNA obtained from AGS cells gradually fragments with increasing dosages. **Figure 2.4** depicts the DNA fragmentation seen after 24 hours of I3C treatment. Chromosomal DNA cleavage and the development of an apoptotic body are characteristics of apoptosis.



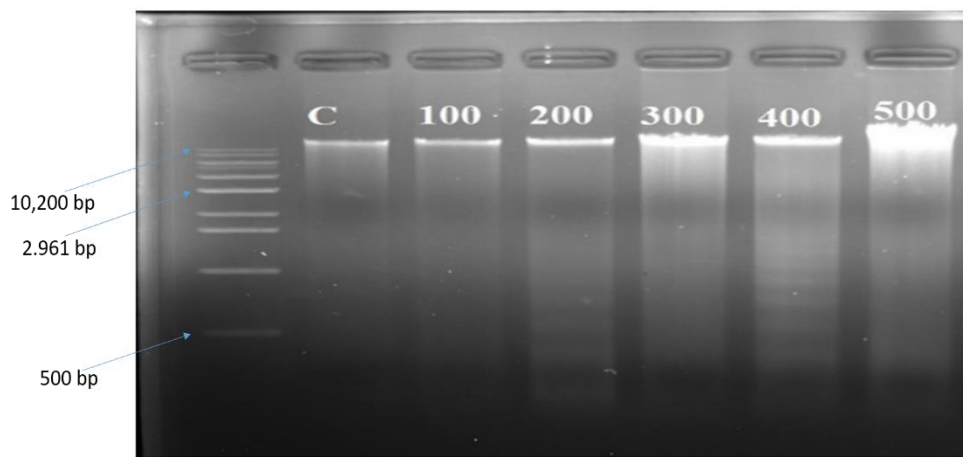
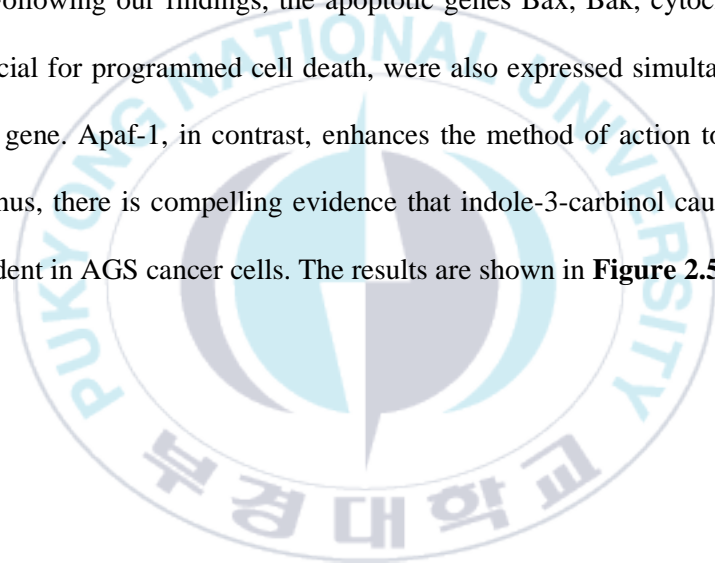


Figure 2.4. DNA fragmentation of I3C treated AGS cells on dose-dependent manner.

I3C (0 μM to 500 μM) treated AGS cells for 24h. AGS genomic DNA was extracted and separated by 1.5% agarose gel electrophoresis.

2.4.4. Apoptosis induction via mitochondrial pathway by expressing BH-3 subfamily genes.

The expression of apoptotic genes connected to the mitochondrial pathway has been examined using RT-qPCR. Our research suggests a process that is closely related to mitochondria-mediated cell death. Bax and Bak, known to generate the pore and aid in releasing cytochrome-c from the mitochondria into the cytosol, were increased during apoptosis. Following our findings, the apoptotic genes Bax, Bak, cytochrome-c, and Apaf-1, crucial for programmed cell death, were also expressed simultaneously with the caspase gene. Apaf-1, in contrast, enhances the method of action to activate the caspases. Thus, there is compelling evidence that indole-3-carbinol causes apoptosis dose-dependent in AGS cancer cells. The results are shown in **Figure 2.5**.



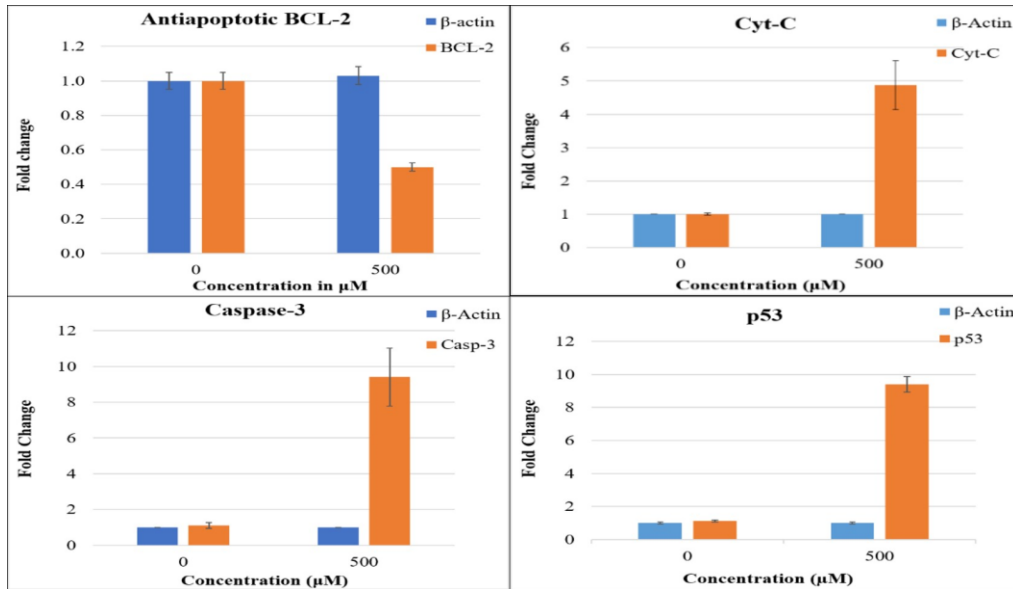


Figure 2.5 continued to the next page.

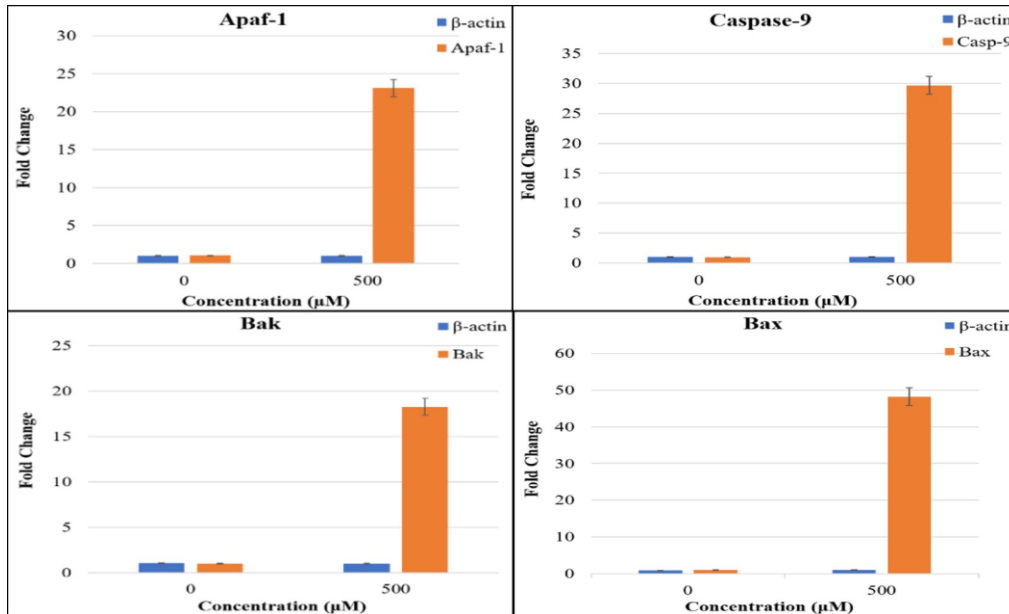


Figure 2.5. RT-qPCR results of relative gene expression in AGS cells after I3C treatment.

The data has been presented as mean \pm SE. Fold change demonstrates upregulation and downregulation of apoptotic and anti-apoptotic gene expression levels relative to the treatment control group.

2.4.5. Molecular docking between I3C and p53 protein

The P2Rank method is based on classifying points distributed over proteins' Solvent-Accessible Surfaces (SAS points). These points represent the local 3D spherical neighborhoods centered at these locations. They can also be considered as simultaneous possible ligand contact atom locations. First, SAS sites are described using a vector of physio-chemical, geometrical, and statistical properties extracted from the surrounding geometry. High-estimated ligand-ability regions are gathered to build predicted ligand binding sites. The high-ranking score binding pockets were taken for docking. The P53 protein structure was generated using UniProtKB/Swiss-Prot modeling based on amino acid sequences from Uniprot, not from the protein data bank (PDB) database. The PubChem website was used to obtain the I3C chemical structure. The binding pocket with the most excellent rank score underwent docking. In **Figure 2.6**, the I3C interacted with the p53 (PDB ID:3DCY) binding site through Pi- anion in GLU326, Pi-alkyl PRO300, and LEU323. LEU130, LYS132, LYS164, PRO322, LEU299, and HIS273's Van der Waals interaction. TRY327's unfavorable acceptor-acceptor interaction. The calculated coordinates of the hypothesized putative protein binding site were X-22.986, Y-37.339, and Z-3.7117. The binding affinity of a compound for a protein was found to be -5.9 kcal/mol.

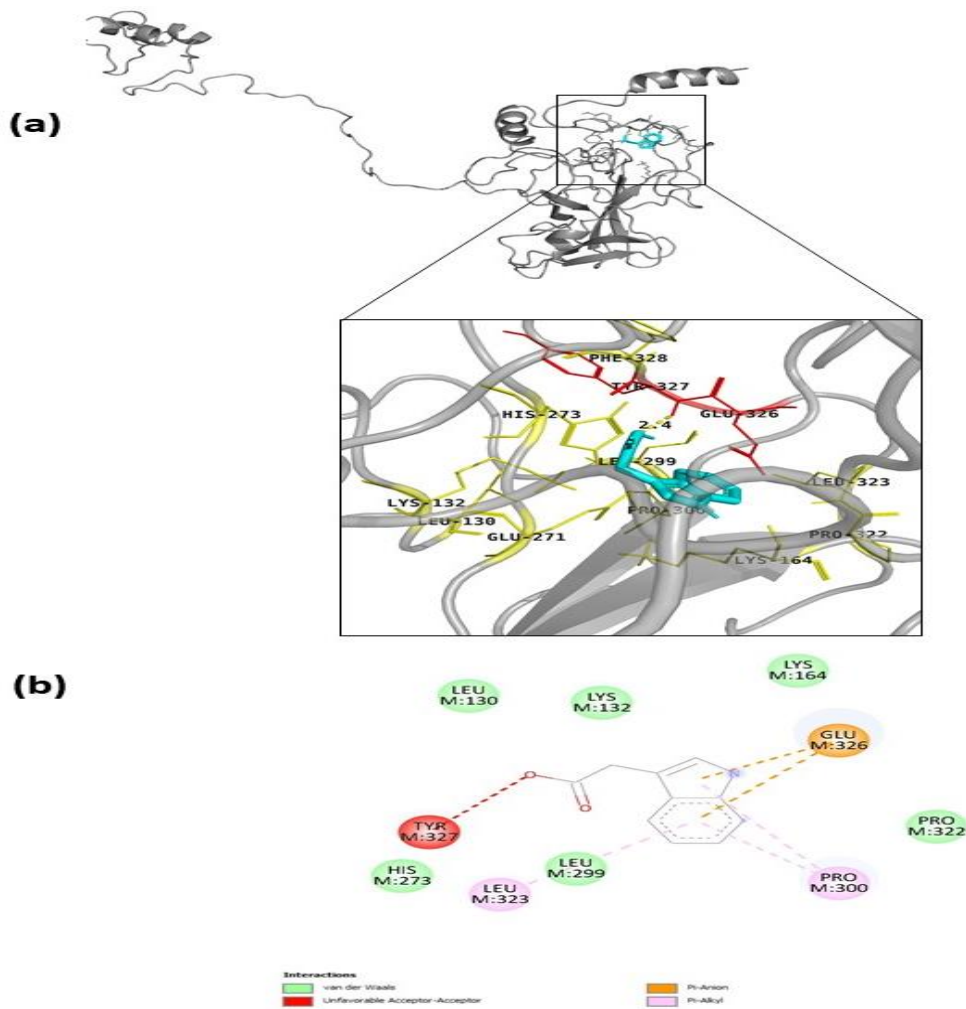


Figure 2.6. (a)Molecular docking analysis of 13C with p53; and (b) The ligand interactions with p53 shown in 2D diagram.

A simplified two-dimensional schematic of the binding interactions between the ligand (13C) and the p53 protein. Amino acids interacting with the ligand are represented by circles with residue names and numbers. The types of interactions are color-coded: hydrogen bonds (green), hydrophobic interactions (yellow), and others specified in the legend.

2.5. Discussion

Cruciferous vegetables tend to neutralize the carcinogens that humans are frequently exposed to I3C and DIM, which are derived from cruciferous vegetables, can prevent procarcinogens from becoming carcinogens (Mao *et al.*, 2014). A naturally occurring substance produced by the hydrolysis of glucobrassicin is indole-3-carbinol. Due to its condensation processes and capacity to transform in vivo into DIM, which may be active against several forms of tumor inhibition, it has demonstrated preventive promise against various limitations. In cancer cells, I3C promotes apoptosis and inhibits cell growth. The division of cells is crucial for tumor development. The four cell cycle phases tumor cells undergo are G1, S, G2, and M. The phase sequence is regulated by several unique protein kinases and their inhibitors (Moiseeva *et al.*, 2007). I3C has demonstrated the ability to inhibit the growth of various types of cancer cells within the range of 500 μM . By downregulating and inhibiting CDK6 expression in MCF-7, the cutaneous melanoma cell lines G-361, SK-MEL-2, and SK-MEL-24, as well as the hormone-dependent prostate cancer cells LNCaP and PC3, as well as by promoting p53 levels thereby making P21 CDK inhibitor available, it inhibits the proliferation of several cancer cells (Singh *et al.*, 2021). The potency of the biological activity of I3C has been demonstrated in several clinical investigations in various studies, including breast cancer, in a double-blind placebo-controlled experiment employing a variety of I3C dosage ranges (Wong *et al.*, 1997). Encouraging the formation of 2-hydroxy estrone, it altered the development of human papilloma (Rosen and Bryson 2004). I3C and its derivatives have potential mechanisms to prevent the growth of bacteria and

viruses that cause chronic illnesses in addition to their anti-tumor activities. Through modulation of the mitogen-activated protein kinase (MAPK) pathway, indole derivatives have a potent inhibitory effect on the uncontrolled proliferation of vascular smooth muscle cells (VSMCs) (Guan *et al.*, 2013). The differentiation of a lung tumor caused by 4-(methylnitrosamino)-1-(3-pyridyl)-1-butanone+lipopolysaccharides (NNK+LPS) has been reduced by the combination of I3C and Silibinin (standardized extract of the milk thistle seeds) (Song *et al.*, 2015). Chemotherapy is often required for the effective management of metastatic cancers. Multiple drugs are commonly utilized as drug resistance is so prevalent that it hardly fades completely. Recent clinical studies have shown the benefits of combining I3C and hydroxychloroquine (HCQ) to assess antineoplastic actions on the Ehrlich ascites carcinoma (EAC) model in mice alone and in combination with HCQ. Furthermore, EAC cell-based apoptosis and autophagy indicators, serum, hepatic, and renal biochemical parameters, histological changes, and anti-tumor response markers were examined (Donia *et al.*, 2022).

I3C and its metabolites have a wide range of anti-tumor efficacy and moderate toxicities in cancer, highlighting its translational potential. I3C and its metabolites have ant-proliferative and anticancer characteristics. However, the exact mechanism(s) behind these effects is/are unclear. The mechanism(s) through which I3C functions in human gastric cancer cells may inspire the development of a cutting-edge strategy for detecting and treating gastric cancer cells. In this research, we provide some proof that I3C could promote apoptosis by altering chromatin condensation, possibly through the mitochondrial pathway. According to our study, I3C promotes the expression of

Caspase-3, Cytochrome-c, P53, Apaf, Caspase-9, Bak, and Bax. A valuable target for developing new anticancer medicines, apoptosis is considered a vital curative mechanism in cancer treatment. I3C is one of the natural chemicals that has long been acknowledged as a significant source of new anticancer medicines since it can be isolated from various natural sources and has been discovered to have remarkable pharmacological effects. Many Studies have shown that various indole derivatives cause apoptosis through multiple mechanisms and pathways. Apoptosis is a natural process of cell self-destruction that is genetically and physiologically determined to have a short life span and plays a significant role in carcinogenesis.

The intrinsic or extrinsic pathways are the two possible mechanisms that might initiate apoptosis. The Bcl-2 family of proteins, which control apoptotic signaling pathways, is the class of proteins in apoptosis that have been the subject of the most extensive research. Through pro- and anti-apoptotic proteins interplay, these pathways control apoptosis by promoting or preventing mitochondrial malfunction (Warren *et al.*, 2019). To carry out its anti-apoptotic actions, the Bcl-2 protein regulates the integrity of the mitochondrial and endoplasmic reticulum membranes and the release of cytochrome-c. The Bcl-2 protein significantly inhibits apoptosis (Campbell and Tait 2018). The pro-apoptotic Bcl-2 family greatly influences the intrinsic regulation of apoptosis. The pro-apoptotic Bcl-2 family greatly influences the intrinsic regulation of apoptosis. The BCL-2 homology domain is often found in the BCL-2 family members Bik, Bim, Hrk, Bad, NOXA, and Bid. The BID is notable within the BH-3 family of proteins that connect the extrinsic and intrinsic pathways. The bid protein is a member of a different

subgroup of the BCL-2 family that triggers apoptosis and concurrently connects both intrinsic and extrinsic pathways by integrating two major apoptotic pathways. A bid is cleaved by caspase-8 while also being essential for the intrinsic pathway. However, within the intrinsic pathway, caspase-3 can interact with its own. The bid protein turns into tBID by caspase-8, and tBID then activates the Bax and Bak proteins, which make pores in the mitochondria or mitochondrial membrane, causing the release of cytochromes and activating the intrinsic pathway (Lee *et al.*, 2004).

A stimulant stimulus, such as a chemical, or the elimination of repressor agents might cause apoptosis. "Programmed cell death" is when a cell dies by dividing into membrane-bound particles and being phagocytosed to be consumed. The prosurvival BCL-2 protein family can be bound by the Bid, Bim, and PUMA proteins. Cytotoxicity tests on fibroblasts reveal that Bid, Bim, and PUMA are strong apoptosis inducers (Chen *et al.*, 2005). At low dosages, apoptosis can be induced by heat, radiation, hypoxia, and cytotoxic chemotherapeutic drugs; however, these same stresses can also result in necrosis. In addition, apoptosis is a regulated and energy-dependent process that requires the activation of a cysteine protease network known as "caspase," as well as a convoluted series of actions that link the initial stimulation to the cells' final demise. The most important protein in the apoptotic scenario is cytochrome-c.

In the mitochondrial pathway, essential for energy consumption, cytochrome-c is the primary apoptosis signaling molecule. The mitochondrial pathway results in cell death by causing mitochondrial swelling, producing reactive oxygen species (ROS), losing osmotic control, and causing cell death. I3C activates the caspase protein, increases the

ratio of anti-apoptotic proteins, changes the permeability of the mitochondrial membrane, and causes the release of cytochrome-c from the mitochondria. When cytochrome-c release in Fas-activated apoptosis is distal to caspase activation, both caspase and cascade activations are triggered once mitochondrial cytochrome-c is transferred from the intermembrane gap into the cytoplasm (Cai *et al.*, 1998). Activating these proteolytic enzymes, which follow the release of cytochrome c and other substances from the mitochondria, organizes the systematic demise of cancer cells. The two primary processes, necrosis and apoptosis, which can occur concurrently, successively, or independently, must also be distinguished. In some circumstances, whether cells die by apoptosis or necrosis depends on the kind of stimuli and the potency of the incentives. Some cancer cells experience DNA damage from radiation or chemotherapy medications, which can trigger apoptosis through p53-dependent pathways. Apoptosis, or programmed cell death, is a crucial cellular process that must work effectively for a cell to maintain its malignant transformation and resist treatment. Through shared binding structures, the dynamic balance of pro- and anti-apoptotic family members, including BCL-2, can control whether a cell lives or perishes. Normal cells and specific cancer cells will upregulate pro-apoptotic family proteins in response to stress; this increases the expression of pro-apoptotic proteins, sufficient to cause apoptosis in cancer cells.

An important flavoprotein known as "apoptosis-inducing factor" (AIF) is produced from mitochondria during apoptotic execution. It can cause the nuclear structure to condense at the nuclear periphery (Toné *et al.*, 2007). According to a recent study, the

other circumstance in which nuclear condensation takes place without fragmentation is during hypoxia-induced caspase-independent cell death. Several factors that trigger apoptosis, including radiation, toxins, and hypoxia, do not have a specific cause and can produce alterations in the inner mitochondrial membrane that result in the opening of the mitochondrial permeability transition (MPT) pore. The release of pro-apoptotic genes into the cytosol has been shown to occur when AIF activates nuclease activity, which can produce high-molecular-weight DNA fragments (Elmore, 2007). However, the current work highlights the crucial function of caspase genes in executing apoptosis. I3C has been shown in multiple trials to have many therapeutic applications when coupled with other medications. The suggested study found that the anti-tumor activity of I3C on MCF-7 and C6 cells was boosted roughly twice by rosehip oil (RHO) nanocapsules without affecting astrocyte cell survival (Gehrcke *et al.*, 2017).

Apoptosis is an essential biological process in vitro and in vivo studies. The fragmentation of nuclear DNA characterizes the self-destruction of the cells into nucleosomal units. This cellular and molecular process involves a specific caspase-activated DNase (CAD) cleaving chromosomal DNA in a caspase-dependent manner that is synthesized with an inhibitor of CAD (ICAD) in cell proliferation. It occurs in various cell types with multiple apoptotic receptors (Nagata, 2000). A vital component of the apoptotic process is the caspase genes. These genes are essential for cleavage of many cellular genes and the death signal transduction that causes other genes to be activated or inactivated, altering apoptotic genes' biochemical makeup and morphology. The apoptotic caspase can play an initiator or effector caspase role in apoptosis,

depending on where they thrive in the apoptotic cascade. Multiple apoptotic signals combine to permeabilize the mitochondria's outer membrane, causing cytochrome-c to be released. As soon as cytochrome-c is released, it activates Apaf-1, which helps caspases break cellular proteins, causing the biochemical and morphological changes associated with apoptosis (Kim *et al.*, 2009). The intrinsic pathway is triggered in response to oxidative stress or other chemical processes that release cytochrome c from the mitochondria into the cytosol.

Caspase-3, one of the caspase proteins, is essential for apoptosis. Truncated bid (tBID), BIM, and PUMA are examples of activator BH3s that activate Bax and Bak to facilitate cytochrome-c efflux and caspase activation during apoptosis. Bak and Bax are crucial for mitochondrial apoptosis, with Bax existing as a monomer with its c-terminal $\alpha 9$ helix in the cytoplasm (Cheng *et al.*, 2001). The transmembrane domain, which binds the proteins in the mitochondrial outer membrane (MOM), is carried by the C-terminal $\alpha 9$ helix. The induction of Bax/Bak upregulation and Bcl-2 downregulation, which supports programmed cell death, significantly alters the release of cytochrome-c. The overexpression of p53, a sign of apoptosis, was triggered by the enhanced activity of the caspase group protein (Lim *et al.*, 2021). In response to various genotoxic stimuli, the p53 protein is recognized as a critical tumor suppressor that significantly contributes to cell cycle arrest, apoptosis, accelerated cell aging, and DNA repair (Chen, 2016).

Furthermore, it is expected that Bax and Bak expression might occur when proapoptotic BH3 domains attach to the grooves of Bax and Bak (Westphal *et al.*, 2014). Because this inhibitor contains a nuclease enzyme that is in a deactivated state, once

caspase-3 is activated, it will break down the inhibitor that is holding onto the nuclease enzyme. That inhibitor may be degraded or broken down by caspase-3. After the inhibitor is degraded by caspase-3, the nuclease gets released and can begin to begin functioning. When the nuclease is active, it may enter the nucleus and start eliminating the nucleic acid, which will cause the cell to die. Despite recent developments in therapy and diagnostic technologies, medical professionals and researchers still haven't discovered a reliable way to treat stomach cancer. In humans, several caspases (caspase-8, caspase-9, and caspase-10) are known to operate as an upstream "initiator" of apoptosis by activating a downstream "effector" caspase (caspase-3, caspase-7) (Walsh *et al.*, 2008). Caspase-3 substantially impacts the morphological changes and DNA fragmentations connected to apoptosis (Jänicke *et al.*, 1998). Caspase-7 and Caspase-9 are also crucial factors in executing programmed cell death. Caspase-3 mediates DNA fragmentation during apoptosis (Wolf *et al.*, 1999). By releasing cytochrome-c, caspase-3 can interact with the intrinsic pathway where Bax/Bak makes pores in the mitochondria or mitochondrial membrane to cause apoptosis.

A crucial component of the respiratory chain, cytochrome c induces cell death and encourages the activation of Apaf-1/caspase-9. The apoptotic executors known as caspases 3, 6, and 7 are controlled by caspase-9 (Green and Kroemer 1998). When cytochrome-c attaches to Apaf-1 in adenosine triphosphate (ATP) presence, a series of processes enable Apaf-1 to oligomerize into a complex ring-like structure with a molecular weight of around 700 kDa (Acehan *et al.*, 2002). Once released, cytochrome-c will interact with Apaf-1, activating caspase-9 and boosting its autocatalytic

activation (Jänicke *et al.*, 1998). Cytochrome-c was the first pro-apoptotic factor connected to mitochondria. By binding to Apaf-1 and activating procaspase-9, released into the cytoplasm when the mitochondrial membrane potential increases, cytochrome-c causes apoptotic cell death (Shakeri *et al.*, 2017). Apoptosis now takes place due to the support of cytochrome-c and Apaf-1 in apoptosome formation. The capacity of cytochrome-c to accumulate in the nucleus does not prevent it from inducing caspase-dependent apoptosis, which is connected to caspase-independent apoptosis and encourages cell death (González-Arzola *et al.*, 2019).

The proposed study on fluorescence loss in photobleaching (FLIP) and fluorescence recovery after photobleaching (FRAP) has been reported; the localization of Bax to mitochondria is observed in healthy cells. Retro, however, translocated to the cytosol when it was active, and this reduction of retro translocation after mitochondrial apoptosis made cells more susceptible to apoptosis, which is the last stage of cell death. The transitory binding of BH3-only proteins to Bax and Bak is consistent with the "hit and run" hypothesis. BH3-only proteins have been linked to the activation and binding of Bax and Bak in several investigations employing genetics, biochemical, or structural methods (Edlich *et al.*, 2011). A protein called Bax, which is pro-apoptotic, inhibits Bcl-2 from functioning. Tumorigenesis is frequently associated with abnormal expression of Bcl-2 family members (Edwards *et al.*, 2013). One of the essential elements of the mitochondrial death process is the *apf-1* gene (Campioni *et al.*, 2005). Apaf-1 functions as a tumor suppressor gene and is crucial for apoptosis (Zlobec *et al.*, 2007). The non-appearance of Apaf-1 inhibits caspase-3 from activating, which is

essential for releasing cytochrome-c via splitting the mitochondrial membrane. A recent study discovered that hepatocellular carcinoma could potentially inhibited by molecular docking of the I3C crystal structure (Alkhalaf 2020). The docking score shows the I3C has a high affinity for p53 (3DYC). By releasing cytochrome-c from the mitochondria, 3DYC is a crucial component of apoptosis in AGS cells. The preceding computational results suggest that the I3C is a more effective anticancer drug in the AGS cell line.



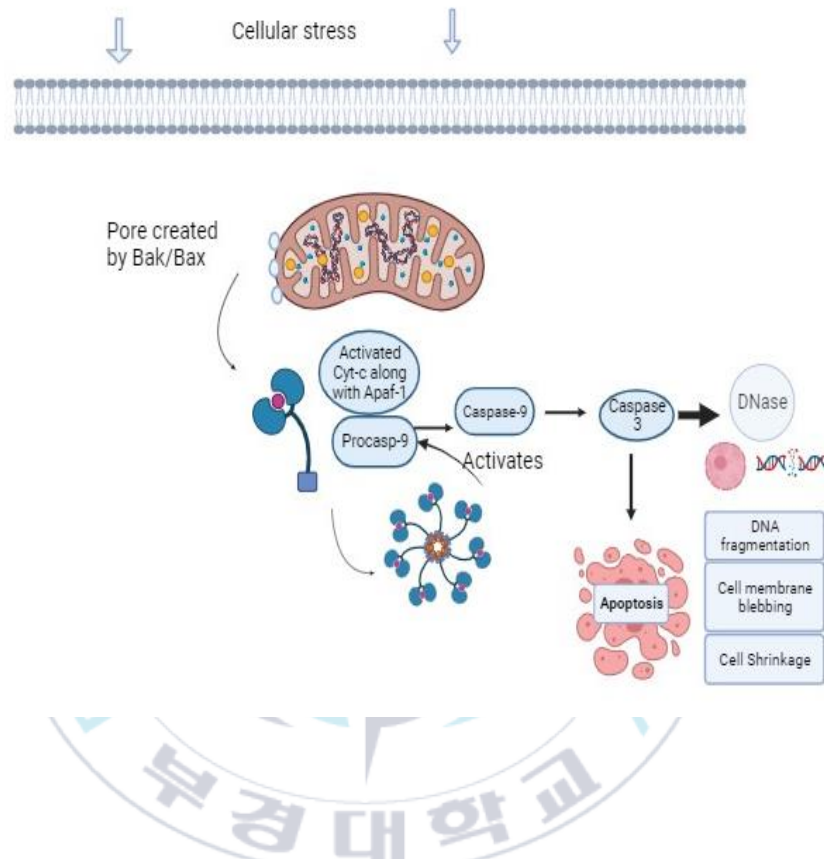


Figure 2.7. Schematic diagram of the intrinsic pathway of apoptosis involved in I3C-treated AGS cells.

This is the process of programmed cell death characterized by certain morphological and molecular features, such as DNA fragmentation, cell membrane blebbing, and cell shrinkage.

2.6. Conclusion

It is significant to note that, so far, there have been no reports of I3C on AGS cells that exerted similar molecular processes to cause apoptosis. These results conclude that Bax translocation to the mitochondria triggers the mitochondrial death pathway during I3C-induced apoptosis in AGS cells. A recent study discovered that hepatocellular carcinoma might be prevented by molecular docking of the I3C crystal structure. As the docking score shows, the I3C has a high affinity for p53 protein. By releasing cytochrome-c from the mitochondria, p53 is a critical component of apoptosis in AGS cells. Based on the computational results mentioned earlier, it is suggested that I3C could serve as a more potent anticancer drug for the gastric cancer. Results from I3C's anticancer efficacy and its molecular mechanism against stomach cancer provide encouraging feedback for reducing the chance of developing cancer. This result suggests potential mechanisms for preventing nuclear condensation, cell growth, and the differentiation and proliferation of gastric cancer cells in a dose-dependent manner, as well as for triggering caspase proteins through the upregulation of the BH-3 family group of genes. According to our research on I3C and its molecular mechanism, a healthy diet, including I3C, may work as a tumor suppressor against many cancers, and foods high in I3C may also lower the chance of developing many cancers. Additional study is required to comprehend the diverse impacts of I3C within cellular pathways fully. However, no further supporting evidence using several cell lines with equivalent properties was supplied, and the tests were solely done in vitro. Future research may also focus on the advantages of I3C and 3,3'-diindolylmethane (DIM) in numerous

clinical trials in combating the cancer epidemic among people worldwide by utilizing a variety of technologies. We'll test additional fundamental pathways using animal models and more cell lines. This research might progress anticancer treatments and offer other therapeutic options.



Chapter 3. *Angelica keiskei*: A potential antioxidant and anticancer agent for photothermal drug delivery applications

3.1. Abstract

Cancer remains one of the leading causes of mortality worldwide, necessitating the continuous search for novel and effective therapeutic strategies. This work explored the potential anticancer properties of *Angelica keiskei* leaf and root extracts (AKLE) for Photothermal therapy (PTT)-mediated drug delivery applications and the compound's antibacterial, antioxidant, and hemolytic activity. AKLE were obtained using a green subcritical water extraction technique. Identification and characterization of extracts were performed by using gas chromatography-mass spectrometry (GC-MS), Total Phenolic Content (TPC), and antioxidant activities by Folin-Ciocalteu colorimetric assay, and 2,2'-diphenyl-1-picrylhydrazyl radical scavenging assay (DPPH), respectively. The crystal structure and chemical properties of Hydroxyapatite (HAp) were analyzed using X-ray powder diffraction (XRD). The characterization of AKLE optical properties, including absorption and photothermal conversion efficiency, revealed strong absorption in the near-infrared (NIR) region, suggesting an ideal candidate for PTT. HAp-loaded AKLE exhibited a controlled and sustained release under NIR laser irradiation, supporting its potential use as a drug carrier for targeted therapy. MTT assay revealed the compound's anticancer activity on MDA-MB231 cells.

HAp was used for drug delivery, and a UV-Vis study was performed to check the photothermal efficacy, drug loading, and releasing capacity. A hemolysis research determined the biocompatibility and safety of the compounds. The study also analyzed the efficiency of the identified compound from AKLE, 2,3-Dihydro-3,5-dihydroxy-6-methyl-4H-pyran-2-one (DDMP) currently repurposed against the specific kind of bacterial proteins that have become resistant to more than one antibiotic strain are known as multidrug-resistant bacteria, and this makes them challenging to cure with standard antibiotic treatments for beta-lactamase and methicillin resistance bacterial proteins. Using docking studies, DDMP showed a great binding affinity with those bacterial proteins that is -5.5 kcal/mol and -4.8 kcal/mol. This work explores the remarkable anticancer, antioxidant, and antibacterial properties and the safest drug delivery applications.

3.2. Introduction

The *Angelica keiskei* (Miq.) Koidz. (Umbelliferae), Asitabha, in Japan, is a flowering shrub that resembles carrots and is rich in nutrients. It is extensive and provides various minerals and amino acids, which have different beneficial effects in biological domains to guard against many severe illnesses and disorders (Du *et al.*, 2019). The biological advantages conferred by crude extracts and parts of *A. keiskei* have been demonstrated for several ailments, including cancer. It contains several active substances, including chalcone and coumarins. Xanthoangelol and 4-hydroxyderricin, two necessary chalcone chemicals, are recognized for enhancing anticancer activity (Okuyama *et al.*, 1991). The botanical, phytochemical, and biological studies on *A. keiskei* extracts and

pure components are summarized in this study. *A. keiskei* inhibits tumor growth in several cancer cell lines through various signaling pathways. Research employing A.K. compounds and raw materials from the other portion of the plant has also reported antioxidant, anti-depressant, antiviral, antithrombotic, anti-hypertensive, anti-inflammatory, and anti-allergic activity (Kil *et al.*, 2017). Due to its distinctive combination of bioactive chemicals with strong pharmacological characteristics, AKLE, produced from the *Angelica keiskei* plant, has attracted much interest recently. Previous research has shown that AKLE has anti-inflammatory, antioxidant, and anticancer properties. This study investigates its potential as a drug carrier and photothermal sensitizer for enhancing cancer therapy. The preliminary breakdown of AKLE's optical properties covered absorption and photothermal conversion effectiveness. The near-infrared (NIR) region was found to have significant absorption, which made it a prime option for PTT (Bian *et al.*, 2021). The drug release profile was then assessed after loading AKLE with anticancer drugs. Positively, under NIR laser irradiation, AKLE demonstrated regulated and sustained drug release, indicating its promise as a drug carrier for targeted treatment. Studies were carried out in vivo and in vitro to assess the efficacy of the treatment. AKLE-mediated PTT significantly raised cancer cell mortality compared to PTT alone or medication therapy alone, according to in vitro studies employing cancer cell lines. The mechanism underlying this increased effectiveness was investigated, and it was discovered that drug-induced cytotoxicity and photothermal ablation had synergistic effects. The therapeutic promise of AKLE-based PTT was further demonstrated in vivo experiments using a mouse xenograft model. In contrast to the control groups, tumor shrinkage, and extended survival were

shown in the AKLE-mediated PTT group. Significantly, little systemic toxicity and adverse effects were seen, highlighting AKLE's safety profile as a therapeutic drug. The safety profile of AKLE as a medicinal agent was highlighted by the observation of low side effects and systemic toxicity. This work emphasizes the enormous potential of *Angelica keiskei* extract as a versatile agent for photo thermally improved medication delivery in cancer therapy. AKLE is an ideal choice for additional preclinical and clinical studies because of its unique mix of photothermal characteristics, prolonged drug release, and therapeutic effectiveness. Utilizing AKLE's potential might lead to a targeted, practical therapeutic strategy with few side effects, transforming cancer therapy. Previous studies have demonstrated the anti-tumor and anti-metastatic actions of two chalcones isolated from the roots of *Angelica keiskei*, and these outcomes can be related to their capacity to obstruct tumor-induced angiogenesis (Kimura *et al.*, 2008). An investigation carried out with MDA-MB 231 human breast cancer cells and reported in the "Journal of the Korean Society of Food Science and Nutrition" demonstrated how AK ethanol extract suppresses the anti-apoptotic gene Bcl-2 (Jeong and Kang 2011). A549 (lung), AZ521 (stomach), CRL1579 (melanoma), and HL60 (leukemia) human tumor cell lines were all susceptible to the cytotoxic effects of an extract of *Angelica keiskei* roots that is soluble in ethyl acetate (EtOAc), according to different research published in the "Journal of Oleo Science." However, caspase-dependent apoptosis occurred in HL 60 human leukemia cells (Nishimura *et al.*, 2007). Since hydroxyapatite [$\text{Ca}_{10}(\text{PO}_4)_6(\text{OH})_2$, (HAp)] materials are extensively employed in biomedical applications due to their exceptional biocompatibility, osteoconductive properties, and resemblance to the inorganic component, researchers have taken a

strong interest in materials (Lin and Chang 2015). There is an ongoing study on the drug loading of *Angelica keiskei* on HAp nanoparticles. One strategy is to use HAp as a viable candidate when designing a drug delivery system (DDS). A further investigation conducted in 2018 and reported in the journal "Materials Science and Engineering: C" focused on loading *Angelica keiskei* extract on HAp nanoparticles coated in chitosan. According to the investigation, the final composite material demonstrated a high drug-loading capacity and features of sustained drug release. The research claimed that the chitosan-coated, *Angelica keiskei*-loaded HAp nanoparticles may be exploited as a possible medication delivery mechanism for the treatment of osteoporosis (Benedini, 2019). Drug resistance in infectious diseases has developed into a severe medical issue. Due to their possibly positive impacts on human health, phytochemicals play a crucial role. Their antibacterial, anti-inflammatory, anti-tumor, and antioxidant action has also been noted. The numerous effects of *Angelica-keiskei* on human health are demonstrated in this study.

This study explores the use of *Angelica keiskei* leaf extract (AKLE) in photothermal therapy (PTT) for targeted cancer treatment. Employing subcritical water extraction and GC-MS analysis, the research identifies the chemical composition and antioxidant properties of AKLE. The focus is on AKLE's photothermal conversion efficacy, particularly in the near-infrared region, making it suitable for PTT. The study also examines AKLE's potential as a drug carrier under NIR laser irradiation, demonstrating controlled drug release. In vivo tests on a mouse xenograft model highlight AKLE-mediated PTT's effectiveness in tumor regression and survival rates. Additionally,

molecular docking assesses AKLE's binding affinity with methicillin-resistant bacterial proteins, exploring its broader therapeutic applications.

3.3. Materials and methods

3.3.1. Sample collection

Dried *Angelica keiskei* stem and leaves were bought from www.handshrub.co.kr.

3.3.2. Crude extraction

Sample treatment and subcritical water extraction conditions are as follows:

Dry samples of *Angelica keiskei* (AK) (leaves) were ground in a lab blender, sieved through a 450 μ m mesh, and then treated in a batch subcritical water reactor described in **Figure 3.1**. Subcritical water (100% distilled water) was performed at different temperatures from 140°C to 170°C with an increment of 10°C between conditions. The pressure was maintained at 3MPa, reaction time (10 min), and solid/liquid ratio was 30 mg/mL, except for a variation on one condition (160°C, 45mg/mL), which was added to test the potential effect of varying solid/liquid ratio. To optimize the extraction efficiency of molecules with lower polarity, 50% ethanol was used instead of 100% water as an exceptional condition at 160°C. All treatments and their acronyms are shown in Table 3.1. Extracts were concentrated using a rotary evaporator prior to freeze-drying for 48 hours. Freeze-dried extracts were reconstituted with distilled water before use in further experiments (An *et al.*, 2023).

Table 3-1. List of the parameters for extracting bioactive components from Angelica Kieskei using subcritical water extraction method.

	Temperature (°C)	Pressure (MPa)	Reaction Time (min)	solid/liquid ratio (mg/mL)	Ethanol	Acronyms
1	160	30	10	30	NO	B1
2	160	30	10	45	NO	B2
3	170	30	10	30	NO	B3
4	140	30	10	30	NO	B4
5	150	30	10	30	NO	B5
6	160	30	10	30	50 %	B-E-1

The acronym NO stands for no ethanol was added, and B1, B2, B3, B4, and B5 denote different Batch treatments, as B-E-1 denotes batch 1 with ethanol. Water was employed as the only solvent. Acronyms are closely connected to the circumstances indicated in the table.

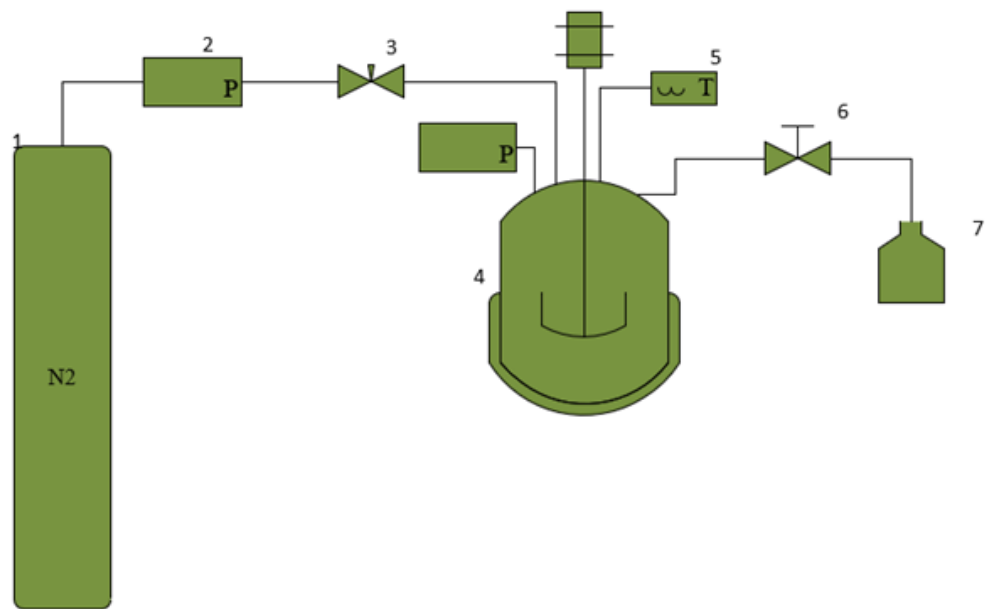


Figure 3.1. Schematic diagram of a batch subcritical water extractor.

The numbers are used to describe each component as follows: (1) nitrogen gas cylinder, (2) pressure gauge, (3) Needle valve, (4) High-pressure extraction vessel, (5) Thermostat, (6) Screw-down valve, (7) Sample collector.

3.3.3. Total phenolic content (TPC) and antioxidant activity assay

Following the Folin-Ciocalteu calorimetric test, TPC analysis was performed. The syringe was then filtered using 45 m filter paper after concentrated extracts were diluted ten times and well combined. After that, 400 μ L of Folin reagent at a ratio of 1/10 (v/v) was added to an aliquot and vortexed for 30 seconds. After 4 minutes, sodium carbonate (7.5% w/v) was added to the mixture and vortexed again. For two hours, the solution was allowed to react. Gallic acid was a common phenolic component and processed similarly to extracts. An absorbance reading was taken at 765 nm using a synergy multi-mode 96-well plate reader. Based on the powdered sample's milled dry weight, the results were reported as equal to gallic acid. [mgGAE/g, Dw]. The previous technique was used to measure the antioxidant activity using the DPPH radical scavenging test. In brief, 3.85 mL of DPPH solution (made in 80% methanol) was combined with 150 L of extracts diluted ten times. The combination was allowed to react for 30 min before being read at 517 nm. The following formula was used to compute the % inhibition of radicals by extracts:

$$\% \text{ Inhibition} = (1 - AS/AC) * 100$$

Where AC is the absorbance of the DPPH radical solution (control), and AS is the treatment's absorbance.

3.3.4. GC-MS

Gas chromatography coupled with mass spectrometry (GC-MS; equipment type GCMS QP-2010Ultra; manufacturer location Kyoto, Japan; column model DB-5MS Ultra)

was used to identify the compounds. (30*0.25*0.25). The substance is dissolved in water and then further diluted with methanol. The precipitated fraction was centrifuged, after which the supernatant was examined.

3.3.5. Synthesis of Hydroxyapatite (HAp)

Dissolve calcium nitrate ($\text{Ca}(\text{NO}_3)_2$) in distilled water to make a calcium precursor solution. Similarly, disperse diammonium hydrogen phosphate ($(\text{NH}_4)_2\text{HPO}_4$) in distilled water to create a phosphate precursor solution. To attain the correct calcium-to-phosphate ratio, prepare both solutions in stoichiometric amounts. Using an appropriate alkaline agent, such as ammonium hydroxide (NH_4OH) or sodium hydroxide (NaOH), the pH of the suspension can be adjusted to a slightly basic range (pH 9–10). This pH range encourages the development of HAp. Add the phosphate precursor gradually while stirring constantly into the calcium precursor solution. To get a homogenous mixture, the mixing is done slowly. Allow the combined solution to mature for a predetermined time, usually at room temperature or slightly higher. The interaction of the calcium and phosphate ions during this aging process leads to the formation and development of HAp particles (Sadat-Shojai *et al.*, 2013).

3.3.6. UV-Vis study

A standard analytical method for determining how much light is absorbed and transmitted in the ultraviolet and visible portions of the electromagnetic spectrum is called UV-Vis (ultraviolet-visible) spectroscopy. Compared to a reference sample or blank test, a sample's ability to transmit or absorb UV or visible light is measured using UV-Vis spectroscopy (Al-Buriahi *et al.*, 2022). This feature may show the sample

composition and concentration (Carroll *et al.*, 2023). It offers valuable details regarding the concentration of chromophores and electronic transitions in a sample. Analysis of substance structure, concentration, and purity is done using UV-Vis research. Researchers may learn more about compounds' chemical and physical characteristics by analyzing their absorption spectra, making it easier to characterize and analyze molecules for use in various applications. The UV-Vis spectrophotometer GENESYS (Thermo Fisher Scientific, USA) was used in this research to examine the absorbance characteristics of an extract of *Angelica keiskei* leaf in the 320–1100 nm wavelength range.

3.3.7. Drug loading and releasing study

Angelica keiskei leaf extract holds promise as a potential drug loaded on HAp nanoparticles. The extract's bioactive components, namely chalcones and flavonoids, have anti-inflammatory and antioxidant characteristics, making them desirable candidates for drug delivery approaches. *Angelica keiskei* leaf extract can improve the therapeutic potential of HAp nanoparticles and encourage drug-controlled release, providing new therapeutic options for the biomedical treatment of cancer.

The drug loading and releasing study involved several steps to assess the loading capacity of *Angelica keiskei* leaf extract onto hydroxyapatite (HAp) nanoparticles and the subsequent controlled release of the loaded drug.

Drug Loading Process:

Angelica keiskei leaf extract was loaded onto the surface of synthesized HAp nanoparticles using adsorption. This process involved incubating the nanoparticles with the extracts for 24 hours to ensure adequate adsorption onto the nanoparticle surface.

Confirmation of Loading Amount:

A UV-Vis study was conducted to quantify the loading amount. This involved comparing the absorbance of the solution containing the loaded extract to a control solution. The results showed that the loading capacity of the HAp nanoparticles was approximately 44.6%, indicating successful adsorption of a significant amount of the *Angelica keiskei* leaf extract onto the nanoparticle surface.

Drug Release Studies:

Drug release studies were performed at different pH conditions to evaluate the sustained release of the drug.

At pH 4.5 over 72 hours, the study showed a moderate drug release, suggesting a controlled and sustained release profile.

At pH 7.0 without any external stimulus (laser treatment), the drug release was minimal, with only about 25% of the loaded drug released over 72 hours. This indicated limited drug release without any external trigger.

When the drug release study was conducted at pH 7.0 with 530 nm laser irradiation, a significant increase in drug release was observed. Around 61% of the loaded drug was released over 72 hours, indicating that laser irradiation at a specific wavelength could trigger the release of the drug from the loaded HAp nanoparticles.

3.3.8. Cell cytotoxicity test

The MTT experiment was performed to examine the cytotoxicity of *Angelica keiskei* extracts on MDA-MB231 cells. MDA-MB 231 cells were seeded in 96-well plates, and the plates were then incubated for 24 hours at standard atmospheric conditions. Old media was removed after 24 hours. The cells were incubated for 24 hours after receiving multiple doses of *A. keiskei* (ranging from 50 µg/ mL to 300 µg/ mL) in a fresh medium in a dose-dependent manner. The old media were replaced with a new DMEM medium and subjected to 10 µl of MTT (Sigma Aldrich, USA) solution treatment following the manufacturer's instructions. Each well, including the one used as a control, has been treated with the MTT solution. MTT was applied to 96-well microplates, which were then incubated for 4 hours at 37° C. After 4 hours, the plate was placed on a microplate reader and shaken for 5 seconds at a medium speed. A microplate scanner with an optical density of 570 nm was used to scan the microplate. The information gathered was used to calculate the number of viable cells and make a graphical representation of the viability of the cells (Kim *et al.*, 2018). The following formula was used to determine the proportion of cytotoxic efficacy seen in an in vitro cell study.

Cell viability (%) = Absorbance of treated cells/absorbance of non-treated cells×100.

3.3.9. Fluorescence imaging of MDA-MB 231 cells

Acridine Orange (AO) and Propidium Iodide (PI) stains were used to create the fluorescent microscopic image of MDA-MB 231 cells. The cells were plated onto a 12-well dish after being incubated for 24 hours. To distinguish between live (green) and

nonliving (red) cells, cells were stained with AO and PI after 15 minutes of incubation. The images were taken using a Leica DMI300B fluorescence microscope from Wetzlar, Germany.

3.3.10. Photothermal therapy

A targeted treatment alternative with minimal systemic adverse effects is photothermal therapy. The photosensitizer has to be converted from electromagnetic to thermal energy by the incoming radiation. In medical circumstances, this phenomenon is called hyperthermia (Eskiizmir *et al.*, 2017). The use of light-absorbing substances to produce localized heat to treat a disease, is known as photothermal treatment. Photothermal treatment may target and eradicate cancer cells or pathogens by turning near-infrared light into heat using components like gold nanoparticles or carbon nanotubes (Zhang *et al.*, 2019). With potential applications in cancer treatments, the treatment of bacterial infections, and other medical conditions, precise control over the heat produced enables less invasive medical procedures (Vines *et al.*, 2019).

3.3.11. Hemolysis study

According to "MedlinePlus," a hemolysis study is a lab examination examining how red blood cells (erythrocytes) break down or lyse. It evaluates various substances' potential toxicity or biocompatibility on red blood cells, including drugs, chemicals, and medical devices. In the research, red blood cells are exposed to the test chemical, and the amount of hemoglobin released is measured to determine the degree of hemolysis. Researchers can use this information to assess a substance's appropriateness and safety for biological use.

3.3.12. Molecular docking analysis to check antibacterial activities

Plant leaf extract has better antibacterial properties than any chemical product, and the extraction process is affordable and safe (Yasmin *et al.*, 2014). Using *Angelica keiskei* (Miq.) Koidz. Leaves, AuNPs, and CuNPs with potent antibacterial properties were produced without hazardous agents (Schäffler *et al.*, 2014). To further understand the mechanism of inhibition between the ligand and the protein, the 2,3-Dihydro-3,5-dihydroxy-6-methyl-4H-pyran-2-one ligand was docked into the active domain of the penicillin-binding protein and beta-lactamases. After docking, the Autodock Vina model with the lowest binding energy level was chosen. A prank web tool was used to find the binding pockets (<https://prankweb.cz/>). The grid box defined by the binding site residues contained all key site residues. The Discovery Studio visualizer program was used to study the molecular interactions in the complexes carefully (Koshy *et al.*, 2022).

3.4. Results

3.4.1. Total phenolic content (TPC) and Radical Scavenging Activity

Figure 3.2a and **3.2b** shows the TPC and radical scavenging activity results. The TPC values in B1 (Batch 1) were around 10.81 mg GAE/g at 160°C and 30 mg/ml, and they significantly dropped with a higher mixing ratio (45 mg/ml) at the same temperature settings. A decrease in mass transfer and solvent diffusivity brought on by an increase in solid material will harm the solubility of subcritical water and result in ineffective extraction. The TPC value increased slightly with a 10°C rise in temperature (B3, 170°C,

30 mg/ml); nevertheless, temperatures over 170°C were avoided to prevent phenolic compounds from degrading (Zhao and Zhao 2012).



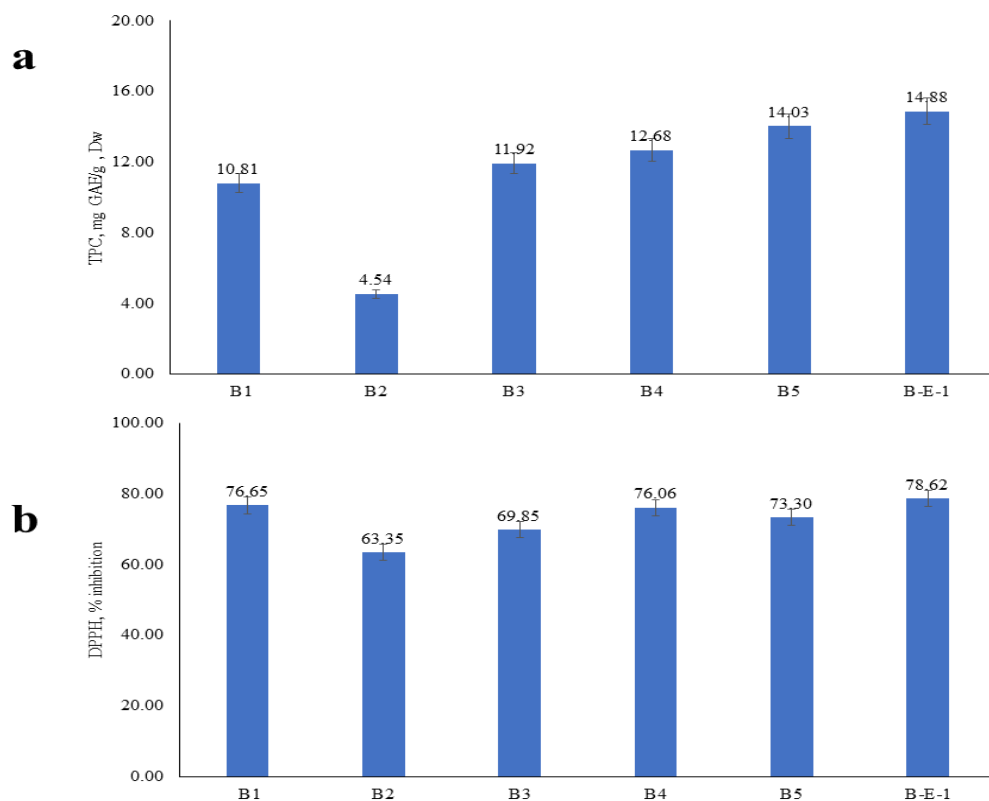


Figure 3.2. Total phenolic content (a) and radical scavenging activity (b) of *Angelica keiskei* extracts obtained from subcritical water treatment at different temperatures.

Using 50% ethanol at 160°C was shown to be more efficient in recovering TPC, and it produced the most significant antioxidant activity results (**Figure 3.2b**), with a radical inhibition rate of 78.62%. The extracts produced by the water-ethanol reaction were chosen for use in subsequent research based on findings for TPC and antioxidant activity.

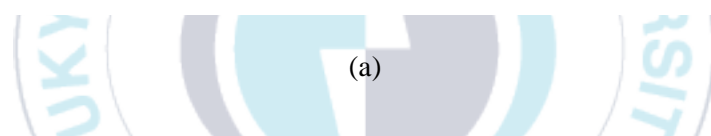
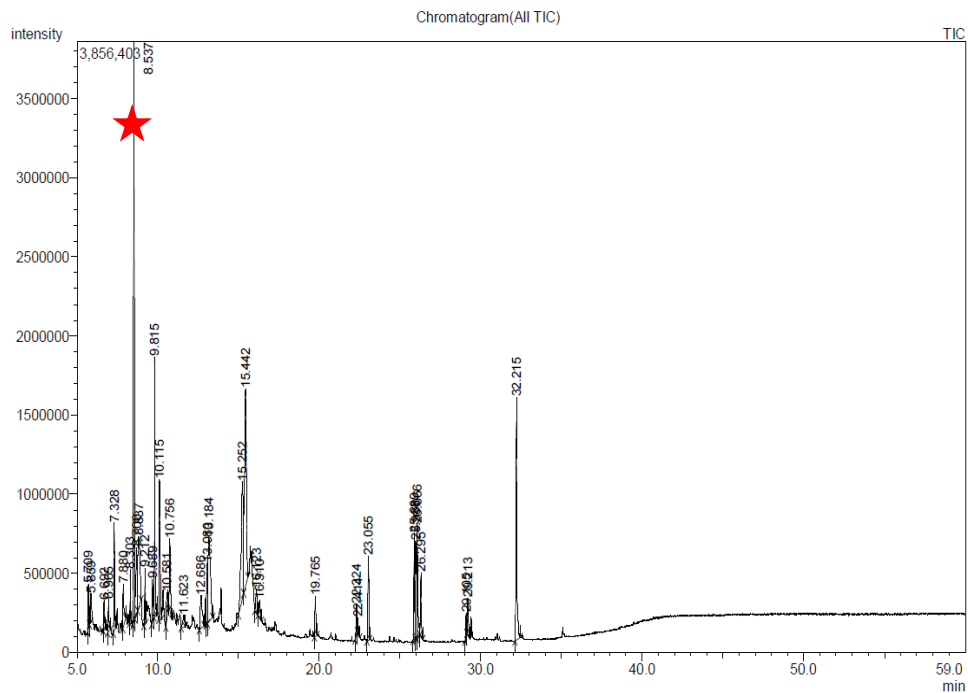
3.4.2. Compound identification and chromatogram by GC-MS analysis based on Wileylib.

A total of 19 chemicals were identified in the AK extract by GC-MS analysis (Table 3.2). Following the findings, 2,3,-Dihydro-3,5 dihydroxy-6-methyl-4H-pyran-4-one (DDMP) isolated from AK showed significant antioxidant activity.



Table 3-2. List of identified compounds by GC-MS analysis

Peak#	R.Time	Area%	Name
1	5.709	0.7	2,4-Dihydroxy-2,5-dimethyl-3(2H)-furan-3-one
2	5.859	0.65	2-Hydroxy-gamma-butyrolactone
3	6.692	0.69	1,3-Dioxol-2-one,4,5-dimethyl-
4	6.965	0.84	2,5-Dimethyl-4-hydroxy-3(2H)-furanone
5	7.88	1.47	3-Pyridinol
6	8.303	0.92	2-acetyl-2-hydroxy-.gamma.-butyrolactone
7	8.537	10.98	2,3-Dihydro-3,5-dihydroxy-6-methyl-4H-pyran-4-one
8	9.815	5.08	5-Hydroxymethylfurfural
9	10.115	4.71	1,2,3-Propanetriol, 1-acetate
10	19.765	0.89	Hexadecanoic acid (CAS)
11	22.324	0.76	9,12-Octadecadienoic acid (Z,Z)-
12	22.414	0.33	9,12,15-Octadecatrienoic acid, (Z,Z,Z)-
13	23.055	1.85	Hexadecanamide (CAS)
14	25.889	2.51	9-Octadecenamide (CAS)
15	25.988	2.84	9-Octadecenamide (CAS)
16	26.066	3.77	9-Octadecenamide (CAS)
17	26.295	1.58	Octadecanamide
18	29.105	0.47	9-Octadecenamide (CAS)
19	32.215	6.93	9-Octadecenamide (CAS)

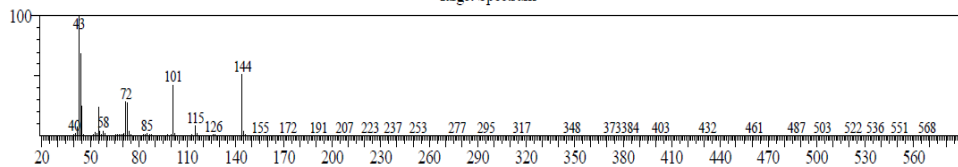


(a)

<< Target >>

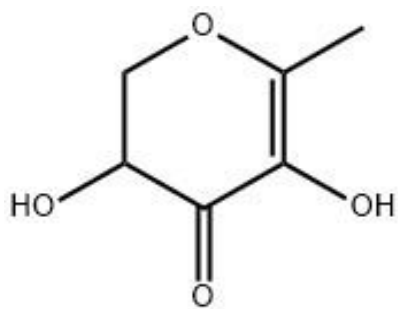
Line#:8 R.Time:8.535(Scan#:708) MassPeaks:325
 RawMode:Averaged 8.530-8.540(707-709) BasePeak:43.00(814735)
 BG Mode:Calc. from Peak Group 1 - Event 1

Target Spectrum



Hit#:1 Entry:42591 Library:Wiley9.lib
 SI:96 Formula:C6H8O4 CAS:28564-83-2 MolWeight:144 RetIndex:0
 CompName:2,3-Dihydro-3,5-dihydroxy-6-methyl-4H-pyran-4-one

(b)



(c)

Figure 3.3. (a) GC-MS chromatogram of crude *Angelica keiskei* extract, (b) The compound identification from *Angelica keiskei* extract based on Wileylib, (c) Chemical structure of DDMP.

The GC-MS plot of the detected compounds 2,3-Dihydro-3,5-dihydroxy-6-methyl-4H-pyran-4-one (DDMP) with a retention time of 8.537 minutes, (the longest peak) is indicated with red star marked on the plot. The size of the points represents the area percentage of each peak.

3.4.3. The biological function of the 2,3-dihydro-3,5-dihydroxy-6-methyl-4H-pyran-4-one (DDMP):

It is well known that 2,3-dihydro-3,5-dihydroxy-6-methyl-4H-pyran-4-one (DDMP) is usually formed in the Maillard reaction, and it contributes to the antioxidant properties of Maillard reaction intermediates (Chen *et al.*, 2021).

The biological function of 2,3-dihydro-3,5-dihydroxy-6-methyl-4H-pyran-4-one (DDMP) is primarily associated with its antioxidant properties. Antioxidants are molecules that help neutralize free radicals, which are highly reactive and potentially damaging molecules produced during various metabolic processes in the body. Free radicals can contribute to oxidative stress, which has been implicated in the development of various diseases, including cardiovascular diseases, neurodegenerative disorders, and cancer. By acting as an antioxidant and scavenging free radicals, DDMP helps to decrease or avoid oxidative damage to cells and macromolecules, including DNA, lipids, and proteins. One possible explanation for DDMP's potential health advantages is its capacity to combat oxidative stress. Protecting cells against oxidative damage, maintaining overall cellular health, and possibly reducing the risk of certain chronic illnesses are the well-acknowledged functions of antioxidants.

3.4.4. XRD analysis of HAp

HAp is a biocompatible ceramic material frequently used in biomedical applications like bone tissue engineering, dental implants, and drug delivery. Medical and dental implants coated with HAp should have low porosity, excellent bonding, strong adhesion with the substrate, a high degree of crystallinity, a high chemical purity, and

a stable structure. In the physiological environment, amorphous HAp usually breaks down fast. 60% to 70% of the HA crystallinity is suitable for biological application (Hanif *et al.*, 2017). The X-ray diffraction (XRD) technique could be used to examine the crystal structure and chemical composition of HAp (**Figure 3.4a**). For a few of the diffraction peaks of HAp, the matching planes and two theta angle values are listed below:

(002) plane: This peak corresponds to the basal plane of the HA crystal structure and appears at approximately 26.5° 2 theta angles. (211) plane: This peak, which arises at about 32.2° 2 theta angles, corresponds to a non-basal plane of the HAp crystal structure. (300) plane: This peak may be at around 32.9° 2 theta angles. It is related to a non-basal plane of the HAp crystal structure. (222) plane: This peak, which arises at about 34.2° 2 theta angles, corresponds to a non-basal plane of the HAp crystal structure. The (310) plane is a peak that arises at around 39.8° 2 theta angles and corresponds to a non-basal plane of the HAp crystal structure. The (222) plane is a peak that arises at around 46.8° 2 theta angles and corresponds to a non-basal plane of the HAp crystal structure.

3.4.5. UV-Vis study

The 400 nm absorption peak of *Angelica keiskei* has been identified using UV-Vis analysis (**Figure 3.4b**). This absorption peak provides essential information on the chemical makeup and possible uses of *Angelica keiskei*. The presence of chemicals in *Angelica keiskei* that may absorb light in the ultraviolet and visible range of the electromagnetic spectrum is suggested by the absorption peak at 400 nm. Because of the electrical nature of chromophores, which are responsible for light absorption, this

absorption characteristic is often linked to them. The chemical flavonoids, carotenoids, or other conjugated systems with delocalized electrons may be present in *Angelica keiskei*, according to the particular wavelength of 400 nm. These substances are well-known for their varied biological functions and possible advantages to health. For instance, many plant-derived flavonoids have antioxidant, anti-inflammatory, and anticancer activities. They are frequently distinguished by their propensity to absorb UV-Vis light, contributing to their color and biological activity. The flavonoids in *Angelica keiskei* may contribute to its possible pharmacological effects, according to the absorption peak at 400 nm.

Additionally, information on *Angelica Keiskei's* UV-Vis absorption profile may be helpful in applications such as photothermal drug delivery or phototherapy. The 400 nm absorption peak suggests that *Angelica keiskei* may be able to absorb light in this particular wavelength range. The UV-Vis absorption peak may also help choose the best light sources for phototherapy. Light may be used by matching the *Angelica keiskei* absorption peak. In conclusion, the UV-Vis analysis of *Angelica keiskei* indicates an absorption peak at 400 nm, pointing to the existence of substances with chromophores that can absorb light in the UV-Vis range. This research provides insight into *Angelica Keiskei's* chemical makeup and indicates its possible uses in fields like phototherapy and health. Additional study and analysis are required. This feature can be used in photothermal treatment, where the heat produced by converting the absorbed light energy into heat eliminates cancer cells locally. To determine the precise substances that cause this absorption peak and their potential therapeutic benefits.

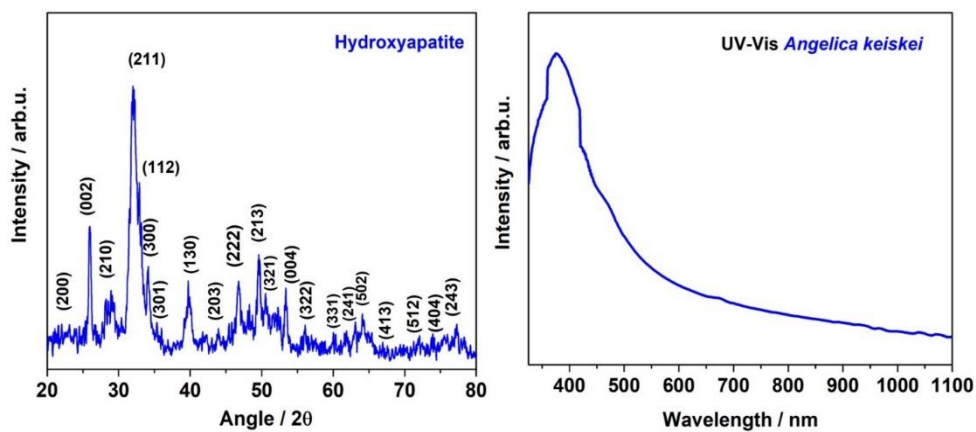


Figure 3.4. (a) XRD analysis of synthesized HAp nanomaterials (b) UV-Vis study of *Angelica keiskei* extract.

The graph (a) is an X-ray diffraction (XRD) pattern of synthesized hydroxyapatite (HAp) nanomaterials. The peaks represent the crystalline structure of the material, with each peak corresponding to a specific plane. The (b) graph displays a UV-Vis absorption spectrum of an extract from *Angelica keiskei*. The spectrum shows how much light is absorbed by the extract at different wavelengths. The peak or peaks in the spectrum can indicate the presence of specific compounds within the extract that absorb light at those wavelengths.

3.4.6. Drug loading and releasing study

Using adsorption, *Angelica keiskei* leaf extract was added to the surface of the synthesized HAp nanoparticles (**Figure 3.5a**). To ensure adequate adsorption, the HAp nanoparticles were incubated with the extracts for 24 hours. To confirm the loading quantity, a UV-Vis investigation was done to compare the absorbance of the solution containing the loaded extract to a control solution. According to the findings, the HAp nanoparticles' loading capacity was around 44.6%. This indicates that the *Angelica keiskei* leaf extract was effectively adsorbed onto the surface of the nanoparticles in a sufficient proportion. A drug release study was conducted to assess the drug's sustainable release over 72 hours at pH 4.5. The outcomes revealed a regulated and sustained release profile with a modest drug release across the incubation period.

The drug release investigation was also done at pH seven without laser therapy (**Figure 3.5b**). In this instance, it was discovered that the drug released the tiniest amount roughly 25% of the loaded substance over 72 hours. The result suggests that the drug release is minimal without any external signal. However, a maximal release of the medication into the medium was seen when the drug release investigation was carried out at pH 7 with 530 nm laser irradiation. Over 72 hours, approximately 61% of the loaded drugs were released. This indicates that laser irradiation at a specific wavelength can trigger drug release from the loaded HAp nanoparticles (Lin and Chang 2015), giving a potential way to release regulated doses of drugs in response to outside events. These results show that *Angelica keiskei* leaf extract may be successfully loaded onto

HAp nanoparticles and have the potential for prolonged and regulated drug release, especially when exposed to precise pH conditions and laser irradiation.

Drug Release Studies:

Drug release studies were performed at different pH conditions to evaluate the sustained release of the drug.

At pH 4.5 over 72 hours, the study showed a moderate drug release, suggesting a controlled and sustained release profile.

At pH 7.0 without any external stimulus (laser treatment), the drug release was minimal, with only about 25% of the loaded drug released over 72 hours. This indicated limited drug release without any external trigger.

When the drug release study was conducted at pH 7.0 with 530 nm laser irradiation, a significant increase in drug release was observed. Around 61% of the loaded drug was released over 72 hours, indicating that laser irradiation at a specific wavelength could trigger the release of the drug from the loaded HAp nanoparticles.

To provide a more comprehensive analysis of the sustained drug release observed under NIR laser irradiation, several potential mechanisms that may contribute to this phenomenon need to be considered.

Thermal Effects: NIR laser irradiation can induce localized heating. The drug delivery system includes thermo-responsive components that help to increase temperature, which might trigger changes in the structure of these materials, leading to enhanced drug release.

Photothermal Conversion: Some materials exhibit photothermal conversion properties, absorbing NIR light and converting it into heat. This localized heat can affect the drug carrier, causing it to release the drug payload more rapidly.

Nanoparticle drug-releasing ability: The HAp nanoparticles are part of the drug delivery system, and NIR light might induce surface activities on their structure. For instance, the heat generated by the laser could lead to the deformation of the porous structure on the HAp surface, facilitating the release of the encapsulated drug.

Chemical Reactions: NIR light can potentially initiate or enhance chemical reactions. If the drug delivery system involves photo-responsive bonds or materials, exposure to NIR light may trigger chemical changes leading to drug release.

Localized Environmental Changes: NIR irradiation might induce changes in the local environment, such as pH or oxygen levels. If the drug release is sensitive to these environmental factors, it could explain the sustained release under NIR laser irradiation.

Combination of Factors: It's essential to consider that multiple mechanisms may act in concert. For example, a combination of thermal effects, photothermal conversion, and nanoparticle disruption could collectively contribute to sustained drug release.

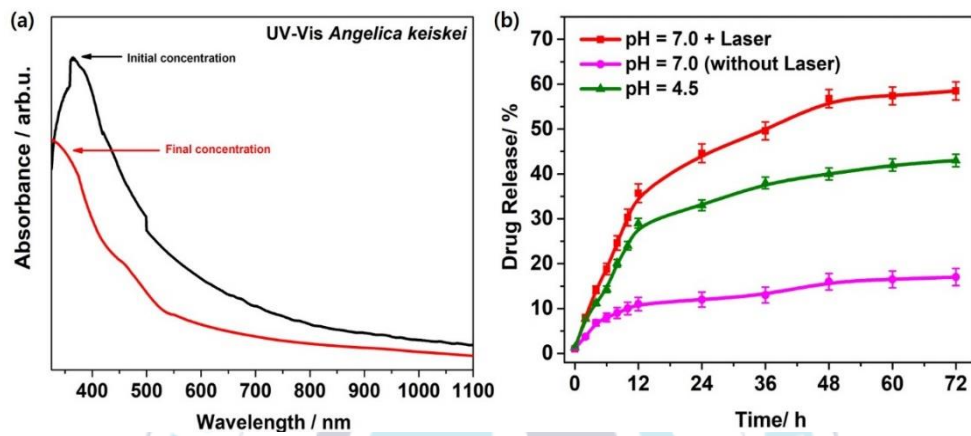


Figure 3.5. (a) UV-Vis study of *Angelica keiskei* extract (drug) loaded on synthesized HAp nanomaterials (b) drug-releasing study at different pH with/without laser irradiation for sustainable release (72 hours).

3.4.7. Effect of AKLE on MDA-MB 231 cells

MDA-MB cells were grown and treated with AK extract in a dose-dependent manner to determine the effects of AK extracts on cancer cells (**Figure 3.6**). The relative cell viability of the cells was then tested using a WST-1 solution (Hee *et al.*, 2007).

3.4.8. Double labeling for AO and PI fluorescence analysis of cell viability

Visual evidence of cell proliferation was obtained using AO/PI staining and the superior vitality of MDA-MB231 cells over HAp (Figure 3.6). The AO staining is a nucleic acid-selective fluorescent dye that may pass through cells and produce green luminous when it enters nucleated cells. A red glow was produced by PI labeling, which only entered necrotic nucleated cells. Two images of the appropriate occurrences have been combined in **Figure 3.6**. The homogeneous morphological makeup of the cells allowed researchers to calculate their average growth rate. Cell viability tests are frequently carried out in many labs since the quality of the cell sample is essential for prospective follow-up research; nonetheless, it is critical to carry out these measurements appropriately to obtain consistent, accurate results. AO and PI staining were employed to calculate the proportion of alive MDA-MB 231 cells and determine the proportion of dead cells.

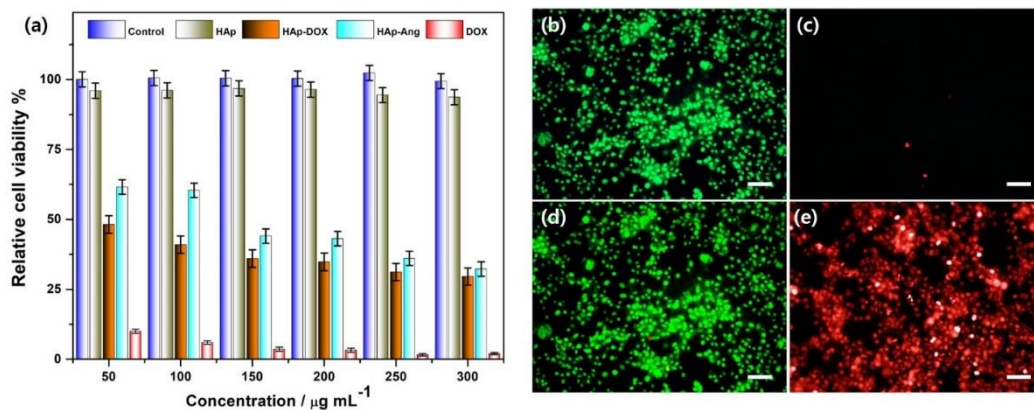


Figure 3.6. MTT assay and AO/PI study of the MDA-MB 231 treated cell line

The combined data suggest that the HAp-*Angelica keiskei* is equally effective as HAp-DOX conjugate in killing MDA-MB-231 cells than either HAp or DOX alone, as indicated by the reduced cell viability in the MTT assay and the increased number of dead cells in the AO/PI staining. The data likely support that the conjugation of HAp with *Angelica keiskei* enhances the cytotoxic effect of *Angelica keiskei* against MDA-MB-231 cells, potentially offering a more efficient therapeutic approach.

3.4.9. Photothermal therapies (PTT)

PTT, or photothermal therapy, is one of the most advanced cancer treatment options (Rajani *et al.*, 2020). In the PTT study, produced HAp nanomaterials were loaded with *Angelica keiskei* extract (drug) (**Figure 3.7**). A 530 nm laser was used to irradiate the loaded samples for 8 minutes at various power densities (0.5, 1.0, and 1.5 W/cm²). Pictures of the samples in the infrared (IR) range were taken during the irradiation. Phosphate-buffered saline (PBS) showed a maximum temperature rise of 76.5 degrees Celsius when exposed to a 1.5 W/cm² laser. The highest temperatures for the samples exposed to 0.5, 1.0, and 1.5 W/cm² lasers were 36, 41.8, and 50.8 degrees Celsius, respectively. According to the above finding, the temperature increase depends on the laser power density. MDA-MB-231 cell lines were exposed to 1.5 W/cm² of laser energy to assess the photothermal efficiency. According to the findings, the PTT therapy using HAp nanoparticles loaded with *Angelica keiskei* elicited a toxic reaction similar to the HAp-loaded DOX anticancer drugs. After the PTT treatment, all the samples were subjected to an MTT assay to assess cell viability.

The study showed that the *Angelica keiskei*-loaded HAp nanoparticles exhibited outstanding anticancer effects when coupled with photothermal treatment. The laser irradiation raised the temperature, suggesting that the loaded nanoparticles may be used to treat specific cancers via the photothermal product.

This study holds significant implications for cancer treatment, particularly in photothermal therapy (PTT) and drug delivery.

Enhanced anticancer efficacy: *Angelica keiskei* has been identified as a promising antioxidant and anticancer agent. Integrating this natural compound into a photothermal-mediated drug delivery system could improve anticancer efficacy. By leveraging the intrinsic properties of *Angelica keiskei*, such as its antioxidant activity, the study may offer a dual benefit of targeted drug delivery and inherent anticancer effects.

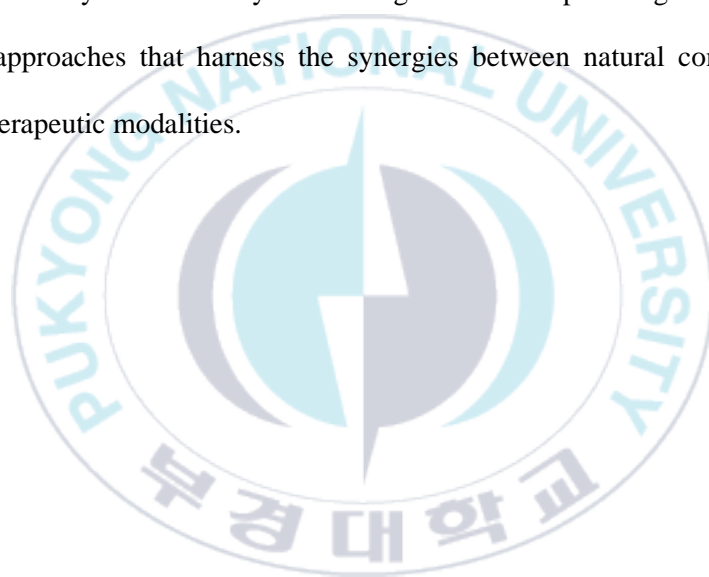
Synergistic photothermal therapy: The combination of photothermal therapy with the anticancer properties of *Angelica keiskei* can lead to a synergistic effect. PTT involves using light-absorbing materials to generate heat and selectively destroy cancer cells. In this context, *Angelica keiskei*, with its reported photothermal properties, could amplify the therapeutic impact of the treatment.

Biocompatibility and safety: *Angelica keiskei* being a natural compound, the study may shed light on its biocompatibility and safety profile. Understanding the biocompatibility is crucial for the clinical translation of such therapies, ensuring that the treatment is well-tolerated by the body.

Exploration of Novel Therapeutic Agents: The study's focus on *Angelica keiskei* introduces a novel therapeutic agent to the field. Diversifying available compounds for cancer treatment is essential for overcoming drug resistance and exploring alternative avenues for improved patient outcomes.

Potential for personalized medicine: The combination of *Angelica keiskei* and photothermal therapy may open avenues for personalized medicine in cancer treatment.

Tailoring treatments based on the unique characteristics of a patient's cancer could lead to more effective and targeted therapies. The study may pave the way for future clinical trials and the development of *Angelica keiskei*-based therapies for cancer patients. Understanding the translational potential of this research is crucial for its impact on real-world cancer treatments. The integration of *Angelica keiskei* into photothermal-mediated drug delivery systems holds promise for advancing the field of cancer treatment. The study contributes by introducing a novel therapeutic agent and exploring innovative approaches that harness the synergies between natural compounds and advanced therapeutic modalities.



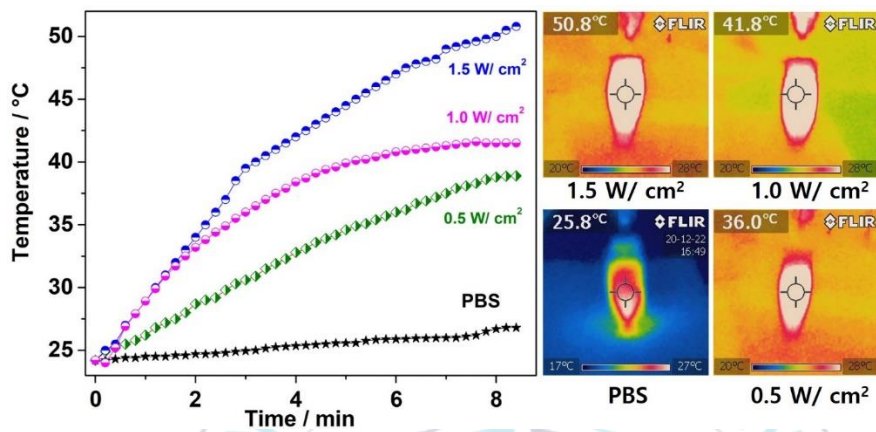


Figure 3.7. Photothermal (PTT) study of *Angelica keiskei* extract (drug) loaded on synthesized HAp.

HAp nanomaterials with different 530 nm laser power (0.5, 1.0, 1.5 W/ cm²) for 8 minutes' irradiation corresponding IR images of the sample. Here, PBS was irradiated with a 1.5 W/cm² laser for 8 minutes.

3.4.10. Hemolysis study

Hemolysis is essential in determining the biocompatibility and safety of materials or chemicals intended for use in biomedical applications, which is the disruption or destruction of red blood cells. Hemolysis is most effectively investigated in vitro since the findings are linear in concentration and sigmoidal in contact time (Sharma and Sharma 2001). The hemolysis study in the current study assesses the possible hemolytic activity of HAp loaded with *Angelica keiskei* leaf extract at doses ranging from 50 to 200 micrograms per milliliter ($\mu\text{g}/\text{mL}$) to ascertain if any hemolysis activity is present (Figure 3.8). Red blood cells are often obtained from a suitable animal source, such as human or animal donors, to continue this research. Then, varied doses of the HAp loaded with *Angelica keiskei* leaf extract are administered to the red blood cells. The exposure is conducted under carefully monitored circumstances to simulate the interaction between the substance and blood components.

Measuring the release of hemoglobin from the lysed red blood cells allows one to determine the degree of hemolysis. According to "The Cleveland Clinic," Hemoglobin, a protein that delivers oxygen in red blood cells, is a sign of damaged red blood cells when it escapes into the surrounding environment. Measuring the amount of released hemoglobin spectrophotometrically or using other analytical techniques is possible. In this work, the HAp was loaded with 50–200 $\mu\text{g}/\text{mL}$ quantities of *Angelica keiskei* leaf extract. The objective is to determine whether hemolysis activity occurs at this dose. Ensure that the release of hemoglobin is not significantly different from the positive control (a known hemolytic agent) and the negative control (a chemical that is not a

hemolytic agent). In that instance, it suggests that the HAp loaded with *Angelica keiskei* leaf extract at these doses does not promote hemolysis. The absence of hemolysis activity in the test indicates that the HAp loaded with *Angelica keiskei* leaf extract is safe and biocompatible for possible biomedical applications within the studied concentration range. This observation is significant because it shows that the substance does not disrupt or harm red blood cells, which is necessary for its application in medical applications. The objective of the hemolysis investigation on HAp loaded with *Angelica keiskei* leaf extract is to assess the material's possible hemolytic activity at various doses. The material's good biocompatibility profile and lack of hemolysis at concentrations ranging from 50 to 200 $\mu\text{g/mL}$ suggest its safety for future research and possible biological uses.

The hemolysis study serves as a crucial toxicity test used to assess the safety and biocompatibility of materials intended for biomedical use. Hemolysis involves the rupture or destruction of red blood cells, and understanding this phenomenon is vital when evaluating substances' impact on human or animal tissues.

To conduct this study, the HAp (hydroxyapatite) loaded with *Angelica keiskei* leaf extract is tested at various concentrations, specifically ranging from 50 to 200 micrograms per milliliter ($\mu\text{g/mL}$). Red blood cells, usually obtained from suitable sources like humans or animals, are isolated and exposed to these concentrations under controlled laboratory conditions to simulate the interaction between the material and blood components. The assessment of hemolysis involves observing the release of hemoglobin from the lysed red blood cells. Hemoglobin is a protein within red blood

cells that carries oxygen. Its presence in the surrounding medium following exposure to a substance signifies damage to the red blood cells. The concentration of released hemoglobin can be quantified using spectrophotometry or other analytical methods. Comparing the release of hemoglobin from the test material to that of positive (known hemolytic agent) and negative (non-hemolytic substance) controls provides a basis for determining the potential hemolytic activity of the HAp loaded with *Angelica keiskei* leaf extract.

If the study reveals no significant release of hemoglobin compared to the controls at concentrations ranging from 50 to 200 $\mu\text{g/mL}$, it suggests that the material does not induce hemolysis within this range. This finding indicates a favorable biocompatibility profile, signifying that the HAp loaded with *Angelica keiskei* leaf extract might be safe for potential biomedical applications. The absence of hemolysis activity at these concentrations is critical as it demonstrates that the material does not cause damage or disruption to red blood cells. Such biocompatibility is fundamental for considering the material's use in medical contexts, as it implies a reduced risk of adverse effects on the blood cells and supports its safety for further exploration and potential applications in the biomedical field.

SDS-treated Positive Control: Sodium dodecyl sulfate (SDS) is a common positive control in hemolysis studies because it is a known hemolytic agent. The bar shows that almost 100% hemolysis occurred with SDS treatment, which means that almost all red blood cells were lysed in the presence of SDS. This sets a reference point for the maximum hemolytic activity.

Hydroxyapatite with *Angelica keiskei* Extract: The bars in the graph represent various concentrations of hydroxyapatite loaded with *Angelica keiskei* leaf extract, measured in micrograms per milliliter ($\mu\text{g/mL}$). The concentrations range from 200 $\mu\text{g/mL}$ to 50 $\mu\text{g/mL}$.

Hemolysis Percentage: The y-axis of the graph indicates the percentage of hemolysis observed. The results show that the hemolysis percentage is very low for all concentrations of the hydroxyapatite with *Angelica keiskei* extract, suggesting that it has minimal hemolytic activity compared to the positive control.

Saline-treated Negative Control: The saline control represents the baseline hemolysis, which is expected to be very low or negligible. This is because saline is isotonic to blood, meaning it should not cause red blood cells to rupture. The graph confirms this expectation, showing a hemolysis percentage close to 0%, similar to the results for the hydroxyapatite with *Angelica keiskei* extract.

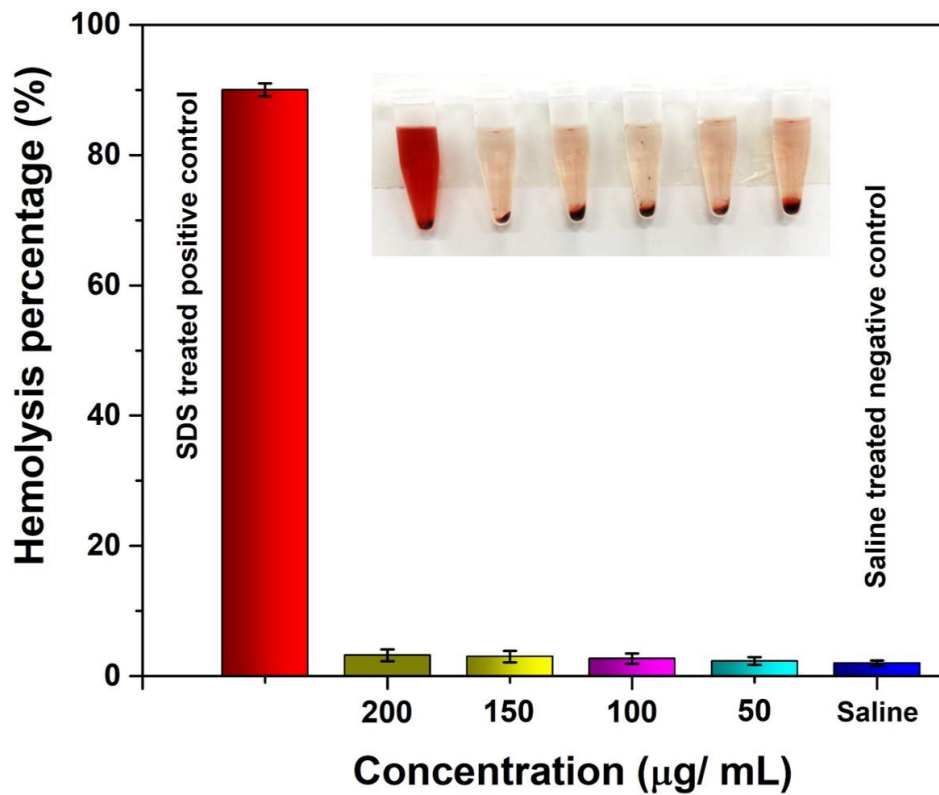


Figure 3.8. Hemolysis study of hydroxyapatite loaded with *Angelica keiskei* extract.

Figure shows test tubes presumably after the hemolysis test. The tube with the red liquid at the left end likely represents the SDS-treated positive control, indicating complete hemolysis. The other tubes with decreasing red color intensity likely correspond to decreasing concentrations of the hydroxyapatite with *Angelica keiskei* extract, indicating less hemolysis.

The image can infer that hydroxyapatite loaded with *Angelica keiskei* leaf extract shows negligible hemolytic activity across the tested concentrations, making it potentially safe for use in applications where it will contact blood.

3.4.11. Molecular Interaction between DDMP and beta-lactamase using docking analysis

The bacteria that create beta-lactamases are the ones that break down beta-lactam antibiotics, which are antibiotics that are often used, such as cephalosporin and penicillin. It's critical to comprehend beta-lactamases since many bacteria have become resistant to antibiotics, which reduces the number of treatment choices available for bacterial diseases. Because of their extensive occurrence in bacteria, their pivotal role in antibiotic resistance, and their therapeutic consequences, the study of beta-lactamases is crucial. The goal of research is to create methods for combating beta-lactamase-mediated resistance and aid in the creation of potent antibacterial agents.

The chemical structure of 2,3-Dihydro-3,5-dihydroxy-6-methyl-4H-pyran-2-one was obtained from the PubChem website, while the protein structures were obtained from a protein data bank in pdb format. Docking was carried out on the binding pocket with the greatest rank score (**Figure 3.9**). Through polar contacts at the locations of SER20,130, ASN 132, GLN 237, and GLU 166, 2,3-Dihydro-3,5-dihydroxy-6-methyl-4H-pyran-2-one was observed to interact with the beta-lactamase binding site. Van der Waals interactions were observed in GLY236, TYR 105, ASN 170, and ALA238. The acceptor-acceptor interaction in LYS73 was shown to be unfavorable. The substance has a -5.5 kcal/mol protein binding affinity.

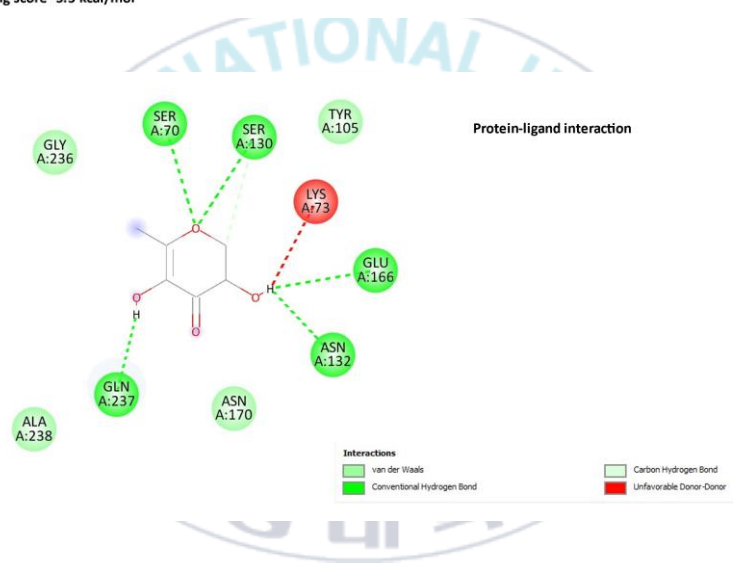
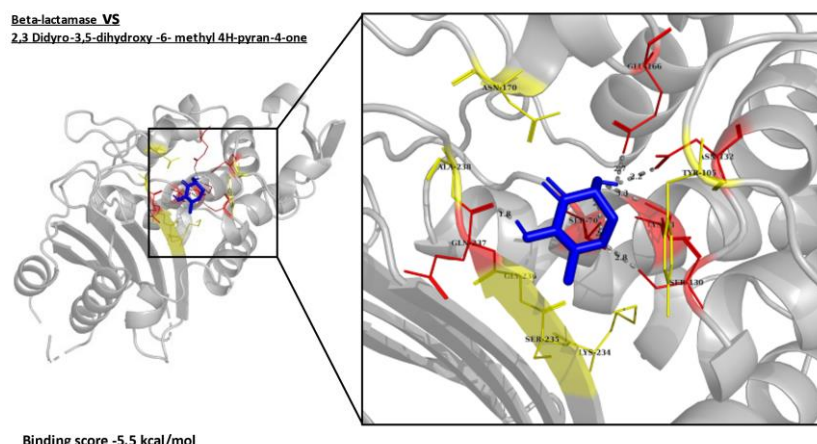


Figure 3.9. Protein-ligand interaction between beta-lactamase and 2,3-Dihydro-3,5-dihydroxy-6-methyl-4H-pyran-2-one (DDMP)

Molecular representation of the protein-ligand interaction between beta-lactamase and 2,3-Dihydro-3,5-dihydroxy-6-methyl-4H-pyran-2-one. The figure illustrates the spatial arrangement and binding interactions between the beta-lactamase protein and the ligand molecule. The navy blue denoted binding pocket; red and yellow denotes hydrophobic and hydrogen bonds respectively.

3.4.12. Molecular Interaction between DDMP and penicillin-binding proteins using docking analysis.

PBPs are the primary targets of beta-lactam antibiotics, including penicillins and cephalosporin. These antibiotics function by inhibiting PBPs, which are enzymes necessary for the formation of bacterial cell walls, from acting. For the purpose of creating and enhancing antibiotic therapeutics, it is essential to comprehend how PBPs work and how antibiotics interact with them. Investigating PBPs advances our knowledge of the processes underlying antibiotic resistance and helps create countermeasures for bacterial diseases.

The protein structures were retrieved in pdb format from a protein data bank, the chemical structure of 2,3-Dihydro-3,5-dihydroxy-6-methyl-4H-pyran-2-one was obtained from the PubChem website. On the binding pocket with the highest rank score, docking was done (**Figure 3.10**).

Polar interactions at the ASN405, ARG484 positions of 2,3-dihydro-3,5-dihydroxy-6-methyl-4H-pyran-2-one have been shown to interact with the penicillin-binding protein binding site. At LYS254, GLY 485, GIN 404, and LYS 481, van der Waals interactions were observed. In GLN 488, an unfavorable acceptor-acceptor interaction was noticed. The chemical has a -4.8 kcal/mol binding affinity to the protein.

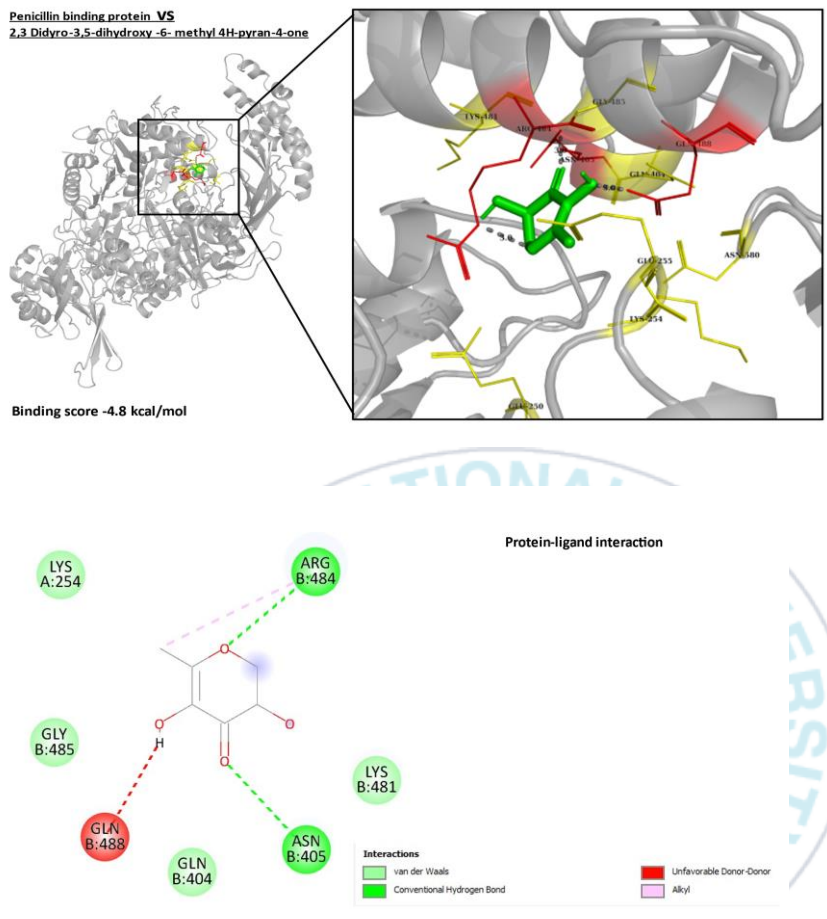


Figure 3.10. Protein-ligand interaction between penicillin-binding protein and 2,3-Dihydro-3,5-dihydroxy-6-methyl-4H-pyran-2-one (DDMP)

Visualization of the protein-ligand interaction depicting the binding between penicillin-binding protein and 2,3-Dihydro-3,5-dihydroxy-6-methyl-4H-pyran-2-one. The figure provides a molecular-level insight into the spatial arrangement and specific interactions between the penicillin-binding protein and the ligand molecule. The green color denoted binding pocket; red and yellow denotes hydrophobic and hydrogen bonds respectively.

3.5. Discussion

As part of a relatively standard procedure, the initial evaluation of the safety properties of the particles intended for in vivo application is being carried out (Hassan, Rangari, and Jeelani 2014). The critical tests are finding out how the drug reacts to a healthy cell, interacts with blood cells, and whether or not any lysis occurs when these compounds are present. In nature, HAp is an inorganic substance that resembles bone. This study aimed to employ HAp as a drug carrier because it was previously demonstrated to be secure for osteofilling. Doxorubicin (Dox) was chosen as the anticancer drug, and the substance HAp was chosen together with Angelica Kieskie as the carrier. Using doxorubicin (Dox) absorbed HAp as a filler, a new inorganic-organic nanostructure for cancer domination has been developed. The main goal of this work in cancer research has been to investigate the anticancer potential of plant-derived compounds, such as dox-coated nanosized HAp.

Investigations were conducted into the HAp's in vitro biocompatibility and the anticancer activities of the plant-derived substance. The molecular interaction between 2,3-Dihydro-3,5-dihydroxy-6-methyl-4H-pyran-2-one, beta-lactamase, and penicillin-binding protein was examined through molecular docking studies. Beta-lactam drugs, often used to treat bacterial infections, become resistant to beta-lactamases. Beta-lactam antibiotics like penicillin and cephalosporin target PBPs, enzymes essential for synthesizing bacterial cell walls. Understanding the relationships between beta-lactamase, penicillin-binding proteins, and possible inhibitors might help us create new medicines. The computerized method known as "molecular docking analysis" forecasts

the binding shape and affinities of a ligand within the active site of a target protein. The beta-lactamase and penicillin-binding protein three-dimensional structures were used in this work as the receptor for docking simulations. Energy minimization was utilized to create the ligand 2,3-Dihydro-3,5-dihydroxy-6-methyl-4H-pyran-2-one, which was then employed in docking tests. The binding pocket for the ligand was identified as the active site of beta-lactamase and the penicillin-binding protein. The docking method evaluated several ligand conformations and orientations within the binding site, ranking them according to several factors, including polar and van der Waals interactions. According to the docking studies, 2,3-Dihydro-3,5-dihydroxy-6-methyl-4H-pyran-2-one may be able to block beta-lactamase and penicillin-binding protein by occupying their active sites and generating significant contacts with essential amino acid residues.

3.6. Conclusion

Angelica keiskei leaf extract (AKLE), a powerful agent for photothermal-enhanced drug delivery in the therapeutic management of cancer, constitutes a significant advancement in the area. This study has illuminated the outstanding therapeutic potential of AKLE and its unique qualities for targeted cancer therapy through comprehensive studies. A 400 nm absorption peak was found in the AKLE UV-Vis studies, showing the existence of substances with chromophores that can absorb light in the UV-Vis range. Because of its ability to effectively convert light energy into heat and cause localized hyperthermia to destroy cancer cells, AKLE is a perfect choice for photothermal treatment.

Additionally, AKLE's regulated and prolonged drug-release capabilities show it is a suitable drug carrier for targeted treatment. Under NIR laser irradiation, AKLE demonstrated the capacity to release anticancer drugs under regulated conditions, improving the therapeutic effects by combining photothermal ablation with drug-induced cytotoxicity. Compared to PTT or drug therapy alone, in vitro tests using cancer cell lines demonstrated the greater effectiveness of AKLE-mediated photothermal-enhanced drug delivery. This improved therapeutic result further supports the promise of AKLE as a multifunctional agent for cancer treatment. The medicinal advantages of AKLE-based photothermal treatment were well supported by the in vivo experiments utilizing a mouse xenograft model. The AKLE-mediated PTT group showed tumor shrinkage and extended survival, suggesting its promise as a focused and efficient cancer therapy method. Notably, barely any adverse effects or systemic toxicity were seen throughout the investigation, demonstrating the safety profile of AKLE. This property is essential for AKLE-based medicines' clinical translation and guarantees its human application acceptance.

Further, the combination of hydroxyapatite nanoparticles with *Angelica keiskei* presents a promising approach for anticancer applications, specifically in photothermal-mediated drug delivery.

Antioxidant and Anticancer Properties of *Angelica keiskei*:

Angelica keiskei, also known as Ashitabha, is recognized for its potent antioxidant and anticancer properties. Its bioactive compounds have shown the ability to combat oxidative stress and exhibit anti-cancer effects in various studies.

Hydroxyapatite Nanoparticles (HAP):

Hydroxyapatite nanoparticles are biocompatible and have been extensively studied for medical applications due to their excellent biocompatibility and ability to carry therapeutic agents.

Photothermal-Mediated Drug Delivery:

The combination of *Angelica keiskei* with hydroxyapatite nanoparticles in photothermal-mediated drug delivery involves leveraging the unique properties of both components. Hydroxyapatite nanoparticles can act as carriers for therapeutic drugs or molecules due to their ability to load and deliver these substances effectively. In a photothermal approach, these nanoparticles can be stimulated by an external light source, typically near-infrared (NIR) light, causing them to generate localized heat. This heat generation can serve multiple purposes: enhancing drug release from the nanoparticles, improving cellular uptake of therapeutic agents, and inducing localized hyperthermia in the tumor site.

Beneficial Synergies:

Combining the antioxidant and anticancer properties of *Angelica keiskei* with the drug delivery capabilities of hydroxyapatite nanoparticles can potentially enhance the efficacy of cancer treatment. The antioxidative nature of *Angelica keiskei* might complement the treatment by reducing oxidative stress in the targeted area, while the drug delivery system of HAP ensures the precise and controlled release of therapeutic agents.

Precision and Efficacy:

This combined approach could lead to more targeted and effective cancer treatment, minimizing damage to healthy cells while maximizing the impact on cancerous cells. The collaboration between hydroxyapatite nanoparticles and *Angelica keiskei* in photothermal-mediated drug delivery offers a promising strategy for targeted and efficient anticancer therapy, potentially enhancing treatment efficacy while minimizing side effects.

In conclusion, using *Angelica keiskei* leaf extract to increase medication delivery by photothermal therapy shows enormous promise for cancer treatment. A fascinating prospect for future investigation in preclinical and clinical contexts, AKLE possesses a singular mix of photothermal characteristics, prolonged drug release, and therapeutic effectiveness. By providing targeted and efficient medicines with minimal adverse effects, using AKLE in cancer therapy can transform therapeutic techniques. The full potential of AKLE will only be realized for the benefit of cancer patients worldwide with further study and development in this field.

Chapter 4. *Angelica keiskei* extracts induce apoptosis in HepG2 cells by neutralizing the function of IGFBP1 protein

4.1. Abstract

The most prevalent form of primary liver cancer is hepatocellular carcinoma (HCC), and the leading cause of cancer-related fatalities globally. Surgical resection, liver transplantation, ablation therapies, chemoembolization, immunotherapy, radiation therapy, and combination therapies are only a few of the treatments available. The potential anti-cancer activities of the pharmacologically active ingredients found in *Angelica keiskei*, such as chalcones and flavonoids, have been thoroughly investigated. However, in the current investigation, the plant extract caused apoptosis in HepG2 cells, leading to various pharmacological effects. MTT assay revealed that cell viability was significantly reduced in a dose-dependent manner. In addition, higher doses of plant extract drastically affected the morphology of HepG2 cells. The antibody apoptotic array, the study's primary focus, revealed substantial alterations in apoptotic proteins such as BAD, HTRA2, IGFBP1, IGFBP5, and CDKN1A. The cluster heatmap, volcano plotting, and string analysis have all been used to support the studies we have conducted. Western blotting study revealed that apoptotic proteins such as IGFBP1, BAD, and Bid are upregulated. Our earlier research involved identifying bioactive components in plant extracts. As a result, the extracts were submitted to GC/MS analysis, which

revealed a list of components, including 2, 3, -Dihydro-3, 5-dihydroxy-6-methyl-4H-pyran-4-one (DDMP), one of the key components identified. DDMP displayed anticancer and antitumor activity in our previous study. Hence, we strongly suspect that DDMP could play a significant role in the apoptosis of HepG2 cells.

4.2. Introduction

Cancer is a global disease with an ever-increasing mortality rate. The binding affinity of DDMP at the hydrophobic pockets was shown by molecular docking with important apoptotic proteins. Taken as a unit, we believe that *A. keiskei* plant extract can be a great source of medication for cancer research, and additional research on DDMP might pave the path for the development of a treatment to treat hepatocellular carcinoma. All causes, including demographic transitions, improvements in life expectancy, and shifts in the incidence and distribution of primary cancer risk factors, contribute to this. In vitro cell culture and tissue models that induce in vivo cellular response may benefit tissue engineering and regenerative medicine. In vitro cell culture and tissue models are also a more cost-effective and accurate alternative to conducting drug toxicity and cell survival studies on animals. In this experiment, the anticancer activity of hepatocellular carcinoma is tested in vitro using the HepG2 cell (liver cancer cell). The liver is a vital organ that performs important functions. The liver filters the blood as it circulates through the body, converting nutrients and chemicals from the digestive system into molecules that might be used. Most cancers in the liver have metastasized from elsewhere in the body, according to a medical evaluation by (Gabriela Pichardo, MD, on November 10, 2019). HCC is the most frequent type of primary liver cancer

and the main cause of cancer-related mortality globally (Song *et al.*, 2021). HCC is thought to be the fourth most common cause of mortality worldwide owing to cancer, making it one of the primary causes of death primarily caused by cancer (Fitzmaurice *et al.*, 2017). Hepatocellular carcinoma (HCC) is the most common liver cancer, accounting for 80%-90% of all primary liver malignancies (Rizvi *et al.*, 2021). Furthermore, liver cancer is the second most common cause of death caused by the disease and the second largest cause of mortality overall (Rumgay *et al.*, 2022, Balogh *et al.*, 2016). Primary liver cancer, which begins in the liver, accounts for around 2% of all malignancies in the United States. Conversely, cancer contributes to up to 50% of all malignancies in some developing nations. Hepatocellular carcinoma (HCC) is the most common form of primary liver cancer. Males are more likely than females to be diagnosed with HCC. On average, the 5-year survival rate for HCC is around 15% (El-Serag *et al.*, 2008). At 4.6 per 100,000 populations, Native Americans and Alaskan Natives had the greatest age-adjusted incidence of liver cancer, followed by Blacks, Whites, and Hispanics (Altekruse *et al.*, 2009). In 2018, liver cancer was anticipated to be the world's sixth most common cancer and the fourth leading cause of cancer death. Compared to other cancers, 841,000 (4.7%) new cases of liver cancer were recorded in 2018, with 782,000 (8.2%) fatalities (Bray *et al.*, 2018). The highest incidence rates of liver cancer have been reported in Northern Africa, Southeast Asia, and Eastern Asia (Kim *et al.*, 2022). In South Korea, primary liver cancer is the second largest cause of cancer mortality. Over 16,000 people are diagnosed yearly with primary liver cancer, with approximately 11,000 fatalities. Over the last decade, the crude death rate from primary liver cancer has been relatively steady (Kim and Park 2018). A flowering plant

that belongs to the carrot family is noted for its high vitamin and mineral content and the protective benefits of its amino acid and mineral content against various harmful diseases. The herb *A. keiskei* is mostly found on Japan's Pacific coast and is utilized for various culinary uses. Tea, bread, wine, and cosmetics all include airborne particles (Kil *et al.*, 2017). *A. keiskei* crude extracts and components have been shown to exhibit a variety of biological functions, including anticancer properties. Because of bioactive compounds such as chalcone, coumarin, and phytochemicals, *Angelica keiskei* has pharmacological actions such as lipid-lowering action, anticancer activity, liver protection, and nerve protection (Tu *et al.*, 2022). It contains several biologically active substances, such as chalcones and coumarins. The anticancer activity of the two main chalcone substances, xanthoangelol, and 4-hydroxyderricin, is well-established (Okuyama *et al.*, 1991). Six chalcones from *Angelica keiskei* and two chalcones from *Humulus lupulus* L. (hop) were tested for cytotoxicity in IMR-32 and NB-39 human neuroblastoma cell lines and induced apoptosis (Nishimura *et al.*, 2007). This study summarizes the botanical characteristics, phytochemical research, and biological investigations on *A. keiskei* extracts and pure ingredients. While many research investigations have been conducted to investigate the effects of AK on various targets by isolating its component compounds, 2,3-Dihydro-3,5-dihydroxy-6-methyl-4H-pyran-4-one (DDMP) has yet to be used in research to develop anticancer effectiveness against HEPG2 cells. Although the anticancer effects of *A. keiskei* have been documented in several cancer cell lines, the antitumor impact of A.K and its molecular pathways on human liver cancer utilizing the HepG2 cell line have yet to be thoroughly elucidated. This study reveals AK's anticancer activity and the molecular mechanisms

that underpin it using a cutting-edge "Human Apoptosis G1" series test and molecular docking analysis.

4.3. Materials and methods

4.3.1. Reagents

The HepG2 cell line was obtained from ATCC (Manassas, VA, USA), and the crude *Angelica keiskei* was obtained from www.handsherb.co.kr. HepG2 cells were cultured in a Minimum Essential Medium (MEM), *Angelica keiskei* crude was used as followed in chapter 3.

4.3.2. Cell culture

The cells were grown in MEM medium using a standard atmospheric process with 5% CO₂ at 37°C and 95% humidity. To assess the compound's anticancer effectiveness, HepG2 cell lines were grown to 85% confluence and treated with A.K in a time- and dose-dependent manner from passages one through four.

4.3.3. MTT assay

HepG2 cells were cultivated in MEM media until they were 85 percent confluent, then put in 96-well plates and incubated for 24 hours at room temperature. After a 24-hour duration in which the old media was removed and replaced, the cells were treated to a dose-dependent treatment with a range of dosages of A.K. in a fresh medium. After 24 hours of incubation, the cells were treated with a new MEM medium and then treated

with a ten-microliter solution of EZ-Cytox (WST-1; Daeil Lab Services, Seoul, Republic of Korea), and the samples were analyzed. WST solution was added to each well, and the experiment also contained a control well that did not include any A.K. dosages. WST-1-treated 96-well microplates were then incubated at 37 °C for 2 hours while kept dark. The plates were shaken for five seconds at a medium speed after being placed on a microplate scanner. The data was used to do a quantitative analysis of the viable cells and to provide a graphical representation of the viability of the treated cell group. ELISA was used to get microplate readings at an optical density of 460 nm. The collected data were used to display a graphical representation of the treated cells' viability and offer a quantitative analysis of the viable cell count.

4.3.4. Human Apoptotic Array Screening

A human apoptotic array has been performed to check the molecular pathway involved in *Angelica keiskei* treated HepG2 cells.

4.3.5. Sample preparation

Protein 1X Cell Lysis Buffer was used to extract the protein, which should be adequately diluted 2-fold with ddH₂O before use. A 1% protease inhibitor cocktail and a 1% phosphatase inhibitor cocktail are included. Sigma (St. Louis, Missouri). After protein extraction, it is advised to freeze for at least 20 minutes at -80 degrees. The frozen material was centrifuged for 20 minutes to thaw it. Repeat the technique three times more. By following the processes mentioned above, the sample was refined. (100 µl of sample volume is required for each array. That matrix effect can be avoided. For bodily fluids like serum, plasma, and cell culture medium, a minimum of a 2x dilution

is suggested or 500 µg/ml-1 mg/ml (diluted 5- to 10-fold to reduce detergent effects)). The BCA protein assay kit (Pierce, Rockford, IL) was used with a Multi-Skan FC (Thermo, USA) to determine protein content in the concentrated sample. The UV spectrum confirmed the purity of the purified sample.

4.3.6. Antibody array assay

Blocking and Incubation:

To block slides, 100 µl of 1X Blocking Buffer was added to each well, followed by a 30-minute incubation period at room temperature. Following removing the buffer from each well, 100 µl of each sample was added to the wells corresponding to those samples. The arrays were incubated at room temperature for two hours. After being removed from the wells, the samples were washed five times in 150 µl of 1X Wash Buffer I at room temperature with moderate rocking for two minutes each. The wash buffer was removed at each stage of the wash procedure. H₂O was used to dilute 20x Wash Buffer I. Each well was emptied of its 1x Wash Buffer I and washed twice for two minutes with 150 µl of 1X Wash Buffer II while gently rocking at room temperature. After each wash, the wash buffer was successfully rinsed, and Wash Buffer II (20X) was diluted with H₂O.

Incubation with a Biotinylated Antibody Cocktail and Wash:

After 2 hours of incubation at room temperature, 70 µl of the detection antibody cocktail was added to each well. After acquiring the samples from each well, they were washed at room temperature with moderate rocking five times for two minutes each

with 150 microliters of 1X Wash Buffer I, followed by two washes with 150 microliters of 1X Wash Buffer II for two minutes each. At each stage of the wash procedure, the wash buffer was removed.

Incubation with Cy3 Equivalent Dye-Streptavidin and Wash:

Each well-received 70 μ l of dye-conjugated streptavidin conjugated with the Cy3 equivalent. The device was coated in aluminum foil to protect it from light and allow it to be incubated in a dark atmosphere. The device was left at room temperature for two hours. After removing the samples from each well, they were washed twice at room temperature in a gently rocking motion with 150 microliters of 1X Wash Buffer I. The wash buffer was removed entirely at each stage of the wash process. After carefully releasing the slide from the gasket, the device was dismantled by pushing the clips on the slide side outward and then withdrawing the slide. The slide was placed in the Slide Washer/Dryer (a 4-slide holder/centrifuge tube), and enough 1x Wash Buffer I (approximately 30 ml) was added to cover the whole slide before gently shaking at room temperature for 10 minutes (2 times). The slide was then washed with 1x Wash Buffer II (about 30 ml) and gently shaken for 10 minutes at room temperature. This was done after decanting the Wash Buffer I. Before examination, the slide was washed with distilled water.

4.3.7. Data analysis

The slide was scanned with a GenePix 4100A scanner from Axon Instrument in the United States. We ensured the slides were dry before scanning them, and we scanned them within the next 24 to 48 hours. The slides were scanned with an optimum laser

power setting, a PMT, and a 10-um resolution. After receiving the scanned picture, they were grided and quantified with GenePix software version 7.0 (Axon Instrument, USA). UniProt DB was utilized to annotate the data relevant to protein information. ExDEGA (E-biogen, Inc., Korea) was used for data mining and graphic visualization.

4.3.8. Protein extraction and Western blotting

Protein was recovered from A.K.-treated and controlled HepG2 cells by washing them in cold PBS and lysing them in lysis buffer. (50 mM Tris-cl, pH 7.5), 150 mM NaCl, one mM DTT, 0.5 percent NP-40, 0.1 percent SDS, 1 percent Triton X-100, and 1 percent deoxycholate). The cell lysate was kept on ice for 30 minutes before being centrifuged at 4 °C for 25 minutes at 18x. The sediment was removed when the protein lysate was transferred to a fresh Eppendorf tube. Protein quantification was performed after collecting the total protein lysate using the albumin standard and Bradford reagent. The ELISA microplates were read on ELISA reader equipment while the plates were shielded from light. Then, use the result of the reading in Excel to determine the appropriate quantity of protein to utilize in the western blot. Western blot analysis was performed on extracted protein lysate using 12% running gel and 5% stacking gel. The gel membrane was placed between two filter sheets and a fiber pad in a positive electrode after separating the protein mixture in an electrophoresis tank. The membrane was then blocked with 1XPBST and 5% skim milk before incubating the primary antibody at a 1:1000 ratio. The concentration of the antibodies, on the other hand, is established by the manufacturer's procedure, and the secondary antibodies, anti-IgG mouse and anti-IgG rabbit, were employed in place of the primary antibodies. A tagged

antibody coupled to horseradish peroxidase (HRP) was used to detect the resultant membrane. Immunoreactive protein bands or signals were seen at varied exposure periods using a chemiluminescence plus detection system.

4.3.9. Molecular docking analysis

To better understand the process of inhibition between the ligand and the protein, the 2,3-Dihydro-3,5-dihydroxy-6-methyl-4H-pyran-2-one ligand was docked into the active domain of the Insulin growth factor binding protein 1. After docking, the Autodock Vina model with the lowest binding energy level was chosen. The binding pockets were discovered using a prank web tool (<https://prankweb.cz/>). All binding site residues fit inside the grid box defined by the binding site residues. The molecular interactions in the complexes were thoroughly investigated using the Discovery Studio visualizer tool.

4.4. Results

4.4.1. Cytotoxic effect and morphological alteration of *Angelica keiskei* on HepG2 cells

The cytotoxic impact of AK was investigated using the MTT assay on HepG2 cells at different dosages. The cells' vitality is reduced in a dose-dependent manner (**Figure 4.1**). AK was demonstrated to exert growth inhibition on HepG2 cells at a 100 µg/ml dose by providing the IC₅₀ value. MTT was used to investigate the preliminary findings of AK against HepG2 cells. A dose-dependent morphological change was seen in HepG2 cells after AK treatment.

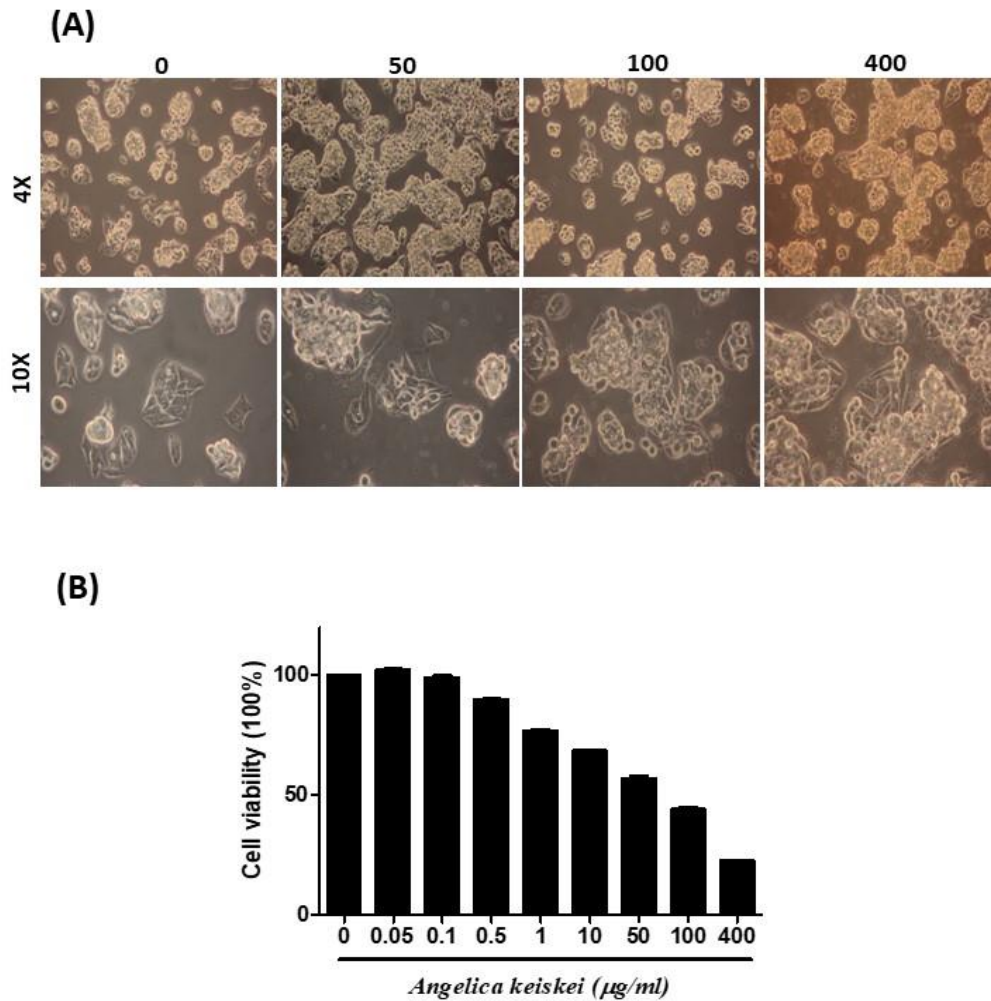


Figure 4.1. Morphological alteration and cell viability representation of HepG2 cell after treatment with *Angelica keiskei* on dose-dependent manner.

Cell viability assay shows physical and physiological alteration within the HepG2 cells treated with *Angelica keiskei* extracts. IC₅₀ is observed within the range of 50 to 100 µg/ml. Data represent the mean ± standard deviation (SD) from three independent experiments. Statistical significance was determined p-values < 0.05 were considered statistically significant.

4.4.2. Protein expression alteration using the apoptotic array analysis.

Advanced antibody array technology was used to discover changes in apoptotic proteins in AK-treated HepG2 cells at four doses. A total of 43 proteins have been investigated. (**Table 4.1**) depicts the effects of AK on the expression of proteins such as BAD, HTRA2, IGFBP1, IGFBP5, and CDKN1A at 50, 100, and 400 μg doses.

Employing advanced antibody array technology with meticulous precision, we conducted a thorough examination to discern intricate variations in apoptotic proteins within the cellular milieu of HepG2 cells. The investigation focused on the impact of A.K. treatment across a spectrum of concentrations, specifically at four distinct levels. This in-depth analysis encompassed the scrutiny of a comprehensive panel comprising a total of 43 proteins, aiming to unravel the nuanced molecular responses induced by the treatment. In the illustrative data presented in **Figure 4.2**, the differential expression patterns of select proteins, namely BAD, HTRA2, IGFBP1, IGFBP5, and CDKN1A, were meticulously observed (**Figure 4.2**). These proteins exhibited distinctive alterations in their expression profiles in direct response to A.K. treatment at dosages spanning 50, 100, and 400 $\mu\text{g}/\text{ml}$. This granular examination of protein dynamics at varying concentrations provides a nuanced and detailed understanding of how A.K. influences apoptotic proteins within HepG2 cells. These findings, collectively, contribute to a more comprehensive comprehension of the intricate landscape of apoptotic protein modulation under different concentrations of A.K. treatment. The detailed insights derived from this comprehensive analysis enhance our understanding

of the treatment's specific impact on the apoptotic pathways within HepG2 cells, thereby advancing our knowledge in the realm of targeted therapeutic interventions.

Table 4.1. List of the antibodies used to perform the human apoptotic array assay

RayBio® Human Apoptosis Antibody Array G1													
Detect 43 Apoptotic Markers in One Experiment													
	1	2	3	4	5	6	7	8	9	10	11	12	13
1	Pos 1	Pos 2	Pos 3	Neg	Neg	bad	bax	bcl-2	bcl-w	BID	BIM	Caspase 3	Caspase 8
2	Pos 1	Pos 2	Pos 3	Neg	Neg	bad	bax	bcl-2	bcl-w	BID	BIM	Caspase 3	Caspase 8
3	CD40	CD40L	ciAP-2	cytoC	DR6	Fas	FasL	NEG	HSP27	HSP60	HSP70	HTRA	IGF-I
4	CD40	CD40L	ciAP-2	cytoC	DR6	Fas	FasL	NEG	HSP27	HSP60	HSP70	HTRA	IGF-I
5	IGF-II	IGFBP-1	IGFBP-2	IGFBP-3	IGFBP-4	IGFBP-5	IGFBP-6	IGF-1 sR	livin	p21	p27	p53	SMAC
6	IGF-II	IGFBP-1	IGFBP-2	IGFBP-3	IGFBP-4	IGFBP-5	IGFBP-6	IGF-1 sR	livin	p21	p27	p53	SMAC
7	Survivin	sTNF-R1	sTNF-R2	TNF-alpha	TNF-beta	TRAIL R-1	TRAIL R-2	TRAIL R-3	TRAIL R-4	XIAP	NEG	NEG	NEG
8	Survivin	sTNF-R1	sTNF-R2	TNF-alpha	TNF-beta	TRAIL R-1	TRAIL R-2	TRAIL R-3	TRAIL R-4	XIAP	NEG	NEG	NEG

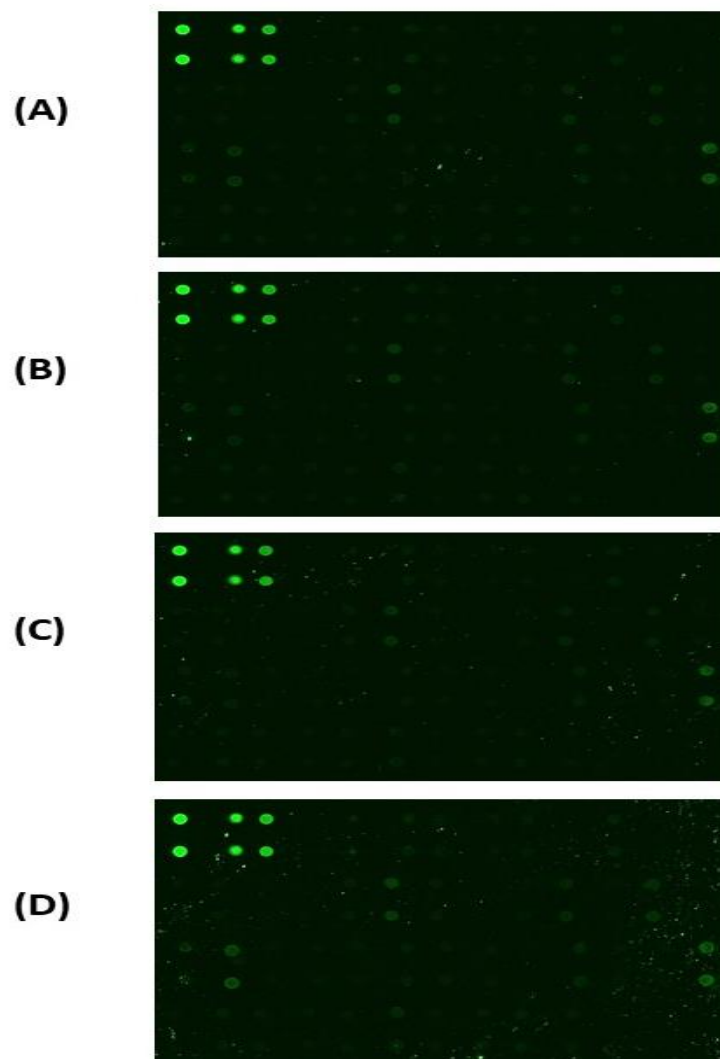


Figure 4.2. The fluorescence image of expressed proteins at different concentrations on dose-dependent manner based on the sequence of the antibodies in the table 4.1.

Fluorescence image capturing antibody screening performed on an immunogen array structured in a 96-well format. The corresponding details are presented in Table 2, providing a comprehensive overview of the proteins analyzed in this experimental setup. (A) control; (B) 50μM, (C) 100μM, (D) 400μM.

4.4.3. Identification of differentially expressed apoptotic proteins using cluster heatmap.

The intricacies of the impact of A.K. treatment on HepG2 cells is further elucidated through the visual representation of a cluster heat map, as illustrated in **Figure 4.3**. This analytical tool not only visually communicates the observed alterations but also provides a comprehensive understanding of the significant response levels induced by the treatment. Upon close examination of the cluster heat map, it becomes evident that A.K. treatment elicits a notable modulation in the relative abundance of specific proteins within HepG2 cells. Notably, BAD, HTRA2, and IGFBP1 exhibit a relative increase in abundance, suggesting an upregulation in their expression levels. Conversely, IGFBP5 and CDKN1A are discernibly downregulated in response to A.K. treatment. These differential expression patterns hold particular significance as these proteins are integral components of apoptotic signaling pathways, playing pivotal roles in cellular responses, particularly those related to programmed cell death. The observed protein expression alterations, as revealed by the cluster heat map, point towards potential co-regulation mechanisms implicated in the induction of hepatocellular carcinoma cell death following A.K. treatment. It is noteworthy that these modulation patterns are not uniform but rather exhibit dosage-dependent trends, emphasizing the nuanced and context-specific nature of the treatment response. The intricate interplay of these proteins in apoptotic pathways, as highlighted by their differential expression patterns, further contributes to our understanding of the molecular intricacies involved in A.K.-mediated responses within HepG2 cells. These detailed insights pave the way

for a more nuanced interpretation of the treatment's impact on apoptotic signaling cascades, fostering a deeper comprehension of the potential therapeutic implications in the context of hepatocellular carcinoma.



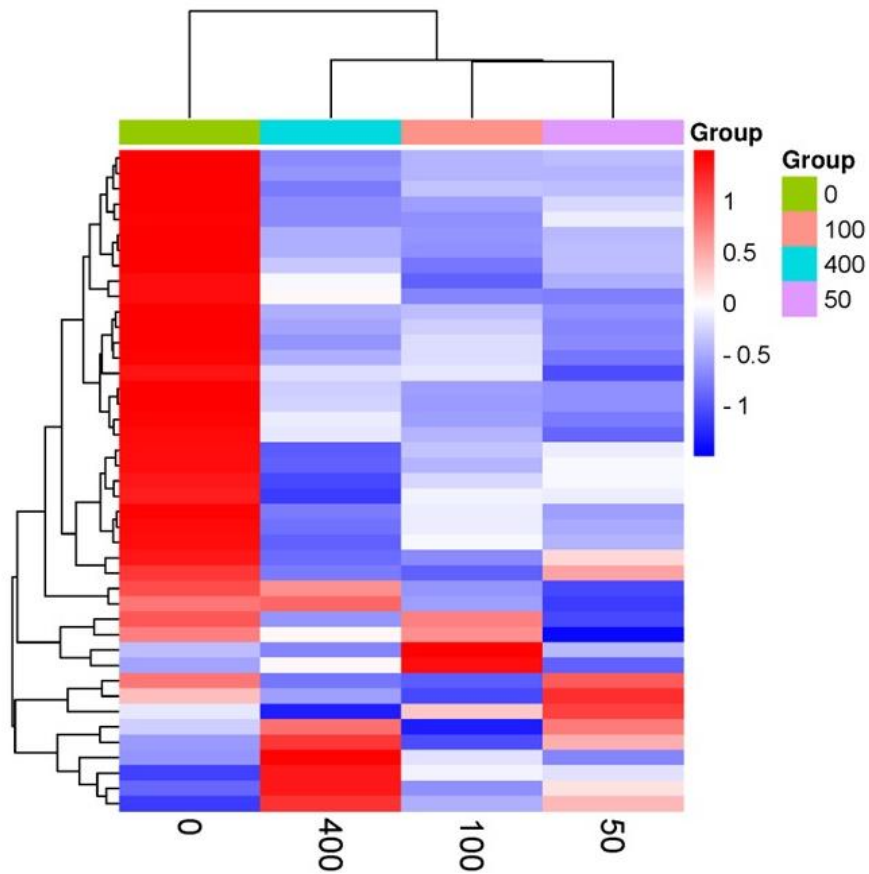


Figure 4.3. The substantial response level of the AK therapy on HepG2 cells.

Assessment of A.K. treatment response in HepG2 cells. The bar graph depicts the observed level of response elicited by A.K. treatment, highlighting the notable impact on cellular dynamics. The green, orange, blue and pink color denotes 0 μ M, 50 μ M, 100 μ M, and 400 μ M respectively. The log-fold changes are represented on a scale ranging from 1 to -1, with color intensity transitioning from red to blue to visually indicate the magnitude and direction of the changes.

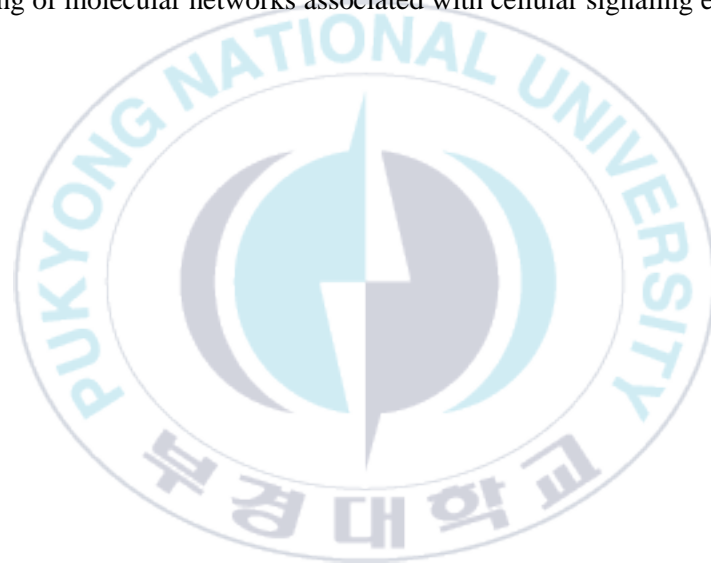
4.4.4. Protein-protein interaction network investigation

Using string analysis, (**Figure 4.4**). shows the protein-protein interactions of BAD, HTRA2, IGFBP1, IGFBP5, and CDKN1A. This research includes predicting interacting protein partners during Signaling, which aids in annotating unknown actions. This portrays the expressed protein interactions, primarily the IGFBP family, related to critical tumor control behaviors such as proliferation, migration, invasion, and adhesion via various molecular pathways. Another intriguing protein is BAD, which regulates apoptosis, and CDKN1A, essential for maintaining DNA damage's survivability. TNFRSF10B (TRAIL R2): Significant changes across all concentrations with fold changes of 0.913, 0.902, and 0.909 for 50, 100, and 400 units, respectively. CD40LG (CD40 Ligand): Significant change at 100 and 400 units with fold changes of 0.886 and 0.926, respectively (Note: The p-value at 50 units is just above the significance threshold). These proteins are involved in various pathways related to apoptosis and cellular stress responses. For instance, BCL2L2 is part of the BCL-2 protein family that regulates cell death by controlling the mitochondrial membrane permeability. CD40LG and TNFRSF10B are both associated with signaling pathways that can lead to apoptosis. HSPB1, or heat shock protein 27, plays a role in protecting cells from stress. IGF1 and IGFBP2 are part of the insulin-like growth factor system, which has various roles including cell growth, development, and survival. BIRC5, known as Survivin, inhibits apoptosis and is involved in cell cycle regulation.

The significance of changes in these proteins could indicate their potential involvement in the biological or pathological processes under study. Further biochemical and

cellular analysis would be necessary to understand the exact role and mechanism of these proteins in the context of the experimental conditions.

Network analysis highlighting the prediction of interacting protein partners during signaling. The nodes represent individual proteins, and the edges denote predicted interactions between them. This analysis provides insights into potential protein-protein interactions within signaling pathways, contributing to a comprehensive understanding of molecular networks associated with cellular signaling events.



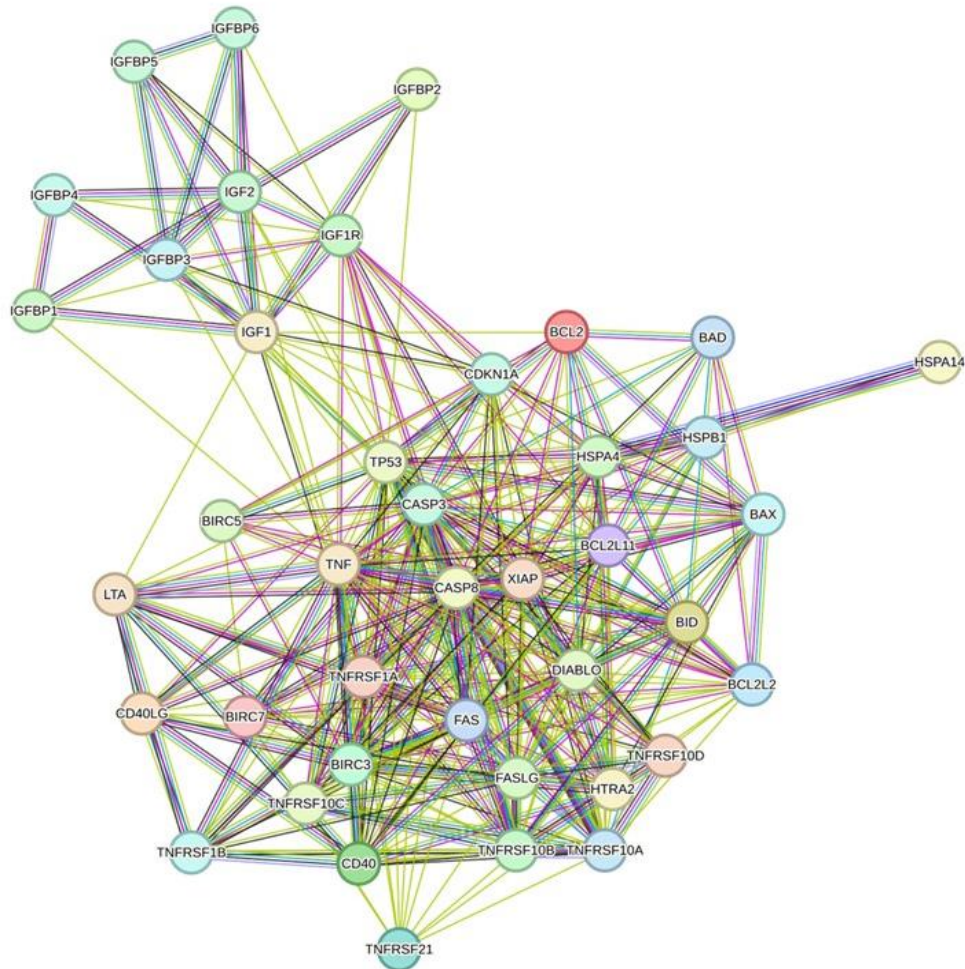
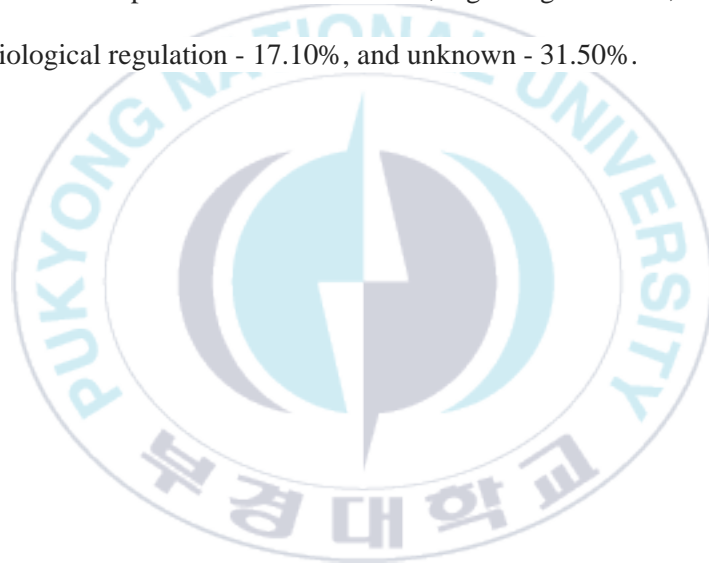


Figure 4.4. Protein-protein interactions of BAD, HTRA2, IGFBP1, IGFBP5, and CDKN1A.

Figure 4.5 summarize the protein that have shown statistically significant changes in expression (p -value < 0.05) under at least one of the condition tested. BCL2L2 (bcl-w): observed significant change at 100 and 400 $\mu\text{g/ml}$ units with fold changes of 0.955, 0.945, and 0.962 for 50, 100, and 400 $\mu\text{g/ml}$ units, respectively. BCL2L2 is responsible to regulate apoptosis along with CD40LG and TNFRSF10B.

4.4.5. Functional enrichment analysis

PANTHER analysis was used to categorize differentially expressed proteins ontologically, as shown in **(Figure 4.5)**. The differentially expressed signaling pathways are as follows: CCKR signaling pathway - 29.60%, p53 pathway feedback loops 2- 35.20%, PI3 kinase pathway - 35.20%, Interleukin signaling pathway - 35.20%, p53 pathway - 35.20%. The following are the biological roles of the differentially expressed proteins: Response to stimuli - 17.10%, Signaling - 17.10%, Cellular process - 17.10%, Biological regulation - 17.10%, and unknown - 31.50%.



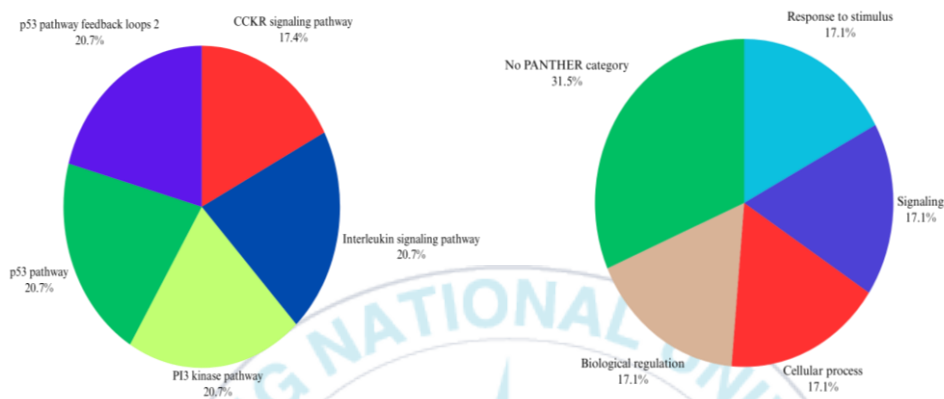


Figure 4.5. The differentially expressed signaling pathways

Pie chart depicting the relative abundance of differentially expressed signaling pathways identified through PANTHER analysis. Distribution of signaling pathways and Molecular functions associated with the differentially expressed proteins. The chart provides a visual representation of the proportionate involvement of distinct signaling pathways and molecular functions influenced by the experimental conditions. Each segment's size corresponds to the percentage of proteins associated with the respective pathway or molecular function.

4.4.6. Western blotting analysis of apoptotic proteins

In order to validate the mechanism of action of AKE, we conducted a Western blot analysis to assess the protein expression profile. The results from the Western blot reveal the presence of key apoptotic proteins known for their regulatory roles in various cancer cell types. Specifically, BAD (Bcl-2 associated agonist of cell death), Bid, and IGFBP1 (Insulin-like growth factor binding protein 1) were detected. Notably, IGFBP1 exhibited a significant upregulation, (**Figure 4.6**) indicating a heightened expression level in response to AKE treatment. These findings provide substantive evidence supporting AKE's impact on apoptotic protein modulation, with a particular emphasis on the notable upregulation of IGFBP1, thereby contributing to a more comprehensive understanding of AKE's mechanism of action.

An analysis of the protein expression using a western blot was done to corroborate the mechanism of action of AKLE. BAD (Bcl 2 associated agonist of cell death), Bid, and IGFBP1 (Insulin-like growth factor binding protein 1) are expressed where IGFBP1 is substantially elevated in the Western blot analysis of several cancer cell types.

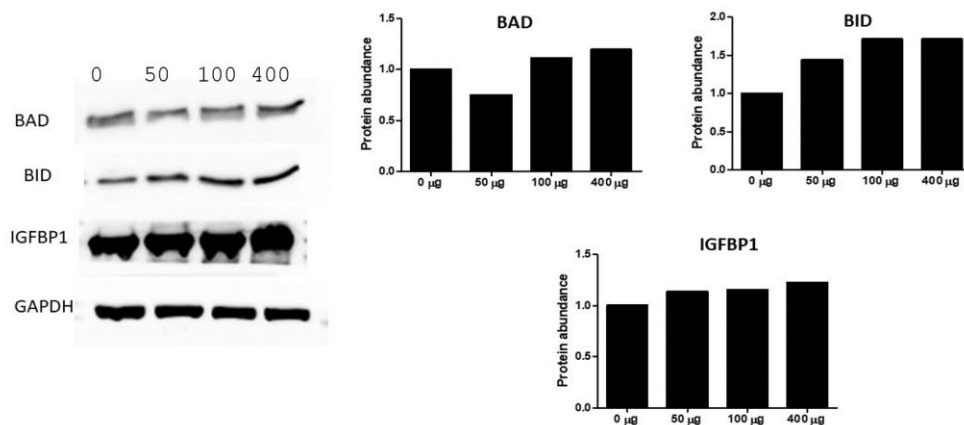


Figure 4.6. Western blot analysis of the BAD, BID, IGFBP1 protein (0, 50, 100, 400µg/ml)

Western blot analysis confirming the expression of apoptotic proteins BAD, Bid, and IGFBP1 for cross-confirmation of apoptosis induction. Data represent the mean \pm standard deviation (SD) from three independent experiments. Statistical significance was determined p-values < 0.05 were considered statistically significant.

4.4.7. Computational analysis of DDMP with IGFBP1, Bcl-2 and P53 protein.

The chemical structure of 2,3-Dihydro-3,5-dihydroxy-6-methyl-4H-pyran-2-one was obtained from the PubChem website, while the protein structures were retrieved from a protein data bank in pdb format. The binding pocket with the most excellent rank score performed the docking procedure (**Figure 4.7**). Insulin growth factor binding protein one engaged with the binding site in 2,3-Dihydro-3,5-dihydroxy-6-methyl-4H-pyran-2-one through Vanderwal interaction at VAL17, GLY54, and ARG32 sites. Conventional hydrogen bond interactions and alkyl interactions were observed at the locations CYS53, CYS59, LEU57, and PHE16. In LYS73, an unfavorable acceptor-acceptor interaction was identified. It was discovered that the compound's binding affinity to the protein was -4.7 kcal/mol.

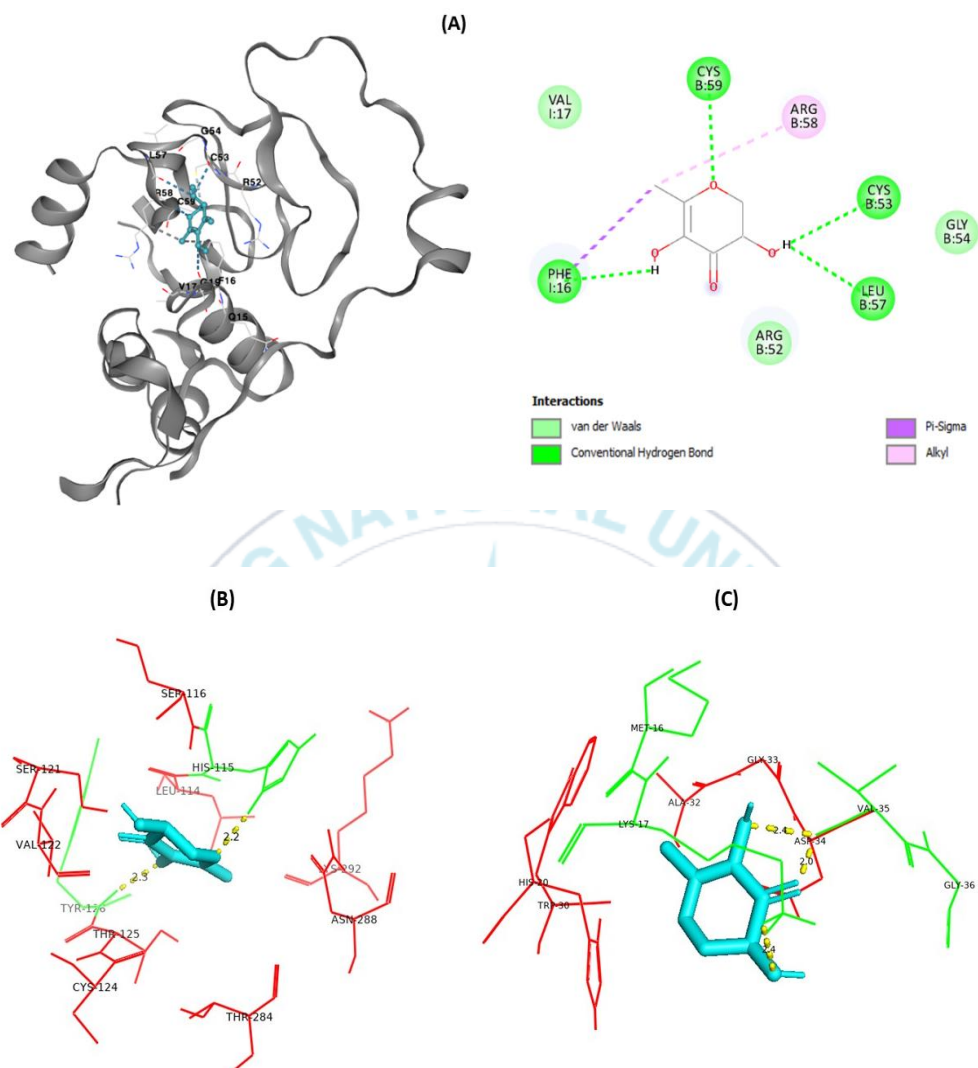


Figure 4.7. (A) IGF1BP1 (B) Bcl-2 and (C) p53 protein docking with DDMP has binding affinity -4.7, -5.3 and -5.4 respectively.

The blue color denotes the binding pocket; green and red color denotes the hydrophobic and hydrogen bonds with respect to the consecutive amino acids. All the docked images were visualized using PyMOL.

4.5. Discussion

Following the surgical removal of several tumors, including breast, colon, and osteogenic sarcomas, distant metastases can form in organs, including the lung, liver, or bone. Therefore, it is necessary to develop innovative anticancer medications with antitumor and antimetastatic

capabilities. The roots of *A. keiskei* have historically been used for their galactagogic, analeptic, diuretic, and laxative properties. There is conflicting evidence to support the idea that *A. keiskei*'s roots and leaves can help avoid coronary heart disease, hypertension, and cancer (DeWys, 1972). This study looked at how different therapies for AKE affected HepG2 cells. The outcome demonstrates that untreated normal cells have regular shapes, and treated cells exhibit granulation and clumping structures. Therefore, it is evident that AKLE has potent anticancer action against HepG2 cells. The intended concentration of AKE on HepG2 cells was then assessed using a further MTT experiment. The cells were exposed to concentrations of "0, 50, 100, and 400 mg/ml, and it is evident that increasing the AKE dosage considerably slows down the growth of cells. The *Angelica keiskei* provides hepatoprotective benefits in leaves, root extract, hydroxyderricin, and separated xanthoangelol found in health-aid food, drink, and food composition. According to the clinical investigation, regular drinkers with impaired liver function tests had significantly lower levels of γ -glutamyl transferase (GGT) after consuming the AK extracts (Noh *et al.*, 2015). BAD is a member of the BCL-2 protein family, known for being a regulator of programmed cell death. When coupled with BCL-xL and BCL-2, the proapoptotic protein BAD prevents these

proteins from acting in a prosurvival manner (Yang *et al.*, 1995). BAD's proapoptotic activity is controlled by phosphorylation, which reduces BAD's proapoptotic activity (Fernando *et al.*, 2007). Down-regulation of p21WAF1 has been seen in human HCC, and it has been linked to tumor growth and a poor prognosis. Additionally, it controls MAP kinase, phosphatase calcium, AKT, and programmed cell death. Proteins are encoded by the insulin-like growth factor binding protein 1 (IGFBP1). IGFBP1 is related to ovarian disease and hepatocellular cancer. One of its associated processes is gene expression (transcription), which also includes cellular responses to stimuli. IGFBP1 is essential for the reciprocal route, just as it was for the differentiation of stem cells dependent on hypoxia-inducible factors. although increased IGFBP-1 expression in HCC significantly impacted lymph angiogenesis (Geis *et al.*, 2015). There have been conflicting results about the blood level and expression of IGFBP1 in HCC patients. According to one research, IGFBP1 may slow tumor development by blunting the IGF axis. Accordingly, our findings showed that IGFBP1, a tumor suppressor, would be a potential target in the therapy of HCC (Dai *et al.*, 2014; Nel *et al.*, 2014; Yang *et al.*, 2016). IGFBP5, the most conserved member of the IGFBP family in all vertebrates, has been shown to regulate cell proliferation, decide the fate of individual cells, and take the role of the metastatic process in cancer growth (Taylor *et al.*, 2010). IGFBP5 has been hypothesized to be a marker for the progression of nonalcoholic steatohepatitis (NASH), a more serious liver disease, from NAFLD in NAFLD patients (Colak *et al.*, 2012). IGFBP5 may play an oncogenic function in the early stages of human hepatocarcinogenesis, according to research by Umemura *et al.*, 2008. They also stated that IGFBP5 significantly reduces the number of cells that make

up human hepatocellular carcinoma (Umemura *et al.*, 2008). The altered expression of CDKN1a may cause apoptosis in HCC cells since it is well-known that this gene is implicated in the intrinsic apoptotic signaling pathway. The heatmap also demonstrated the various manners in which cell cycle-related genes express themselves. While CDK4 was upregulated in HCC, CDKN1A was downregulated. Mechanistic research revealed that the short nucleolar RNA host gene one might exhibit some regulatory mechanisms in the nucleus and cytoplasm and could promote the formation of HCC by regulating the expression of CDKN1A and other proteins (Li *et al.*, 2020). One study demonstrated the gene's inhibitory activity by examining CDKN1a's role as a regulator of proliferation, invasion, and response to anticancer therapy (Fornari *et al.*, 2012). The relationship between HtrA2 and HCC is too tenuous, although it is clear that HtrA2 expression is essential for the frequency of apoptosis in hepatocellular carcinoma cells. The functional enrichment of HtrA2-related genes in HCC and the relationship between HtrA2 and tumor immunity were investigated using a multidimensional approach (Feng *et al.*, 2023). Because HtrA2 regulates the apoptosis of tumor cells, there may be a connection between the two molecules. The facts discussed above could provide a starting point for further research into the relationship between HtrA2 and the network of microRNAs in HCC. According to this study, HtrA2 dysregulation is correlated with various transcription factors, including IPF1, HFH4, PAX4, E4BP4, and ETF. All major transcription factors govern the proliferation and death of different types of human cells (Sachdeva *et al.*, 2009; Zhang *et al.*, 2021; Karunakaran *et al.*, 2020; Zhang *et al.*, 2021; Xu *et al.*, 2012). Our research found that IGFBP5 and CDKN1A proteins were downregulated in HCC cells at higher dosages, which may have led to the cells'

apoptosis. The cluster heatmap and volcano scatter plot further support the altered relative expression of all the apoptosis-related proteins stated previously in HCC cells. AKT phosphorylates some proteins, including the proapoptotic protein BAD, rendering it inactive. The expression of the tumor suppressor gene product phosphatase and tensin homolog, which typically suppresses PI3K activity, was noticeably downregulated in nearly half of the HCC tumors. The BCL-2 family protein BAD and Bid is known to control programmed cell death by activating the kinases AKT and MAP Kinase and calcium phosphatase by building heterodimers of BCL-XL and BCL-2. (National Library of Medicine, National Center for Biotechnology Information) The BAD protein regulates apoptosis by binding to members of the same family that prevent apoptosis. A large number of kinases and phosphatases also directly regulate the BAD protein. When Bax is not phosphorylated, Bad replaces it by preferentially dimerizing with Bcl-xL and Bcl-2. Bax is thus free to initiate the apoptotic process of mitochondrial membrane permeability (Stickles *et al.*, 2015). Bad and Bid proteins cause cell death by inactivating prosurvival Bcl-2 family members (Sinicrope *et al.*, 2008). Next, this study demonstrates the IGFBP1 protein's significant overexpression, preventing MMP-9 from being expressed in HCC cells. As the IGF signaling pathway is known to have a significant role in the initiation and progression of HCC, IGFBP-1, mostly generated by the liver, can inhibit the activation of IGF-R. Studies on HepG2 cells have shown that IL-1 causes IGFBP-1 activation via the MAPK pathway (Rutkute and Nikolova-Karakashian 2007). IGFBP1 may be a transcriptional target of p53 in hepatic cells, according to the increased gene expression in HepG2 cells after treatment with AKE. The tumor suppressor p53 is one of the genes most often mutated in HCC. This

transcription factor regulates several downstream target genes that govern metabolism, senescence, DNA repair, cell cycle progression, and apoptosis (Link and Iwakuma 2017). AKE elevated several proteins according to a protein microarray study. According to molecular docking, IGFBP1 was among these elevated proteins in HepG2 cells. IGFBP1 is mostly found in the liver and binds to insulin growth factors (IGFs) to modulate their actions. This finding shows that the Bcl-2 protein family, which includes the protein Bad, may cause apoptosis under the control of p53. The proapoptotic activity of the Bcl-2 family protein known as Bid is crucial for death receptor-mediated apoptosis in several cell systems. The translocation of Bid's shortened form, tBid (truncated Bid), into the mitochondria, has been hypothesized to contribute to the release of apoptogenic proteins such as cytochrome c. As demonstrated by molecular docking, one of these elevated proteins in HepG2 cells may thus be the cause of apoptosis. Previous studies have suggested that IGFBP1 may function as a tumor suppressor. However, the precise mechanism of action is still unknown. This ongoing study will employ pure AKLE and examine its molecular mechanisms in more depth.

4.6. Conclusion

In conclusion, Effective use of AKLE's potential may result in a focused, functional therapeutic approach with minimal side effects, revolutionizing cancer treatment. Our findings suggest that AKE causes liver cells to die through the mitochondrial pathway by upregulating the apoptotic protein. In light of this, analyzing the molecular docking binding affinity with apoptotic protein, it is hypothesized that DDMP may be a potentially beneficial, safe, and selective anticancer agent for hepatocellular carcinoma.

Furthermore, the morphological alteration in the hepatocellular carcinoma HepG2 cells shows the great anticancer activity of the extracts.



References

- Aaron P Thrift., and Hashem B. El-Serag. 2020. "Burden of Gastric Cancer." *Clinical Gastroenterology and Hepatology* 18 (3): 534–42.
- Acehan, Devrim, Xuejun Jiang, David Gene Morgan, John E Heuser, Xiaodong Wang, and Christopher W Akey. 2002. "Three-Dimensional Structure of the Apoptosome: Implications for Assembly, Procaspase-9 Binding, and Activation." *Molecular Cell* 9 (2): 423–32.
- Al-Buriahi, Abdullah Khaled, Adel Ali Al-Gheethi, Ponnusamy Senthil Kumar, Radin Maya Saphira Radin Mohamed, Hanita Yusof, Abdullah Faisal Alshalif, and Nasradeen A Khalifa. 2022. "Elimination of Rhodamine B from Textile Wastewater Using Nanoparticle Photocatalysts: A Review for Sustainable Approaches." *Chemosphere* 287: 132162.
- Alfarouk, K O, A H Bashir, A N Aljarbou, A M Ramadan, A K Muddathir, S T AlHoufie, and others. "Helicobacter Pylori in Gastric Cancer and Its Management." *Frontiers in Oncology* 9: 75.
- Alkhalaf, Maha Ibrahim. 2020. "Attenuating Effect of Indole-3-Carbinol on Gold Nanoparticle Induced Hepatotoxicity in Rats." *Arabian Journal of Chemistry* 13 (11): 8060–68.

- Alqahtani, Ali, Zubair Khan, Abdurahman Alloghbi, Tamer S. Said Ahmed, Mushtaq Ashraf, and Danae M. Hammouda. 2019. "Hepatocellular Carcinoma: Molecular Mechanisms and Targeted Therapies." *Medicina* 55 (9): 526.
- Altekruse, Sean F, Katherine A McGlynn, and Marsha E Reichman. 2009. "Hepatocellular Carcinoma Incidence, Mortality, and Survival Trends in the United States from 1975 to 2005." *Journal of Clinical Oncology* 27 (9): 1485.
- Amieva, Manuel R, and Emad M El--Omar. 2008. "Host-Bacterial Interactions in Helicobacter Pylori Infection." *Gastroenterology* 134 (1): 306–23.
- An, Jun-Hye, Min-Jung Ko, and Myong-Soo Chung. 2023. "Thermal Conversion Kinetics and Solubility of Soy Isoflavones in Subcritical Water Extraction." *Food Chemistry* 424: 136430.
- Anwanwan, David, Santosh Kumar Singh, Shriti Singh, Varma Saikam, and Rajesh Singh. 2020. "Challenges in Liver Cancer and Possible Treatment Approaches." *Biochimica et Biophysica Acta (BBA)-Reviews on Cancer* 1873 (1): 188314.
- Babavalian, H, Ali Mohammad Latifi, M A Shokrgozar, S Bonakdar, H Tebyanian, and F Shakeri. 2016. "Cloning and Expression of Recombinant Human Platelet-Derived Growth Factor-BB in Pichia Pink." *Cellular and Molecular Biology* 62 (8): 45–51.
- Backert, Steffen, and Matthias Selbach. 2008. "Role of Type IV Secretion in Helicobacter Pylori Pathogenesis." *Cellular Microbiology* 10 (8): 1573–81.

- Badgwell, Brian, Prajnan Das, and Jaffer Ajani. 2017. "Treatment of Localized Gastric and Gastroesophageal Adenocarcinoma: The Role of Accurate Staging and Preoperative Therapy." *Journal of Hematology & Oncology* 10 (1): 1–7.
- Baldwin, David N, Benjamin Shepherd, Petra Kraemer, Michael K Hall, Laura K Sycuro, Delia M Pinto-Santini, and Nina R Salama. 2007. "Identification of Helicobacter Pylori Genes That Contribute to Stomach Colonization." *Infection and Immunity* 75 (2): 1005–16.
- Balogh, Julius, David Victor III, Emad H Asham, Sherilyn Gordon Burroughs, Maha Bektour, Ashish Saharia, Xian Li, R Mark Ghobrial, and Howard P Monsour Jr. 2016. "Hepatocellular Carcinoma: A Review." *Journal of Hepatocellular Carcinoma*, 41–53.
- Benedini, Luciano. 2019. "Adsorption/Desorption Study of Antibiotic and Anti-Inflammatory Drugs onto Bioactive Hydroxyapatite Nano-Rods." *Materials Science and Engineering C*.
- Bian, Wangqing, Zhenxing Pan, Yakun Wang, Wei Long, Zefeng Chen, Niping Chen, Yaoxun Zeng, *et al.*, 2021. "A Mitochondria-Targeted Thiazoleorange-Based Photothermal Agent for Enhanced Photothermal Therapy for Tumors." *Bioorganic Chemistry* 113: 104954.
- Blaser, Martin J., and John C. Atherton. "Helicobacter pylori persistence: biology and disease." *The Journal of clinical investigation* 113, no. 3 (2004): 321-333.

- Bray, Freddie, Jacques Ferlay, Isabelle Soerjomataram, Rebecca L. Siegel, Lindsey A. Torre, and Ahmedin Jemal. 2018. "Global Cancer Statistics 2018: GLOBOCAN Estimates of Incidence and Mortality Worldwide for 36 Cancers in 185 Countries." *CA: A Cancer Journal for Clinicians* 68 (6): 394–424.
- Bray, Freddie, Jacques Ferlay, Isabelle Soerjomataram, Rebecca L. Siegel, Lindsey A. Torre, and Ahmedin Jemal. 2018. "Global Cancer Statistics 2018: GLOBOCAN Estimates of Incidence and Mortality Worldwide for 36 Cancers in 185 Countries." *CA: A Cancer Journal for Clinicians* 68 (6): 394–424.
- Bugaytsova, Jeanna A, Oscar Björnham, Yevgen A Chernov, Pär Gideonsson, Sara Henriksson, Melissa Mendez, Rolf Sjöström, *et al.*, 2017. "Helicobacter Pylori Adapts to Chronic Infection and Gastric Disease via PH-Responsive BabA-Mediated Adherence." *Cell Host & Microbe* 21 (3): 376–89.
- Buzás, György Miklós. 2014. "Metabolic Consequences of Helicobacter Pylori Infection and Eradication." *World Journal of Gastroenterology: WJG* 20 (18): 5226.
- Cai, Jiyang, Jie Yang, and Dean P. Jones. 1998. "Mitochondrial Control of Apoptosis: The Role of Cytochrome C." *Biochimica et Biophysica Acta - Bioenergetics* 1366 (1–2): 139–49
- Campbell, Kirsteen J, and Stephen W G Tait. 2018. "Targeting BCL-2 Regulated Apoptosis in Cancer." *Open Biology* 8 (5): 180002.

- Campioni, Mara, Daniele Santini, Giuseppe Tonini, Raffaele Murace, Emanuele Dragonetti, Enrico P. Spugnini, and Alfonso Baldi. 2005. "Role of Apaf-1, a Key Regulator of Apoptosis, in Melanoma Progression and Chemoresistance." *Experimental Dermatology* 14 (11): 811–18.
- Carroll, Gregory T, Reed C Dowling, David L Kirschman, Mark B Masthay, and Angela Mammana. 2023. "Intrinsic Fluorescence of UV-Irradiated DNA." *Journal of Photochemistry and Photobiology A: Chemistry* 437: 114484.
- Chang, Mei-Hwei, San-Lin You, Chien-Jen Chen, Chun-Jen Liu, Ming-Wei Lai, Tzee-Chung Wu, Shu-Fen Wu, *et al.*, 2016. "Long-Term Effects of Hepatitis B Immunization of Infants in Preventing Liver Cancer." *Gastroenterology* 151 (3): 472–80.
- Chen, Chuan, and Ge Wang. 2015. "Mechanisms of Hepatocellular Carcinoma and Challenges and Opportunities for Molecular Targeted Therapy." *World Journal of Hepatology* 7 (15): 1964.
- Chen, Jiandong. 2016. "The Cell-Cycle Arrest and Apoptotic Functions of P53 in Tumor Initiation and Progression." *Cold Spring Harbor Perspectives in Medicine* 6 (3).
- Chen, Lin, Simon N. Willis, Andrew Wei, Brian J. Smith, Jamie I. Fletcher, Mark G. Hinds, Peter M. Colman, Catherine L. Day, Jerry M. Adams, and David C.S. Huang. 2005. "Differential Targeting of Prosurvival Bcl-2 Proteins by Their

BH3-Only Ligands Allows Complementary Apoptotic Function.” *Molecular Cell* 17 (3): 393–403.

Chen, Zhifei, Qiang Liu, Zhiwei Zhao, Bing Bai, Zhitao Sun, Lili Cai, Yufeng Fu, Yuping Ma, Qingfu Wang, and Gaolei Xi. "Effect of hydroxyl on antioxidant properties of 2, 3-dihydro-3, 5-dihydroxy-6-methyl-4 H-pyran-4-one to scavenge free radicals." *RSC advances* 11, no. 55 (2021): 34456-34461.

Cheng, Emily H.Y., Michael C. Wei, Solly Weiler, Richard A. Flavell, Tak W. Mak, Tullia Lindsten, and Stanley J. Korsmeyer. 2001. “BCL-2, BCL-XL Sequester BH3 Domain-Only Molecules Preventing BAX- and BAK-Mediated Mitochondrial Apoptosis.” *Molecular Cell* 8 (3): 705–11.

Chhikara, Bhupender S., and Keykavous Parang. "Global Cancer Statistics 2022: the trends projection analysis." *Chemical Biology Letters* 10, no. 1 (2023): 451-451.

Chinni, Sreenivasa R., Yiwei Li, Sunil Upadhyay, Prathima K. Koppolu, and Fazlul H. Sarkar. 2001. “Indole-3-Carbinol (I3C) Induced Cell Growth Inhibition, G1 Cell Cycle Arrest and Apoptosis in Prostate Cancer Cells.” *Oncogene* 20 (23): 2927–36.

Colagrande, Stefano, Andrea L Inghilesi, Sami Aburas, Gian G Taliani, Cosimo Nardi, and Fabio Marra. 2016. “Challenges of Advanced Hepatocellular Carcinoma.” *World Journal of Gastroenterology* 22 (34): 7645.

- Colak, Yasar, Ebubekir Senates, Oguzhan Ozturk, Yusuf Yilmaz, Ebru Zemheri, Feruze Yilmaz Enc, Celal Ulasoglu, *et al.*, 2012. "Serum Concentrations of Human Insulin-like Growth Factor-1 and Levels of Insulin-like Growth Factor-Binding Protein-5 in Patients with Nonalcoholic Fatty Liver Disease: Association with Liver Histology." *European Journal of Gastroenterology & Hepatology* 24 (3): 255–61.
- Cover, Carolyn M., S. Jean Hsieh, Susan H. Tran, Gunnell Hallden, Gloria S. Kim, Leonard F. Bjeldanes, and Gary L. Firestone. 1998. "Indole-3-Carbinol Inhibits the Expression of Cyclin-Dependent Kinase-6 and Induces a G1 Cell Cycle Arrest of Human Breast Cancer Cells Independent of Estrogen Receptor Signaling." *Journal of Biological Chemistry* 273 (7): 3838–47.
- Cram, Erin J., Betty D. Liu, Leonard F. Bjeldanes, and Gary L. Firestone. 2001. "Indole-3-Carbinol Inhibits CDK6 Expression in Human MCF-7 Breast Cancer Cells by Disrupting Sp1 Transcription Factor Interactions with a Composite Element in the CDK6 Gene Promoter." *Journal of Biological Chemistry* 276 (25): 22332–40.
- Dai, Bin, Bai Ruan, Juan Wu, Jianlin Wang, Runze Shang, Wei Sun, Xia Li, Kefeng Dou, Desheng Wang, and Yu Li. 2014. "Insulin-like Growth Factor Binding Protein-1 Inhibits Cancer Cell Invasion and Is Associated with Poor Prognosis in Hepatocellular Carcinoma." *International Journal of Clinical and Experimental Pathology* 7 (9): 5645.

- DeWys, William D. 1972. "Studies Correlating the Growth Rate of a Tumor and Its Metastases and Providing Evidence for Tumor-Related Systemic Growth-Retarding Factors." *Cancer Research* 32 (2): 374–79
- Donia, Thoria, Marian N. Gerges, and Tarek M. Mohamed. 2022. "Anticancer Effects of Combination of Indole-3-Carbinol and Hydroxychloroquine on Ehrlich Ascites Carcinoma via Targeting Autophagy and Apoptosis." *Nutrition and Cancer* 74 (5): 1802–18.
- Du, Juan, Zheyuan Hu, Wei-jie Dong, Yubo Wang, Shujing Wu, and Yanhong Bai. 2019. "Biosynthesis of Large-Sized Silver Nanoparticles Using Angelica Keiskei Extract and Its Antibacterial Activity and Mechanisms Investigation." *Microchemical Journal* 147: 333–38.
- Edlich, Frank, Soojay Banerjee, Motoshi Suzuki, Megan M. Cleland, Damien Arnoult, Chunxin Wang, Albert Neutzner, Nico Tjandra, and Richard J. Youle. 2011. "Bcl-XL Retrotranslocates Bax from the Mitochondria into the Cytosol." *Cell* 145 (1): 104–16.
- Edwards, Amanda L., Evripidis Gavathiotis, James L. Labelle, Craig R. Braun, Kwadwo A. Opoku-Nsiah, Gregory H. Bird, and Loren D. Walensky. 2013. "Multimodal Interaction with BCL-2 Family Proteins Underlies the Proapoptotic Activity of PUMA BH3." *Chemistry and Biology* 20 (7): 888–902.

- Elmore, Susan. 2007. "Apoptosis: A Review of Programmed Cell Death." *Toxicologic Pathology* 35 (4): 495–516.
- El-Serag, Hashem B, Jorge A Marrero, Lenhard Rudolph, and K Rajender Reddy. 2008. "Diagnosis and Treatment of Hepatocellular Carcinoma." *Gastroenterology* 134 (6): 1752–63.
- Eskiizmir, Görkem, Aylin T Ermertcan, and Kerim Yapici. 2017. "Nanomaterials: Promising Structures for the Management of Oral Cancer." In *Nanostructures for Oral Medicine*, 511–44. Elsevier.
- Feng, Lei, Zhen Li, Yao Xiong, Ting Yan, Changmin Fu, Qiuyue Zeng, Huamin Wang, and others. 2023. "HtrA2 Independently Predicts Poor Prognosis and Correlates with Immune Cell Infiltration in Hepatocellular Carcinoma." *Journal of Oncology* 2023.
- Fernando, Romaine, James S Foster, Amber Bible, Anders Strom, Richard G Pestell, Mahadev Rao, Arnold Saxton, *et al.*, 2007. "Breast Cancer Cell Proliferation Is Inhibited by BAD: Regulation of Cyclin D1." *Journal of Biological Chemistry* 282 (39): 28864–73.
- Ferro, Anabela, Tânia Mestre, Patrícia Carneiro, Ivan Sahumbaiev, Raquel Seruca, and João M. Sanches. 2017. "Blue Intensity Matters for Cell Cycle Profiling in Fluorescence DAPI-Stained Images." *Laboratory Investigation* 97 (5): 615–25.
- Fitzmaurice, Christina, Christine Allen, Ryan M Barber, Lars Barregard, Zulfiqar A Bhutta, Hermann Brenner, Daniel J Dicker, *et al.*, 2017. "Global, Regional, and

National Cancer Incidence, Mortality, Years of Life Lost, Years Lived with Disability, and Disability-Adjusted Life-Years for 32 Cancer Groups, 1990 to 2015: A Systematic Analysis for the Global Burden of Disease Study.” *JAMA Oncology* 3 (4): 524–48.

Fornari, Francesca, Maddalena Milazzo, Pasquale Chieco, Massimo Negrini, Elena Marasco, Giovanni Capranico, Vilma Mantovani, *et al.*, 2012. “In Hepatocellular Carcinoma MiR-519d Is up-Regulated by P53 and DNA Hypomethylation and Targets CDKN1A/P21, PTEN, AKT3 and TIMP2.” *The Journal of Pathology* 227 (3): 275–85.

Fu, Kunli, Xiang Gao, Puyue Hua, Yuedi Huang, Ruitao Dong, Mingji Wang, Qun Li, and Zichao Li. 2023. “Anti-Obesity Effect of Angelica Keiskei Jiaosu Prepared by Yeast Fermentation on High-Fat Diet-Fed Mice.” *Frontiers in Nutrition* 9: 1079784.

Garcia-Pelaez, José, Rita Barbosa-Matos, Irene Gullo, Fatima Carneiro, and Carla Oliveira. 2021. “Histological and Mutational Profile of Diffuse Gastric Cancer: Current Knowledge and Future Challenges.” *Molecular Oncology* 15 (11): 2841–67.

Gehrcke, Mailine, Laura Minussi Giuliani, Luana Mota Ferreira, Allanna Valentini Barbieri, Marcel Henrique Marcondes Sari, Elita Ferreira da Silveira, Juliana Hofstatter Azambuja, Cristina Wayne Nogueira, Elizandra Braganhol, and Letícia Cruz. 2017. “Enhanced Photostability, Radical Scavenging and

Antitumor Activity of Indole-3-Carbinol-Loaded Rose Hip Oil Nanocapsules.”
Materials Science and Engineering C 74: 279–86.

Geis, Theresa, Rüdiger Popp, Jiong Hu, Ingrid Fleming, Nina Henke, Nathalie Dehne,
and Bernhard Brüne. 2015. “HIF-2 α Attenuates Lymphangiogenesis by up-
Regulating IGFBP1 in Hepatocellular Carcinoma.” *Biology of the Cell* 107 (6):
175–88.

Gilman, Neyda V. 2018. “Analysis for Science Librarians of the 2017 Nobel Prize in
Physiology or Medicine: The Life and Work of Jeffrey C. Hall, Michael
Rosbash, and Michael W. Young.” *Science & Technology Libraries* 37 (1):
22–47.

Green, Douglas, and Guido Kroemer. 1998. “Tceocom” 8924 (98): 267–71.

Guan, Hongjing, Changgui Chen, Lihua Zhu, Changping Cui, Yuanyuan Guo, Mingyue
Fu, Lang Wang, and Qizhu Tang. 2013. “Indole-3-Carbinol Blocks Platelet-
Derived Growth Factor-Stimulated Vascular Smooth Muscle Cell Function
and Reduces Neointima Formation in Vivo.” *Journal of Nutritional
Biochemistry* 24 (1): 62–69

Halkier, Barbara Ann, and Jonathan Gershenzon. 2006. “Biology and Biochemistry of
Glucosinolates.” *Annual Review of Plant Biology* 57: 303–33.

Hamashima, Chisato. 2020. “The Burden of Gastric Cancer.” *Annals of Translational
Medicine* 8 (12).

- Hanif, Ayesha, Saima Qureshi, Zeeshan Sheikh, and Haroon Rashid. 2017. "Complications in Implant Dentistry." *European Journal of Dentistry* 11 (01): 135–40.
- Hartke, Justin, Matthew Johnson, and Marwan Ghabril. 2017. "The Diagnosis and Treatment of Hepatocellular Carcinoma." In *Seminars in Diagnostic Pathology*, 34:153–59.
- Hassan, Tarig A, Vijay K Rangari, and Shaik Jeelani. 2014. "Sonochemical Synthesis and Characterisation of Bio-Based Hydroxyapatite Nanoparticles." *International Journal of Nano and Biomaterials* 5 (2–3): 103–12.
- Hatakeyama, Masanori, and Hideaki Higashi. 2005. "Helicobacter Pylori CagA: A New Paradigm for Bacterial Carcinogenesis." *Cancer Science* 96 (12): 835–43.
- Hatakeyama, Masanori. 2004. "Oncogenic Mechanisms of the Helicobacter Pylori CagA Protein." *Nature Reviews Cancer* 4 (9): 688–94.
- Hee Yu, M., Gwon Im, H., Lee, S.O., Sung, C., Park, D.C. and Lee, I.S. 2007. "Induction of Apoptosis by Immature Fruits of Prunus Salicina Lindl. Cv. Soldam in MDA-MB-231 Human Breast Cancer Cells." *International Journal of Food Sciences and Nutrition*.
- Hirukawa, Sayaka, Hiroshi Sagara, Satoshi Kaneto, Tomoyo Kondo, Kotaro Kiga, Takahito Sanada, Hiroshi Kiyono, and Hitomi Mimuro. 2018. "Characterization of Morphological Conversion of Helicobacter Pylori under Anaerobic Conditions." *Microbiology and Immunology* 62 (4): 221–28.

- Ilver, Dag, Anna Arnqvist, Johan Ogren, Inga-Maria Frick, Dangeruta Kersulyte, Engin T Incecik, Douglas E Berg, Antonello Covacci, Lars Engstrand, and Thomas Borén. 1998. "Helicobacter Pylori Adhesin Binding Fucosylated Histo-Blood Group Antigens Revealed by Retagging." *Science* 279 (5349): 373–77.
- Imai, K, and M Imai. 2008. "Encyclopedia of Wild Herbs and Vegetables." Green Home, Seoul.
- Jänicke, Reiner U., Michael L. Sprengart, Mas R. Wati, and Alan G. Porter. 1998. "Caspase-3 Is Required for DNA Fragmentation and Morphological Changes Associated with Apoptosis." *Journal of Biological Chemistry* 273 (16): 9357–60.
- Jeong, Yu-Jin, and Keum Jee Kang. 2011. "Effect of Angelica Keiskei Extract on Apoptosis of MDA-MB-231 Human Breast Cancer Cells."
- Karunakaran, Denuja, Adam W Turner, Anne-Claire Duche, Sebastien Soubeyrand, Adil Rasheed, David Smyth, David P Cook, *et al.*, 2020. "RIPK1 Gene Variants Associate with Obesity in Humans and Can Be Therapeutically Silenced to Reduce Obesity in Mice." *Nature Metabolism* 2 (10): 1113–25.
- Kelley, Jon R., and John M. Duggan. 2003. "Gastric Cancer Epidemiology and Risk Factors." *Journal of Clinical Epidemiology* 56 (1): 1–9.
- Kiddane, Anley Teferra, Vikash Chandra Roy, Min-Jae Kang, Maheshkumar Prakash Patil, Byung-Soo Chun, and Gun-Do Kim. 2022. "Anticancer and Apoptotic

Activity in Neuroblastoma SK-N-SH Using Phospholipid Extract from Bone of *Scomberomorus Nipponius* .” *Chemical Biology & Drug Design*.

Kil, Yun-Seo, Sally T Pham, Eun Kyoung Seo, and Mahtab Jafari. 2017. “*Angelica Keiskei*, an Emerging Medicinal Herb with Various Bioactive Constituents and Biological Activities.” *Archives of Pharmacal Research* 40: 655–75.

Kim, Bo Hyun, and Joong-Won Park. 2018. “Epidemiology of Liver Cancer in South Korea.” *Clinical and Molecular Hepatology* 24 (1): 1.

Kim, Bo Hyun, Dahhay Lee, Kyu-Won Jung, Young-Joo Won, and Hyunsoon Cho. 2022. “Cause of Death and Cause-Specific Mortality for Primary Liver Cancer in South Korea: A Nationwide Population-Based Study in Hepatitis B Virus-Endemic Area.” *Clinical and Molecular Hepatology* 28 (2): 242.

Kim, H., Mondal, S., Jang, B., Manivasagan, P., Moorthy, M.S. and Oh, J. 2018. “Biomimetic Synthesis of Metal–Hydroxyapatite (Au-HAp, Ag-HAp, Au-Ag-HAp): Structural Analysis, Spectroscopic Characterization and Biomedical Application.” *Ceramics International*.

Kim, Hyungjin, Ho Chou Tu, Decheng Ren, Osamu Takeuchi, John R. Jeffers, Gerard P. Zambetti, James J.D. Hsieh, and Emily H.Y. Cheng. 2009. “Stepwise Activation of BAX and BAK by TBID, BIM, and PUMA Initiates Mitochondrial Apoptosis.” *Molecular Cell* 36 (3): 487–99.

Kim, Jie-Hyun, Kyung-Do Han, Jung Kuk Lee, Hyun-Soo Kim, Jae Myung Cha, Sohee Park, Joo Sung Kim, Won Ho Kim, and Big Data Research Group (BDRG) of

- the Korean Society of Gastroenterology (KSG). 2020. "Association between the National Cancer Screening Programme (NSCP) for Gastric Cancer and Oesophageal Cancer Mortality." *British Journal of Cancer* 123 (3): 480–86.
- Kim, W, and S F Moss. 2008. "The Role of H. Pylori in the Development of Stomach Cancer." *Oncology Review*, December 1 (Suppl 1): 165–68.
- Kimura, Yoshiyuki, Maho Sumiyoshi, and Kimiye Baba. 2008. "Anti-Tumor Actions of Major Component 3'-O-Acetylhamaudol of *Angelica Japonica* Roots through Dual Actions, Anti-Angiogenesis, and Intestinal Intraepithelial Lymphocyte Activation." *Cancer Letters* 265 (1): 84–97.
- Kliebenstein, Dan J, Juergen Kroymann, and Thomas Mitchell-Olds. 2005. "The Glucosinolate--Myrosinase System in an Ecological and Evolutionary Context." *Current Opinion in Plant Biology* 8 (3): 264–71.
- Koshy, Calmly M., Deva Asirvatham, Rikhia Majumdar, and Shobana Sugumar. 2022. "In Silico Structural and Functional Characterization of a Hypothetical Protein from *Stenotrophomonas Maltophilia* SRM01." *Journal of Pure and Applied Microbiology* 16 (2): 1167–78.
- Kunimasa, Kazuhiro, Tomomi Kobayashi, Kazuhiko Kaji, and Toshiro Ohta. 2010. "Antiangiogenic Effects of Indole-3-Carbinol and 3, 3'-Diindolylmethane Are Associated with Their Differential Regulation of ERK1/2 and Akt in Tube-Forming HUVEC." *The Journal of Nutrition* 140 (1): 1–6.

- Kusters, Johannes G, Arnoud H M Van Vliet, and Ernst J Kuipers. 2006. "Pathogenesis of Helicobacter Pylori Infection." *Clinical Microbiology Reviews* 19 (3): 449–90.
- Kweon, Minson, Hyejin Lee, Cheol Park, Yung Hyun Choi, and Jae-Ha Ryu. 2019. "A Chalcone from Ashitaba (*Angelica Keiskei*) Stimulates Myoblast Differentiation and Inhibits Dexamethasone-Induced Muscle Atrophy." *Nutrients* 11 (10): 2419.
- Laird-Fick, Heather S, Shivani Saini, and James Randolph Hillard. 2016. "Gastric Adenocarcinoma: The Role of Helicobacter Pylori in Pathogenesis and Prevention Efforts." *Postgraduate Medical Journal* 92 (1090): 471–77.
- Layke, John C, and Peter P Lopez. 2004. "Gastric Cancer: Diagnosis and Treatment Options." *American Family Physician* 69 (5): 1133–41.
- Lee, C. M., S. H. Park, and M. J. Nam. 2019. "Anticarcinogenic Effect of Indole-3-Carbinol (I3C) on Human Hepatocellular Carcinoma SNU449 Cells." *Human and Experimental Toxicology* 38 (1): 136–47.
- Lee, Jong Heun, Young Hwa Soung, Jong Woo Lee, Won Sang Park, Su Young Kim, Yong Gu Cho, Chang Jae Kim, *et al.*, 2004. "Inactivating Mutation of the Pro-Apoptotic Gene BID in Gastric Cancer." *The Journal of Pathology: A Journal of the Pathological Society of Great Britain and Ireland* 202 (4): 439–45.
- Lee, Yi-Chia, Tsung-Hsien Chiang, Chu-Kuang Chou, Yu-Kang Tu, Wei-Chih Liao, Ming-Shiang Wu, and David Y Graham. 2016. "Association between

- Helicobacter Pylori Eradication and Gastric Cancer Incidence: A Systematic Review and Meta-Analysis.” *Gastroenterology* 150 (5): 1113–24.
- Li, Bei, Ang Li, Zhen You, Jingchang Xu, and Sha Zhu. 2020. “Epigenetic Silencing of CDKN1A and CDKN2B by SNHG1 Promotes the Cell Cycle, Migration and Epithelial-Mesenchymal Transition Progression of Hepatocellular Carcinoma.” *Cell Death & Disease* 11 (10): 823.
- Lim, Heui Min, See Hyoung Park, and Myeong Jin Nam. 2021. “Induction of Apoptosis in Indole-3-Carbinol-Treated Lung Cancer H1299 Cells via ROS Level Elevation.” *Human and Experimental Toxicology* 40 (5): 812–25.
- Lin, K, and J Chang. 2015. “Structure and Properties of Hydroxyapatite for Biomedical Applications.” In *Hydroxyapatite (HAp) for Biomedical Applications*, 3–19. Elsevier.
- Link, Tim, and Tomoo Iwakuma. 2017. “Roles of P53 in Extrinsic Factor-Induced Liver Carcinogenesis.” *Hepatoma Research* 3: 95.
- Llovet, Josep M, and Michel Beaugrand. 2003. “Hepatocellular Carcinoma: Present Status and Future Prospects.” *Journal of Hepatology* 38: 136–49.
- Lordick, F., F. Carneiro, S. Cascinu, T. Fleitas, K. Haustermans, G. Piessen, A. Vogel, and E. C. Smyth. "Gastric cancer: ESMO Clinical Practice Guideline for diagnosis, treatment and follow-up☆." *Annals of Oncology* 33, no. 10 (2022): 1005-1020.)

- Luedde, Tom, and Robert F Schwabe. 2011. "NF- κ B in the Liver—Linking Injury, Fibrosis and Hepatocellular Carcinoma." *Nature Reviews Gastroenterology & Hepatology* 8 (2): 108–18.
- Maio, Massimo Di, Bruno Daniele, Sandro Pignata, Ciro Gallo, Ermelinda De Maio, Alessandro Morabito, Maria Carmela Piccirillo, and Francesco Perrone. 2008. "Is Human Hepatocellular Carcinoma a Hormone-Responsive Tumor?" *World Journal of Gastroenterology: WJG* 14 (11): 1682.
- Mao, Cheng Gang, Ze Zhang Tao, Zhe Chen, Chen Chen, Shi Ming Chen, and Li Jia Wan. 2014. "Indole-3-Carbinol Inhibits Nasopharyngeal Carcinoma Cell Growth in Vivo and in Vitro through Inhibition of the PI3K/Akt Pathway." *Experimental and Therapeutic Medicine* 8 (1): 207–12.
- Marin, J J G, R Al-Abdulla, E Lozano, O Briz, L Bujanda, J M Banales, and R I R Macias. 2016. "Mechanisms of Resistance to Chemotherapy in Gastric Cancer." *Anti-Cancer Agents in Medicinal Chemistry (Formerly Current Medicinal Chemistry-Anti-Cancer Agents)* 16 (3): 318–34.
- Minsky, B D. 1996. "The Role of Radiation Therapy in Gastric Cancer." In *Seminars in Oncology*, 23:390–96.
- Mise, Kotaro, Seiki Tashiro, Shiro Yogita, Daisuke Wada, Masamitsu Harada, You Fukuda, Hidenori Miyake, Masashi Isikawa, Keiske Izumi, and Nobuya Sano. 1998. "Assessment of the Biological Malignancy of Hepatocellular Carcinoma: Relationship to Clinicopathological Factors and Prognosis." *Clinical Cancer*

Research: An Official Journal of the American Association for Cancer
Research 4 (6): 1475–82.

Moiseeva, Elena P., Gabriela M. Almeida, George D.D. Jones, and Margaret M.
Manson. 2007. “Extended Treatment with Physiologic Concentrations of
Dietary Phytochemicals Results in Altered Gene Expression, Reduced Growth,
and Apoptosis of Cancer Cells.” *Molecular Cancer Therapeutics* 6 (11): 3071–
79.

Nagata, Shigekazu. 2000. “Apoptotic DNA Fragmentation.” *Experimental Cell
Research* 256 (1): 12–18.

Nel, Ivonne, Hideo A Baba, Frank Weber, Barbara Sitek, Martin Eisenacher, Helmut
E Meyer, Joerg F Schlaak, and Andreas-Claudius Hoffmann. 2014. “IGFBP1
in Epithelial Circulating Tumor Cells as a Potential Response Marker to
Selective Internal Radiation Therapy in Hepatocellular Carcinoma.”
Biomarkers in Medicine 8 (5): 687–98.

Nishimura, Reiko, Keiichi Tabata, Motoki Arakawa, Yoshihisa Ito, Yumiko Kimura,
Toshihiro Akihisa, Hisashi Nagai, Atsuko Sakuma, Hideki Kohno, and Takashi
Suzuki. 2007. “Isobavachalcone, a Chalcone Constituent of *Angelica Keiskei*,
Induces Apoptosis in Neuroblastoma.” *Biological and Pharmaceutical Bulletin*
30 (10): 1878–83.

Noh, Hye-Mi, Eun-Mi Ahn, Jae-Moon Yun, Be-Long Cho, and Yu-Jin Paek. 2015.
“*Angelica Keiskei* Koidzumi Extracts Improve Some Markers of Liver

Function in Habitual Alcohol Drinkers: A Randomized Double-Blind Clinical Trial.” *Journal of Medicinal Food* 18 (2): 166–72.

Nolte, M, M Werner, A Nasarek, H Bektas, R Von Wasielewski, J Klemnauer, and A Georgii. 1998. “Expression of Proliferation Associated Antigens and Detection of Numerical Chromosome Aberrations in Primary Human Liver Tumours: Relevance to Tumour Characteristics and Prognosis.” *Journal of Clinical Pathology* 51 (1): 47–51.

Oh, Hyun-A, Hyunbeom Lee, Soo-yeon Park, Yeni Lim, Oran Kwon, Ji Yeon Kim, Donghak Kim, and Byung Hwa Jung. 2019. “Analysis of Plasma Metabolic Profiling and Evaluation of the Effect of the Intake of Angelica Keiskei Using Metabolomics and Lipidomics.” *Journal of Ethnopharmacology* 243: 112058.

Okuyama, T, M Takata, J Takayasu, T Hasegawa, H Tokuda, A Nishino, H Nishino, and A Iwashima. 1991. “Anti-Tumor-Promotion by Principles Obtained from Angelica Keiskei.” *Planta Medica* 57 (03): 242–46.

Orditura, Michele, Gennaro Galizia, Vincenzo Sforza, Valentina Gambardella, Alessio Fabozzi, Maria Maddalena Laterza, Francesca Andreozzi, *et al.*, 2014. “Treatment of Gastric Cancer.” *World Journal of Gastroenterology: WJG* 20 (7): 1635.

Papatheodoridis, George V, Henry Lik-Yuen Chan, Bettina E Hansen, Harry L A Janssen, and Pietro Lampertico. 2015. “Risk of Hepatocellular Carcinoma in

- Chronic Hepatitis B: Assessment and Modification with Current Antiviral Therapy.” *Journal of Hepatology* 62 (4): 956–67.
- Petersen, Andreas Munk, and Karen Angeliki Krogfelt. 2003. “Helicobacter Pylori: An Invading Microorganism? A Review.” *FEMS Immunology & Medical Microbiology* 36 (3): 117–26.
- Rajani, Chitra, Vruti Patel, Pooja Borisa, Tukaram Karanwad, Suryanarayana Polaka, Dnyaneshwar Kalyane, and Rakesh K Tekade. 2020. “Photothermal Therapy as Emerging Combinatorial Therapeutic Approach.” In *The Future of Pharmaceutical Product Development and Research*, 297–339. Elsevier.
- Ramakrishna, Gayatri, Archana Rastogi, Nirupama Trehanpati, Bijoya Sen, Ritu Khosla, and Shiv K Sarin. 2013. “From Cirrhosis to Hepatocellular Carcinoma: New Molecular Insights on Inflammation and Cellular Senescence.” *Liver Cancer* 2 (3–4): 367–83.
- Rizvi, Sumera, Juan Wang, and Anthony B El-Khoueiry. 2021. “Liver Cancer Immunity.” *Hepatology* 73: 86–103.
- Rosen, Clark A, and Paul C Bryson. 2004. “Indole-3-Carbinol for Recurrent Respiratory Papillomatosis: Long-Term Results.” *Journal of Voice* 18 (2): 248–53.
- Rumgay, Harriet, Melina Arnold, Jacques Ferlay, Olufunmilayo Lesi, Citadel J Cabasag, Jérôme Vignat, Mathieu Laversanne, Katherine A McGlynn, and

- Isabelle Soerjomataram. 2022. "Global Burden of Primary Liver Cancer in 2020 and Predictions to 2040." *Journal of Hepatology* 77 (6): 1598–1606.
- Rungapamestry, Vanessa, Alan J Duncan, Zoë Fuller, and Brian Ratcliffe. 2006. "Changes in Glucosinolate Concentrations, Myrosinase Activity, and Production of Metabolites of Glucosinolates in Cabbage (*Brassica Oleracea* Var. *Capitata*) Cooked for Different Durations." *Journal of Agricultural and Food Chemistry* 54 (20): 7628–34.
- Rutkute, Kristina, and Mariana N Nikolova-Karakashian. 2007. "Regulation of Insulin-like Growth Factor Binding Protein-1 Expression during Aging." *Biochemical and Biophysical Research Communications* 361 (2): 263–69.
- Sachdeva, Mira M, Kathryn C Claiborn, Cynthia Khoo, Juxiang Yang, David N Groff, Raghavendra G Mirmira, and Doris A Stoffers. 2009. "Pdx1 (MODY4) Regulates Pancreatic Beta Cell Susceptibility to ER Stress." *Proceedings of the National Academy of Sciences* 106 (45): 19090–95.
- Sadat-Shojai, Mehdi, Mohammad-Taghi Khorasani, Ehsan Dinpanah-Khoshdargi, and Ahmad Jamshidi. 2013. "Synthesis Methods for Nanosized Hydroxyapatite with Diverse Structures." *Acta Biomaterialia* 9 (8): 7591–7621.
- Sastre, Javier, Jose Angel García-Saenz, and Eduardo Díaz-Rubio. "Chemotherapy for gastric cancer." *World journal of gastroenterology: WJG* 12, no. 2 (2006): 204.
- Schäffler, Martin, Fernanda Sousa, Alexander Wenk, Leopoldo Sitia, Stephanie Hirn, Carsten Schleh, Nadine Haberl, *et al.*, 2014. "Blood Protein Coating of Gold

- Nanoparticles as Potential Tool for Organ Targeting.” *Biomaterials* 35 (10): 3455–66.
- Schreiber, Sören, Manuela Konradt, Claudia Groll, Peter Scheid, Guido Hanauer, Hans-Otto Werling, Christine Josenhans, and Sebastian Suerbaum. 2004. “The Spatial Orientation of *Helicobacter Pylori* in the Gastric Mucus.” *Proceedings of the National Academy of Sciences* 101 (14): 5024–29.
- Schubert, Mitchell L, and David A Peura. 2008. “Control of Gastric Acid Secretion in Health and Disease.” *Gastroenterology* 134 (7): 1842–60.
- Shakeri, Raheleh, Asma Kheirollahi, and Jamshid Davoodi. 2017. “Apaf-1: Regulation and Function in Cell Death.” *Biochimie* 135: 111–25.
- González-Arzola, Katuska, Alejandro Velázquez-Cruz, Alejandra Guerra-Castellano, Miguel Á. Casado-Combreras, Gonzalo Pérez-Mejías, Antonio Díaz-Quintana, Irene Díaz-Moreno, and Miguel A. De la Rosa. 2019 “New moonlighting functions of mitochondrial cytochrome c in the cytoplasm and nucleus.” *FEBS letters* 593, no. 22 (2019): 3101-3119.
- Sharma, Poonam, and Jayashri Devi Sharma. 2001. “In Vitro Hemolysis of Human Erythrocytes—by Plant Extracts with Antiplasmodial Activity.” *Journal of Ethnopharmacology* 74 (3): 239–43.
- Shukla, Yogeshwer, Annu Arora, and Pankaj Taneja. 2003. “Antigenotoxic Potential of Certain Dietary Constituents.” *Teratogenesis, Carcinogenesis, and Mutagenesis* 23 (S1): 323–35.

- Singh, Alka Ashok, Maheshkumar Prakash Patil, Min Jae Kang, Irvine Niyonizigiye, and Gun Do Kim. 2021. "Biomedical Application of Indole-3-Carbinol: A Mini-Review." *Phytochemistry Letters* 41 (July 2020): 49–54.
- Sinicrope, Frank A, Rafaela L Rego, Nathan R Foster, Stephen N Thibodeau, Steven R Alberts, Harold E Windschitl, and Daniel J Sargent. 2008. "Proapoptotic Bad and Bid Protein Expression Predict Survival in Stages II and III Colon Cancers." *Clinical Cancer Research* 14 (13): 4128–33.
- Smoot, Duane T. 1997. "How Does Helicobacter Pylori Cause Mucosal Damage? Direct Mechanisms." *Gastroenterology* 113 (6): S31--S34.
- Smyth, Elizabeth C, and David Cunningham. 2012. "Targeted Therapy for Gastric Cancer." *Current Treatment Options in Oncology* 13: 377–89.
- Song, Jung Min, Xuemin Qian, Kalkidan Molla, Fistum Teferi, Pramod Upadhyaya, Gerry O'Sullivan, Xianghua Luo, and Fekadu Kassie. 2015. "Combinations of Indole-3-Carbinol and Silibinin Suppress Inflammation-Driven Mouse Lung Tumorigenesis by Modulating Critical Cell Cycle Regulators." *Carcinogenesis* 36 (6): 666–75
- Song, Tianqiang, Mengran Lang, Shaohua Ren, Leijuan Gan, and Wei Lu. 2021. "The Past, Present and Future of Conversion Therapy for Liver Cancer." *American Journal of Cancer Research* 11 (10): 4711.
- Soukupova, Jitka, Andrea Malfettone, Petra Hyroššová, María-Isabel Hernández-Alvarez, Irene Peñuelas-Haro, Esther Bertran, Alexandra Junza *et al.*, "Role of

- the Transforming Growth Factor- β in regulating hepatocellular carcinoma oxidative metabolism." *Scientific reports* 7, no. 1 (2017): 12486.
- Stark, R M, G J Gerwig, R S Pitman, L F Potts, N A Williams, J Greenman, I P Weinzweig, T R Hirst, and M R Millar. 1999. "Biofilm Formation by *Helicobacter Pylori*." *Letters in Applied Microbiology* 28 (2): 121–26.
- Stickles, Xiaomang B, Douglas C Marchion, Elona Bicaku, Entidhar Al Sawah, Forough Abbasi, Yin Xiong, Nadim Bou Zgheib, *et al.*, 2015. "BAD-Mediated Apoptotic Pathway Is Associated with Human Cancer Development." *International Journal of Molecular Medicine* 35 (4): 1081–87.
- Takei, Shogo, Akihito Kawazoe, and Kohei Shitara. 2022. "The New Era of Immunotherapy in Gastric Cancer." *Cancers* 14 (4): 1054.
- Taylor, Karen J, Andrew H Sims, Liang Liang, Dana Faratian, Morwenna Muir, Graeme Walker, Barbara Kuske, *et al.*, 2010. "Dynamic Changes in Gene Expression in Vivo Predict Prognosis of Tamoxifen-Treated Patients with Breast Cancer." *Breast Cancer Research* 12: 1–13.
- Tella, Sri Harsha, Anuhya Kommalapati, Amit Mahipal, and Zhaohui Jin. 2022 "First-line targeted therapy for hepatocellular carcinoma: role of atezolizumab/bevacizumab combination." *Biomedicines* 10, no. 6 (2022): 1304.
- Telloni, Stacy M. "Tumor staging and grading: A primer." *Molecular Profiling: Methods and Protocols* (2017): 1-17.)

- Thorgeirsson, Snorri S, and Joe W Grisham. 2002. "Molecular Pathogenesis of Human Hepatocellular Carcinoma." *Nature Genetics* 31 (4): 339–46.
- Toné, Shigenobu, Kenji Sugimoto, Kazue Tanda, Taiji Suda, Kenzo Uehira, Hiroaki Kanouchi, Kumiko Samejima, Yohsuke Minatogawa, and William C. Earnshaw. 2007. "Three Distinct Stages of Apoptotic Nuclear Condensation Revealed by Time-Lapse Imaging, Biochemical and Electron Microscopy Analysis of Cell-Free Apoptosis." *Experimental Cell Research* 313 (16): 3635–44.
- Torre, Lindsey A, Freddie Bray, Rebecca L Siegel, Jacques Ferlay, Joannie Lortet-Tieulent, and Ahmedin Jemal. 2015. "Global Cancer Statistics, 2012." *CA: A Cancer Journal for Clinicians* 65 (2): 87–108.
- Tsuji, S, N Kawai, M Tsujii, S Kawano, and M Hori. 2003. "Inflammation-Related Promotion of Gastrointestinal Carcinogenesis--a Perigenetic Pathway." *Alimentary Pharmacology & Therapeutics* 18: 82–89.
- Tu, Lanlan, Rui Wang, Zheng Fang, Mengge Sun, Xiaohui Sun, Jinhong Wu, Yali Dang, and Jianhua Liu. 2022. "Assessment of the Hypoglycemic and Hypolipidemic Activity of Flavonoid-Rich Extract from *Angelica Keiskei*." *Molecules* 27 (19): 6625.
- Tu, Lanlan, Rui Wang, Zheng Fang, Mengge Sun, Xiaohui Sun, Jinhong Wu, Yali Dang, and Jianhua Liu. 2022. "Assessment of the Hypoglycemic and

- Hypolipidemic Activity of Flavonoid-Rich Extract from *Angelica Keiskei*.”
Molecules 27 (19): 6625.
- Umemura, Atsushi, Yoshito Itoh, Katsuhiko Itoh, Kanji Yamaguchi, Tomoki Nakajima, Hiroaki Higashitsuji, Hitoshi Onoue, Manabu Fukumoto, Takeshi Okanoue, and Jun Fujita. 2008. “Association of Gankyrin Protein Expression with Early Clinical Stages and Insulin-like Growth Factor-Binding Protein 5 Expression in Human Hepatocellular Carcinoma.” *Hepatology* 47 (2): 493–502.
- Verhoeven, Dorette T H, Hans Verhagen, R Alexandra Goldbohm, Piet A van den Brandt, and Geert van Poppel. 1997. “A Review of Mechanisms Underlying Anticarcinogenicity by Brassica Vegetables.” *Chemico-Biological Interactions* 103 (2): 79–129.
- Viala, J. 2004. “Chaput C, Boneca IG, Cardona A, Girardin SE, Moran AP, Athman R, Memet S, Huerre MR, Coyle AJ, DiStefano PS, Sansonetti PJ, Labigne A, Bertin J, Philpott DJ, Ferrero RL.” Nod1 Responds to Peptidoglycan Delivered by the *Helicobacter Pylori* Cag Pathogenicity Island. *Nat Immunol* 5: 1166–74.
- Villanueva, Augusto, and Tom Luedde. 2016. “The Transition from Inflammation to Cancer in the Liver.” *Clinical Liver Disease* 8 (4): 89–93.
- Vines, J.B., Yoon, J.H., Ryu, N.E., Lim, D.J. and Park, H. 2019. “Gold Nanoparticles for Photothermal Cancer Therapy.” *Frontiers in Chemistry*.
- Walsh, John G., Sean P. Cullen, Clare Sheridan, Alexander U. Lüthi, Christopher Gerner, and Seamus J. Martin. 2008. “Executioner Caspase-3 and Caspase-7

- Are Functionally Distinct Proteases.” Proceedings of the National Academy of Sciences of the United States of America 105 (35): 12815–19.
- Warren, Chloe F.A., Michelle W. Wong-Brown, and Nikola A. Bowden. 2019. “BCL-2 Family Isoforms in Apoptosis and Cancer.” Cell Death and Disease 10 (3).
- Westphal, D, R M Kluck, and G Dewson. 2014. “Building Blocks of the Apoptotic Pore: How Bax and Bak Are Activated and Oligomerize during Apoptosis.” Cell Death & Differentiation 21 (2): 196–205.
- Wolf, Beni B., Martin Schuler, Fernando Echeverri, and Douglas R. Green. 1999. “Caspase-3 Is the Primary Activator of Apoptotic DNA Fragmentation via DNA Fragmentation Factor-45/Inhibitor of Caspase-Activated DNase Inactivation.” Journal of Biological Chemistry 274 (43): 30651–56.
- Wong, George Y.C., Leon Bradlow, Daniel Sepkovic, Stephanie Mehl, Joshua Mailman, and Michael P. Osborne. 1997. “Dose-Ranging Study of Indole-3-Carbinol for Breast Cancer Prevention.” Journal of Cellular Biochemistry 67 (SUPPL. 28/29): 111–16.
- Xu, Zongquan, Xiaoping Chen, Cheng Peng, Enyu Liu, Yunguang Li, Changhai Li, and Jun Niu. 2012. “Hypoxia-Inducible Factor-1 α Suppressed Hepatocellular Carcinoma Cell Apoptosis through Influencing on Omi/HtrA2 Expression and Its Releasing from the Mitochondrion.” Oncology Research Featuring Preclinical and Clinical Cancer Therapeutics 20 (5–6): 213–20.

- Yang, Elizabeth, Jiping Zha, Jennifer Jockel, Lawrence H Boise, Craig B Thompson, and Stanley J Korsmeyer. 1995. "Bad, a Heterodimeric Partner for Bcl-XL and Bcl-2, Displaces Bax and Promotes Cell Death." *Cell* 80 (2): 285–91.
- Yang, LiJun, Qing Tang, Jingjing Wu, Yuqing Chen, Fang Zheng, Zhenhui Dai, and Swei Sunny Hann. 2016. "Inter-Regulation of IGFBP1 and FOXO3a Unveils Novel Mechanism in Ursolic Acid-Inhibited Growth of Hepatocellular Carcinoma Cells." *Journal of Experimental & Clinical Cancer Research* 35 (1): 1–13
- Yasmin, A., Ramesh, K. and Rajeshkumar, S. 2014. "Optimization and Stabilization of Gold Nanoparticles by Using Herbal Plant Extract with Microwave Heating." *Nano Convergence*.
- Zhang, Jing, Wen-Liang Wang, Qing Li, and Qing Qiao. 2004. "Expression of Transforming Growth Factor- α and Hepatitis B Surface Antigen in Human Hepatocellular Carcinoma Tissues and Its Significance." *World Journal of Gastroenterology* 10 (6): 830.
- Zhang, Keliang, Yin Zhang, Jeffrey L Walck, and Jun Tao. 2019. "Non-Deep Simple Morphophysiological Dormancy in Seeds of *Angelica Keiskei* (Apiaceae)." *Scientia Horticulturae* 255: 202–8.
- Zhang, P., Chen, H., Liu, J. and Liu, G. 2019. "Genetically Engineered Plasma Membrane Nanovesicles for Cancer-Targeted Nanotheranostics." *Theranostics: Methods and Protocols*.

- Zhang, Wenqing, Mingqun Lin, Qi Yan, Khemraj Budachetri, Libo Hou, Ashweta Sahni, Hongyan Liu, *et al.*, 2021. "An Intracellular Nanobody Targeting T4SS Effector Inhibits Ehrlichia Infection." *Proceedings of the National Academy of Sciences* 118 (18): e2024102118.
- Zhang, Yan, Li Ding, Qingfeng Ni, Ran Tao, and Jun Qin. 2021. "Transcription Factor PAX4 Facilitates Gastric Cancer Progression through Interacting with MiR-27b-3p/Grb2 Axis." *Aging (Albany NY)* 13 (12): 16786.
- Zhao, Haifeng, and Mouming Zhao. 2012. "Effects of Mashing on Total Phenolic Contents and Antioxidant Activities of Malts and Worts." *International Journal of Food Science & Technology* 47 (2): 240–47.
- Zhao, Yanting, Jiansheng Wang, Yuanyuan Liu, Huiying Miao, Congxi Cai, Zhiyong Shao, Rongfang Guo, *et al.*, 2015. "Classic Myrosinase-Dependent Degradation of Indole Glucosinolate Attenuates Fumonisin B 1-Induced Programmed Cell Death in A Rabidopsis." *The Plant Journal* 81 (6): 920–33.
- Zhu, Xiao-Dong, Zhao-You Tang, and Hui-Chuan Sun. "Targeting angiogenesis for liver cancer: past, present, and future." *Genes & Diseases* 7, no. 3 (2020): 328-335.).
- Zlobec, Inti, Parham Minoo, Kristi Baker, David Haegert, Karim Khetani, Luigi Tornillo, Luigi Terracciano, Jeremy R. Jass, and Alessandro Lugli. 2007. "Loss of APAF-1 Expression Is Associated with Tumour Progression and Adverse Prognosis in Colorectal Cancer." *European Journal of Cancer* 43 (6): 1101–7.

Indole-3-Carbinol 및 *Angelica keiskei* 추출물을 이용한 AGS 및

HepG2 암세포의 세포사멸 유도

싱 얼카

미생물학교, 대학원,

요약

세계에서 가장 흔한 질병 중 하나는 암입니다. 암에 의해 제기되는 엄청난 글로벌 건강 도전 앞에서 여전히 행동이 필요합니다. 암은 특정 신체 세포가 비정상적으로 무제한으로 증식하고 다른 신체 부위로 이동할 때 발생하는 질병입니다. 질병에 대한 표준적인 관점에 따르면, 암은 종양 억제 유전자, 종양 유전자, 그리고 염색체 이상에 대한 돌연변이로 인해 발생하는 점진적인 유전적 이상의 집합입니다. 암 화학 예방은 건강한 사람들에게 암 발병 위험을 줄이기 위해 천연 또는 생물학적 화합물을 사용합니다. 화학 예방 약물은 DNA 손상을 막거나, 이에도 불구하고 DNA 손상을 가진 예비암 세포의 분열을 뒤집거나 막음으로써 암 성장을 방지합니다. 현재 사용되는 대부분의 의약품은 식물에서 파생되므로, 이들은 약의 더 중요한 출처 중 하나입니다. 차별적인 약물 반응과 안전한 복용량은 그러한 예측의 주요 과제입니다. 정상 세포와 암

세포를 모두 죽이는 약물의 부작용을 피하기 위해 IC50 용량으로 치료하는 것이 안전합니다. 임상 연구는 식물 화학 물질과 허브가 암을 치료하는 가장 효과적인 방법임을 보여주었습니다. 이것은 항암 요법에 추가되거나 부작용 없이 면역 체계를 강화하기 위해 별도로 복용됩니다.

위암은 전 세계적으로 암 관련 사망 원인 중 두 번째입니다. 잘 알려진 사실은 *Helicobacter pylori* 가 위 내벽을 감염시키고 암을 유발한다는 것입니다. 이 연구에서는 인돌-3-카비놀을 AGS 암 세포에 대한 항암 약물로 사용하였습니다. 세포 활성은 화합물의 항암 활동을 확인하기 위해 수행되었습니다. DNA 단편화는 DNA 분해를 평가하기 위해 사용되었으며, DAPI 라벨링은 핵 응축을 식별하는 데 사용되었습니다. qPCR 기법은 세포 사멸 유전자 발현을 측정하는 데 사용되었습니다. 분자 도킹 연구에 따르면 I3C 는 세포 사멸 단백질 3DCY 에 강한 친화력을 보였습니다.

이 연구는 놀라운 항암, 항산화 및 항균 특성과 가장 안전한 약물 전달 응용을 탐구합니다.

Angelica keiskei Crude 는 아열수 추출 방법을 사용하여 추출되었습니다. 항산화 활동은 DPPH 라디칼 소거 분석을 사용하여 평가되었습니다. MTT 분석은 MDA-MB-231

Acknowledgement

I express my gratitude to God for safeguarding me, bestowing remarkable opportunities, and ensuring my excellent health until today. I extend heartfelt thanks to Professor Gun-Do Kim, my supervisor and advisor, for granting me the chance to be part of his research lab and for his invaluable guidance and supporting me in all ups and down. My gratitude goes to members of my thesis committee: Professor Young Tae Kim, Professor Young Jae Jeon, Professor Nam Gyu Park and Professor Soo-Wan Nam, for their insightful comments and their encouragement. I would particularly like to thank Professor Byung-Soo Chun and Professor Sudip Mondal for their academic help and advice. I couldn't have completed this work without my friends Manas R Biswal, Mohan Prakash, Devyani Gawande, Vishal Gawande, Dinesh Myilsami, David Nkurunziza, Deva Asirvatham, Yaseer yanish, Shubhendu Fuladi, Maheshkumar Prakash Patil and Anley Teferra, also thanks to my friends from Pune India who helped me a lot to pursue my doctorate degree. The special thanks to my family for their immense support throughout my Ph.D journey. Thanks to my grandfather and my mother for their encouragement and motivation. Thanks to my sister Nutan Singh and Brothers Mayank Mani Singh and Shashank Sekhar Singh for always being on my side, encouraging me to complete my degree.

I would like to thank my late father Mr. Ashok Singh for giving me strength and hope from another world. Last but not least, I dedicate this thesis to my late father Mr. Ashok Singh. May your soul live in eternal peace. You are always in my prayer.